

“JÚLIO DE MESQUITA FILHO”

Campus de Guaratinguetá - SP

WEIXIAN CHEN

**DESENVOLVIMENTO E APLICAÇÕES DO MODELO
HIDRODINÂMICO SPHERIO**

GUARATINGUETÁ

2017

WEIXIAN CHEN

DESENVOLVIMENTO E APLICAÇÕES DO MODELO HIDRODINÂMICO SPHERIO

Dissertação apresentada à Faculdade de Engenharia do Campus de Guaratinguetá, Universidade Estadual Paulista, para a obtenção do título de Mestre em Física Nuclear na área de Física.

Orientador: Prof. Weiliang Qian

Co-orientador: Prof. Kai Lin

GUARATINGUETÁ

2017

Chen, Weixian

C518d Development and applications of hydrodynamics model SPheRIO /
Weixian Chen – Guaratinguetá 2017.

106 f : il.

Bibliografia: f. 103-106

Dissertação (Mestrado) – Universidade Estadual Paulista, Faculdade de
Engenharia de Guaratinguetá 2017.

Orientador: Prof. Dr. Weiliang Qian

Coorientador: Prof. Dr. Kai Lin

1. Partículas (Física nuclear). 2. Hidrodinâmica. 3. Física nuclear.

I. Título

CDU 539.1(043)

WEIXIAN CHEN

**ESTA DISSERTAÇÃO FOI JULGADA ADEQUADA PARA A OBTENÇÃO DO TÍTULO DE
"MESTRE EM FÍSICA"**

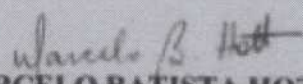
PROGRAMA: FÍSICA

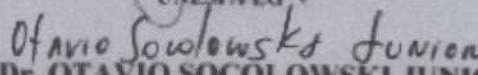
APROVADA EM SUA FORMA FINAL PELO PROGRAMA DE PÓS-GRADUAÇÃO

Prof. Dr. Konstatin Georgiev Kostov
Coordenador

BANCA EXAMINADORA:


Prof. Dr. WEI-LIANG QIAN
Orientador / UNESP/FEG


Prof. Dr. MARCELO BATISTA HOTT
UNESP/FEG


Prof. Dr. OTAVIO SOCOLOWSKI JUNIOR
UFRG/RS

Agosto de 2017



“JÚLIO DE MESQUITA FILHO”

Campus de Guaratinguetá - SP

**DESENVOLVIMENTO E APLICAÇÕES DO MODELO
HIDRODINÂMICO SPHERIO**

WEIXIAN CHEN

Folha de Aprova ção

AGOSTO DE 2017

DADOS CURRICULARES**WEIXIAN CHEN**

NASCIMENTO	16.04.1994 – HENGYANG / HUNAN - CHINA
FILIAÇÃO	CHENGQIANG CHEN YUANQING CHEN
2011/2015	Curso de graduação Física – Universidade Normal de Hunan
2016/2017	Curso de Pós-graduação em Física, nível de mestrado na Faculdade de Engenharia do Campus de Guaratinguetá da Universidade Estadual Paulista.

Dedico a todos que em algum determinado momento da minha vida tenham me ajudado..

AGRADECIMENTOS

Para o Prof. Dr. Philipe Mota, que sempre continua me encorajando. Sem a sua assistência, orientação e dedicação, o trabalho apresentado não teria sido possível.

Ao meu colega Honghao Ma e à minha colega DanWen para dar ajuda e para discutir alguns problemas que eu encontrei durante o processo de pesquisa.

A meus pais por terem me ajudado minha formação como pessoa e a ensinar-me a lutar por meus sonhos.

À FAPESP – Fundação de Amparo à Pesquisa do Estado de São Paulo (2015/06212-5) pelo apoio financeiro.

À UNESP – Universidade Estadual Paulista por fornecer um bom ambiente para estudar e terminar o trabalho de pesquisa.

“Não tenho talento especial. Eu só sou apaixonadamente curioso”

Albert Einstein.

WEIXIAN, CHEN. Desenvolvimento e aplicações do modelo hidrodinâmico SPheRIO. 2017, 107 f. Dissertação (Mestrado em Física) – Universidade Estadual Paulista (Unesp), Faculdade de Engenharia de Guaratinguetá, Campus Guaratinguetá, 2017.

RESUMO

Nesta dissertação, investigamos o algoritmo numérico conhecido como hidrodinâmicos de Partículas Suavizadas (SPH). O algoritmo de interpolação SPH é amplamente utilizado para equações diferenciais e para aplicações como problemas em colisões de íons pesados, por exemplo, modelo Landau unidimensional e expansão transversal de escala longitudinal. Propriedades importantes, precisão, eficiência e estabilidades, são discutidas. Como SPH é um método sem malha, os méritos e desvantagens comparados com os métodos baseados em grade anteriores são resumidos. Para colisão de alta energia, o sistema composto pode ser modelado pela hidrodinâmica. Em particular, a equação de Euler e sua versão relativística são abordadas. Além do método SPH convencional, o método de partículas finitas (FPM), que faz uso da expansão da série Taylor de funções suaves desconhecidas, também é investigado. Para o modelo Landau unidimensional, ambos os algoritmos são aplicados e os resultados são comparados. Devido à melhor precisão do FPM, a equação de movimento hidrodinâmica correspondente é derivada. Mostramos que a equação de movimento derivada garante uma melhor consistência das partículas. Também foram feitos esforços no desenvolvimento de programas para estudar a solução numérica do modelo hidrodinâmico de Landau. Escrevemos alguns programas curtos em c++ para calcular numericamente a evolução temporal do modelo de Landau. Os resultados são então comparados aos da abordagem analítica. Além disso, o código baseado no algoritmo SPH padrão é modificado para investigar o esquema FPM.

PALAVRAS-CHAVE: SPH. Precisão. Eficiência. Estabilidade. FPM

WEIXIAN, CHEN. **Development and applications of hydrodynamic model SPheRIO**. 2017, 107 p. Dissertation (Master in Physics) - Paulista State University (Unesp), Faculty of Engineering of Guaratinguetá, Campus Guaratinguetá 2017.

ABSTRACT

In this dissertation, we investigate the numerical algorithm known as the Smoothed Particle Hydrodynamics (SPH). The SPH interpolation algorithm are widely used for partial differential equations and for applications such as problems in heavy ion collisions for instance one dimensional Landau model and transverse expansion under a longitudinal scaling expansion. Important properties accuracy, efficiency, stability are discussed. As SPH IS a mesh free method, the merits and drawbacks comparing with previous grid based methods are summarized. For high energy collision, the compound system can be modeled by hydrodynamics. In particular, the Euler equation and its relativistic version are addressed. Besides the conventional SPH method, the finite particle method (FPM) which makes use of the Taylor series expansion of unknown smooth functions is also investigated. For the one dimensional Landau model, both algorithms are applied and results are compared. Owing to the better accuracy of the FPM, the corresponding hydrodynamic equation of motion is derived. We show that the derived equation of motion guarantees better particle consistency. Efforts have also been made in developing programs to study the numerical solution of Landau's hydrodynamical model. We write some short programs in c++ to numerically calculate the temporal evolution of Landau's model. The results are then compared to those of the analytic approach. Moreover the code based on the standard SPH algorithm is modified to investigate FPM scheme.

KEYWORDS: SPH. Accuracy. Efficiency. Stability. FPM.

LISTA DE FIGURAS

Figure 1 – The effect of tensile instability.....	30
Figure 2 – Displacement history of the perturbed particle for the bar under the stress.....	31
Figure 3 – Evolution of a double white dwarf binary system consisting of 1.2 and 0.9 solar masses.....	32
Figure 4 – Evolution of a double white dwarf binary system consisting of 1.2 and 0.4 solar masses.....	33
Figure 5 – Evolution of the collision between proto mercury and impactor of 1/6 its mass which hit head-on at 20km/s.....	35
Figure 6 – Evolution of the collision between proto mercury and impactor of 1/6 its mass which hit head-on at 35km/s.....	36
Figure 7 – The particle positions for the evolution of an elliptical drop at two instants $t=0.0008$ and $t=0.0082$	38
Figure 8 – Pressure, density and velocity profiles for the shock tube problem. The upper frames are for Von Neumann Richtmyer viscosity, the lower frame are for the bulk viscosity.....	39
Figure 9 – Pressure, density, velocity and entropy profiles for the shock tube problem, the kernel is Gaussian function.....	40
Figure 10 – Pressure, density, velocity and entropy profiles for the shock tube problem, the kernel is super Gaussian function.....	41
Figure 11 – The comparison for 2D validation between numerical and experimental wave profiles.....	42
Figure 12 – The comparison for 2D validation between numerical and experimental wave profiles which are averaged during the first 3m of the tank.....	43
Figure 13 – The comparison for 2D validation between numerical and experimental wave profiles which are exerted by the incoming wave on the structure.....	43

Figure 14 – The collision between water and disk from the lateral and top view.....	44
Figure 15 – Pressure profiles along the TNT slab during the detonation process.....	47
Figure 16 – Pressure transients at 1 and 2 μ s.....	48
Figure 17 – Density transients at 1 and 2 μ s.....	49
Figure 18 – Pressure transients in the explosive gas and water as well as the shock waves at $t=0.8$ ms and $t=0.12$ ms.....	51
Figure 19 – Density profiles in the explosive gas and water at $t=0.8$ ms and $t=1.2$ ms.....	52
Figure 20 – Velocity profiles in the explosive gas and water at $t=0.8$ ms and $t=1.2$ ms.....	53
Figure 21 – Standard SPH interpolation for original function and its derivative.....	60
Figure 22 –Taylor SPH interpolation for original function and its derivative.....	60
Figure 23 – The profile of the energy density ratio $\varepsilon/\varepsilon_0$ and the flow rapidity y as a function of z/l at different values of t/l is achieved by Riemann solution.....	74
Figure 24 –The profile of the energy density ratio $\varepsilon/\varepsilon_0$ and the flow rapidity y as a function of z/l at different values of t/l is achived by Khalatnikov solution.....	76
Figure 25– Entropy density for different values of t applying standard SPH.....	80
Figure 26 –Entropy density for different values of t applying Taylor SPH.....	81
Figure 27 – Analytical solution for radial distribution of temperature ratio T/T_0 at different instants τ	86
Figure 28 – Numerical solution for radial distribution of temperature ratio T/T_0 at different instants τ	92

LISTA DE ABREVIATURAS E SIGLAS

SPH	Smoothed Particle Hydrodynamics
FPM	Finite Particle Method
SPHERIO	Smoothed Particle Hydrodynamic evolution of Relativistic heavy-Ion collisions
FDM	Finite difference method
FEM	Finite element method
FVM	Finite volume method
GSM	Gradient smoothing methods
W2	Weakened weak method
HVI	High velocity impact
CSPM	Corrective smoothed particle method
DSPH	Discontinuous SPH

LISTA DE SÍMBOLOS

T	Temperature	K
t	Time	s
l	Length	m
M	Mass	kg
τ	Proper time	s
s	Entropy density	J/K
ε	Energy density	J/m ³
E	Energy	J
V	Volume	m ³
y	rapidity	1
c_0	Speed of light	m/s
x	Displacement	m
F	Force	N

Contents

1	Introduction	3
1.1	Motivations	4
1.2	Grid based numerical methods	5
1.3	Meshfree methods	6
1.4	Merits and drawbacks of SPH	6
1.5	Idea of SPH interpolation	8
1.6	Kernel function	13
1.6.1	Kernel properties	13
1.6.2	Kernel general forms	14
1.6.3	Kernel smoothing length	15
1.7	Tensile instability	16
1.8	SPH for discrete system	18
1.9	Efficiency of SPH	21
1.10	different kernel leads to distinct accuracy	25
1.11	SPH extension to three dimensional condition	26
1.12	SPH application to solid	28
1.13	SPH application to underwater explosion	32
1.14	Consistency	37
2	Finite particle method	43
3	Introduction of hydrodynamical equations of motion	48
3.1	Navier-Stokes equations in Lagrangian form	48
3.1.1	The continuity equation	48
3.1.2	The momentum equation	49
3.1.3	The energy equation	50
3.2	Euler's equation	51
3.3	SPH representations for equations	51
3.4	Relativistic hydrodynamical equations of motion	56
3.5	Derivation of relativistic Euler's equation	58
3.6	summary	58
4	One dimensional Landau Model	59
4.1	Analytic solutions	59
4.1.1	The Riemann simple wave solution	60
4.1.2	The Khalatnikov solution	62
4.1.3	summary	62
4.2	Equation of motion for SPH particles	64
4.3	Derivation of EOM	64
4.4	numerical results for entropy density in laboratory frame	66

5	Transverse expansion on longitudinal scaling expansion	66
5.1	Resolution of transverse expansion analytically	67
5.2	Characteristic method	71
5.3	SPH formulation and evaluation for the transverse expansion . .	73
5.3.1	General coordinate system	74
5.3.2	Hyperbolic coordinate system	77
5.4	Conclusions	81
6	Hydrodynamic equation of motion in FPM	81
7	Discussion and Outlook	87
7.1	Numerical Properties of SPH	87
7.2	The kernel function	88
7.3	The SPH implementation	88
7.4	Future research directions	88
8	Publications	89

1 Introduction

In this chapter, many aspects about the SPH method would be addressed. First of all, the motivations of this work are given. As a numerical method to solve partial equation, it's advantages and disadvantages have been summarized as it is compared with other grid based numerical approaches. The important properties such as accuracy, stability and efficiency are emphasized. The main context will focus on these crucial properties and also some applications of the SPH method would be discussed. The detailed illustration would be given as follows. In general a comprehensive understanding of SPH method would be achieved.

Section one introduces the motivation of my work. Through learning a lot of work done by pioneering, the investigation of accuracy, stability and efficiency are tried to be made. By writing own numerical codes and implementing them in lots of test, it will lay a good foundation to the future research work. Section two introduces some well known and state of art grid based numerical methods, like finite difference, finite volume and finite element methods. However with the developments of techniques and appearance of new problems, they are facing great challenges. Section three introduces some mesh free methods like W2 method, GSM method and SPH method. Subsequently section four addresses the merits and drawbacks of the SPH method, which is mainly summarized by comparing with these mentioned grid based methods. Section five focuses on the basic idea of the SPH method, while the interpolation of function and its derivatives have been made. The Euler equation and Navier Stokes equation have been represented in SPH formulation. In section six, the kernel function is addressed in detail, including its properties, forms and concerning smoothing length. Section seven describes an instability named tensile instability which usually arises in problems of material strength. Section eight introduces the SPH method application to the discrete system which shows its powerful ability to deal with such phenomena. Section nine illustrates the SPH method efficiency in handling realistic problems. Section ten involves the accuracy problem by making use of different kernels, which shows that the selection of kernel function plays a important role in different problems. Section eleven introduces the SPH application to three dimensional conditions, in order to demonstrate high efficiency of SPH method comparing with other numerical method in high dimensional problems. Section twelve introduces one of the crucial properties of SPH algorithm named consistency. The definition of consistency, how to calculate it and how to restore it have been discussed in detail.

Chapter two introduces the finite particle method, which has been proposed since a few years ago. Here we review it because it has better accuracy than the conventional SPH method. This is exactly what we are interested. Another reason is that it is proposed from different view of point by Philipe Mota [1] comparing with the first proposal by GR LIU and MB LIU [2].

Chapter three introduces the hydrodynamical equation of motion. First the classical fluid dynamics equation named Euler's equation is derived. Then attention would be transient to the relativistic conditions. Starting from the variational principle, the relativistic equation of motion, in other word, the

conservation of energy momentum tensor has been deducted. In subsequent, the relativistic Euler's equation is derived, which will be used in the subsequent numerical evaluation.

Chapter four introduces the one dimensional Landau model, the physical background of the Landau hydrodynamics in dealing with the high energy collisions has been addressed. Then the analytic solutions consists of Riemann simple wave solution and Khalatnikov solution have been discussed. The related results of the analytic solution have been shown by figures and concerned discussions have been made. Then applying the conventional SPH method and finite particle method to this physical model, the numerical results are obtained and also compared with the analytic solution, which show great performance.

Chapter five studies the transverse expansion on longitudinal scaling expansion, which is more realistic situation than the one dimensional Landau model. Because of the fact that except the longitudinal expansion, the system would expand in transverse direction. Another reason is that the Landau situation does not satisfy the Bjorken scaling which is verified by the experiments.

Chapter six derived the new equation of motion based on the same variational principle but by virtue of the finite particle method. The deduction is not trivial and the obtained equation motion is satisfactory because it guarantee the momentum conservation and can be consistent with those of conventional SPH.

Chapter seven gives some outlook of present work. The deduction of new equation of motion improve the particle consistency. Recently the "ridge" effect in two particle correlation in relativistic heavy ion collisions has been observed. The fluctuating initial conditions have great influence on it. The new equation of motion is useful in the precision and efficiency of the numerical approach. It will be an interesting topic to simulate the obtained equation of motion for realistic physical problems.

1.1 Motivations

SPheRIO is a numerical code which implements the entropy representation of the Smoothed Particle Hydrodynamics (SPH) algorithm for relativistic high energy collisions. It is the abbreviation of Smoothed Particle hydrodynamical evolution of Relativistic heavy-Ion collisions, which has been studied and developed by Sao Paulo and Rio de Janeiro collaboration. The motivation of my work is to study the accuracy, stability and efficiency of the SPH algorithm, as well as participate in the further development of the SPheRIO code. By using numerical simulations, I plan to study the high energy nuclear collisions at RHIC and LHC.

In the following, I am going to address the definition of the SPH numerical method and advantages, disadvantages inherent to it. Comparisons with other numerical approaches have also been made. Then the basic idea and some features relevant to it would be discussed in detail. Finally attention will be focused on the accuracy, stability and efficiency of the SPH numerical algorithm.

From the hydrodynamical model, the system formed by relativistic high energy collisions would behave more like a fluid, instead of a collection of free

particles. In order to study such a system, we need to get familiar with the fluid dynamics at first. In physics and engineering, fluid dynamics is a part of fluid mechanics which gives description of the flow of fluids. The fundamental rules of fluid dynamics are the conservation laws, such as conservation of mass, conservation of linear momentum, and conservation of energy. As far as the governing equations are concerned, they are generally differential or partial differential equations. To handle these equations, some numerical approaches have been proposed and well studied.

The SPH method is a computationally numerical method used for simulating the dynamics of continuum media, such as the fluid flow and solid mechanics. It divides the fluid into a set of discrete points. These points are assigned material properties such as mass and energy, so that they are referred to as particles. The movement of these particles represents the evolution of the whole system, which can be determined by the governing equation of classical hydrodynamical mechanics. The properties of these particles are smoothed by a kernel function, which gives a smoothing length typically represented by h . In consequence, any arbitrary physical quantity such as the derivative appearing in the equation of motion can be obtained by summing over the related property of these particles which interact within the range of the kernel.

1.2 Grid based numerical methods

In fact, there are many other numerical algorithms for solving the differential equations. One large family of algorithm scheme is the grid based or mesh based method, such as the finite difference method (FDM), the finite element method (FEM) and the finite volume method (FVM). In finite difference method, the derivatives of the differential equations are approximated by finite differences and they are written by discrete quantities of dependent and independent variables. In finite element method, the values of the unknowns are approximated at discrete points over the domain. It solves problem by introducing finite elements which are modeled by simple equations and assembled into a system of equations describing the whole problem. In finite volume method, volume integrals in differential equation that includes the divergence term are usually converted into surface integrals by virtue of divergence theorem. In general, all of them are originally defined on meshes of data points, resulting in grids in FDM, elements in FEM and cells in FVM. In such a mesh, each point has a number of fixed predefined neighbors and the connectivity of these points can be used to calculate the operators like derivative. And these operators are usually constructing a part of the equations such as Euler equations or the Navier-Stokes equations. We can also conclude that all values of unknowns are calculated at discrete places on the meshing geometry. In the past a few years, great developments and progresses have been achieved for these grid based numerical methods and they have become dominant in numerical simulations at present [3-7].

However, dealing with problems like free surface, large deformation, moving interface and deformable boundary, the grid based numerical methods have suffered from great difficulties. In grid based numerical methods, the mesh

generation is of first importance. On one hand, for irregular or complicated geometry of the surface and boundary, a regular grid construction is never easy. And usually mesh generation takes up a large portion of computation effort for handling solids and structures. On the other hand, during the occurrence of large deformation, the connectivity of points in mesh is difficult to maintain and can not give good evaluation for the values of quantities. Moreover, for system consists of a set of discrete particles instead of being a continuum, grid based numerical methods are not desirable either. These problems contain the interaction of stars in astrophysics, dynamical behavior of molecules, and movement of large number of atoms in equilibrium or non-equilibrium state. In summary, it is necessary to find a numerical approach showing great adaptivity which is absent from the grid based methods.

1.3 Meshfree methods

Another typical algorithm scheme is called mesh free methods. In recent years, the mesh free methods have been proposed and become the research focus. It can be used to obtain accurate and stable solution for the partial differential equations through a set of discrete particles or nodes [6,8]. In a field of numerical analysis, mesh free methods do not need the connection of nodes, but are based on the interaction of each node with all its neighbours. In a consequence, the extensive property such as mass are not assigned to mesh but to the single nodes. Owing to the introduction of nodes, the mesh free method is capable of simulating some difficult types of problems, which is at the cost of extra computing time and programming effort. There are a lot of applications and theories about the mesh free methods which have been introduced and discussed in many monographs and reviews [6,8,9-13]. For example, it can be used for simulation where nodes may be created or destroyed, such as in cracking simulations. For the recent development of mesh free method, the so-called weakened weak (W2) method and Gradient Smoothing Methods (GSM) are worthwhile to be discussed. The W2 formulation can formulate various models which work well with triangular meshes. The triangular meshes can be created automatically, which makes it much easier in re-meshing and enables automation in modeling and simulation. The W2 models can produce upper bound solutions for force-driving problems and bound the solution from both sides together with stiff models such as fully compatible FEM models [14-17]. The W2 formulation also leads to the combination of mesh free techniques with the well-studied FEM method. And the GSM is similar to the FVM, which works well with the unstructured triangular mesh. It has been developed recently for CFD problems with the implementation of gradient smoothing idea in strong form [18,19].

1.4 Merits and drawbacks of SPH

The SPH method is one of mesh free methods, which entirely removes the spatial grids. It is a relatively new computational method, which was firstly

proposed by Lucy [20], simultaneously by Gingold and Monaghan [21] to solve the astrophysical problems in three dimensional open space. Due to its inherent adaptivity, numerical conservation of physical conserved quantities and capability to handle problems involving many orders of magnitude, it becomes popular and finds widespread use in astrophysics. These applications in astrophysics contain the simulations of binary stars and stellar collisions [22,23], supernova [24,25], formation of galaxies [26,27] and so on. Apart from the large range of applications to astrophysics, it has been extended to a vast range of problems in fluid flow and solid mechanics. For the use in fluid simulation [28-31], this is owing to several benefits over the traditional grid based techniques. First of all, it guarantees mass conservation since particles themselves carry mass. Secondly the SPH method evaluates the pressure from weighted contributions of neighboring particles instead of solving the linear system of equations. Finally in dealing with two phase or multi-phase fluid flow, SPH does not require tracking the boundaries and it can model different fluid using separate particles. For the extension to solid mechanics, the main advantage of SPH is the possibility of tackling large local distortion comparing with grid-based methods. Another merit of SPH is inherent because of its mesh free nature. These features have been exploited in plenty of applications such as metal forming, high die casting, fracture and fragmentation and so on [32-35].

As mentioned before, due to the SPH inherent features, it has been successfully applied to problems in astrophysics, fluid and solid mechanics. Here we want to summarize the advantages of the SPH method based on comparing with the traditional grid based numerical methods. Firstly the concept of SPH is simple. With the help of a few basic assumptions, all of the equations can be derived from physical principles with self-consistence. Secondly, the feature of adaptivity in SPH shows great simplicity in solving changes in density and flow morphology without the complicated procedure of mesh refinement in grid based methods. Thirdly, the free surface, material interface, and moving boundaries can be traced naturally in SPH while present large difficulties for grid based methods. Fourthly, without using the mesh or grid, the large deformations are able to be handled straightforwardly. Therefore SPH method is an ideal choice for modeling application in high energy phenomena such as explosion, underwater explosion and high velocity impact (HVI). Fifthly, because the SPH method is similar to the molecular dynamics, so that it is possible to apply it to deal with complex problems in biophysics and biochemistry. Finally, SPH is suitable for problems which do not involve continuum. Such phenomena includes bio-engineering and nanometer-engineering at nanometer scale, astrophysics at astronomic scale.

As we all know, each numerical method has its own pros and cons. During the development of SPH method, some drawbacks of it have also been identified. First of all, the approximation of a physical quantity in SPH method involves a summation over all SPH particles. As a matter of fact, not all particles make contribution and only the neighbour particles work for the summation according to the range of smoothed function. Consequently a portion of computation cost is used to construct the neighbour list in simulation. Secondly, the establishment

of initial conditions are not easy and requires some experience and experiments. Because a poorer particle deploying can lead to bad simulation results. Thirdly, the SPH algorithm is still developing and a lot of problems involving accuracy, stability, convergency and efficiency requires analysis. Unlike the well studied numerical method like finite difference method and finite volume method, SPH method is still not a mainstream use. Fourthly, it takes large computational time particularly in 3-D simulation. Fifthly, it is not easy in prescribing wall boundary conditions and even greater problems at open boundaries. Finally, it is difficult to deal with variable space resolution for incompressible flows.

We have known the merits and drawbacks of the SPH method. On one hand, it has low requirement on the particle distribution than the grid based methods, therefore it can avoid the accuracy destroy problems when the system subjected to big deformations. On the other hand, as a pure lagrangian method, it is able to avoid the problems which take place between Euler grid and material interface. Consequently it is very suited to high velocity impact problems. However as a new proposed numerical algorithm, a large number of properties require to be investigated. Before going further to them, a clear image of how does the SPH method work should be made.

1.5 Idea of SPH interpolation

The basic idea of SPH method is that for an arbitrary function $f(x)$, we have the trivial identity:

$$f(x) = \int f(x')\delta(x - x')dx'. \quad (1)$$

where the function $\delta(x - x')$ is Dirac delta function given by

$$\delta(x - x') = \begin{cases} \infty, & x = x' \\ 0, & x \neq x' \end{cases} \quad (2)$$

and dx' is the differential volume element. Now for the SPH method interpolation, we introduce the first kernel approximation. In this approximation, the Dirac delta function is substituted by a smooth kernel function $W(x - x', h)$ with finite support h , and the approximation of $f(x)$ is denoted by $\langle f(x) \rangle$

$$\langle f(x) \rangle = \int f(x')W(x - x', h)dx'. \quad (3)$$

where the kernel function is normalized,

$$\int W(x - x', h)dx' = 1. \quad (4)$$

and $W(x - x', h)$ tends to Dirac delta function when the length scale h tends to zero.

$$\lim_{h \rightarrow 0} W(x - x', h) = \delta(x - x'). \quad (5)$$

For the kernel approximation, there exists second order accuracy. If $f(x)$ is differentiable, we can obtain

$$\langle f(x) \rangle = \int f(x') W(x - x', h) dx' \quad (6)$$

$$\langle f(x) \rangle = \int [f(x) + (x' - x)f'(x) + (x' - x)^2 f''(x)] W(x' - x, h) dx' \quad (7)$$

$$\begin{aligned} \langle f(x) \rangle = f(x) \int W(x' - x, h) dx' + \int (x' - x) f'(x) W(x' - x, h) dx' \\ + r(h^2) \end{aligned} \quad (8)$$

where $r(h^2)$ represents the residual. We note that on the r.h.s of equation (8), the first term is the normalization condition. And for the second term, the kernel function $W(x' - x, h)$ is an even function, therefore $(x' - x)W(x' - x, h)$ is an odd function and the integral should be zero. Hence we have

$$\langle f(x) \rangle = f(x) + r(h^2). \quad (9)$$

From the above derivations, it is obvious that the SPH kernel approximation of any function is of second order accuracy.

Now we introduce the second particle approximation. In this approximation, the integral is represented by a summation over finite discrete points,

$$\langle f(x) \rangle = \sum_{i=1}^N f(x_i) W(x - x_i, h) \Delta x_i. \quad (10)$$

where Δx_i is the volume of point.

Considering a set of SPH particles such that particle b has mass m_b , density ρ_b , and position r_b , the interpolation for any physical quantity $A(\vec{r})$, $\langle A(\vec{r}) \rangle$ can be written as

$$\langle A(\vec{r}) \rangle = \sum_b \frac{m_b}{\rho_b} A(\vec{r}_b) W(\vec{r} - \vec{r}_b, h). \quad (11)$$

And for the gradient of $A(\vec{r})$, we can write from equation (2)

$$\nabla A(\vec{r}) = \nabla \int A(\vec{r}') W(\vec{r} - \vec{r}', h) d\vec{r}' \quad (12)$$

$$\nabla A(\vec{r}) = \int A(\vec{r}') \nabla W(\vec{r} - \vec{r}', h) d\vec{r}' \quad (13)$$

$$\nabla A(\vec{r}) = \int \frac{A(\vec{r}')}{\rho(\vec{r}')} \nabla W(\vec{r} - \vec{r}', h) \rho(\vec{r}') d\vec{r}' \quad (14)$$

$$\nabla A(\vec{r}) = \sum_b \frac{m_b}{\rho_b} A(\vec{r}_b) \nabla W(\vec{r} - \vec{r}_b, h). \quad (15)$$

If we want to calculate the density at position \vec{r}_a , we just replace A by the density ρ and the position \vec{r} by \vec{r}_a .

$$\rho_a = \sum_b m_b W(\vec{r}_a - \vec{r}_b, h). \quad (16)$$

According to the kernel approximation and the particle approximation, the SPH simulation of differential or partial differential equations can be derived. For the fluid dynamics, two famous kinds of equations are involved, which are the Euler equations and the Navier-Stokes equations. The Euler equations are a series of quasi-linear hyperbolic equations which govern adiabatic and inviscid flow. Meanwhile, the Navier-Stokes equations describe the motion of viscous fluid substances. In fact, the Euler equation can be taken as a particular Navier-Stokes equations without viscosity and thermal conductivity.

For the Euler equations of inviscid fluid flow, which are the rates of change of density, velocity and position, namely

$$\frac{d\rho}{dt} = -\rho \nabla \cdot \vec{v}, \quad (17)$$

$$\frac{d\vec{v}}{dt} = -\frac{\nabla P}{\rho}, \quad (18)$$

$$\frac{d\vec{r}}{dt} = \vec{v}. \quad (19)$$

For the continuity equation, we have obtained the SPH form of density as previous Eq. (15). Here another SPH form of it is derived

$$\frac{d\rho}{dt} = \vec{v} \cdot \nabla \rho - \nabla \cdot (\rho \vec{v}), \quad (20)$$

$$\nabla_a \rho = \sum_b m_b \nabla_a W_{ab}, \quad (21)$$

$$\nabla_a \cdot (\rho \vec{v}) = \sum_b m_b \vec{v}_b \nabla_a W_{ab}, \quad (22)$$

$$\frac{d\rho}{dt} = \sum_b m_b (\vec{v}_a - \vec{v}_b) \nabla_a W_{ab}. \quad (23)$$

For the equation of motion which was firstly derived by Lucy [20], Gingold and Monaghan [21], it has the following form,

$$\nabla_a P = \sum_b m_b \frac{P_b}{\rho_b} \nabla_a W_{ab}, \quad (24)$$

$$\frac{d\vec{v}_a}{dt} = -\frac{1}{\rho_a} \sum_b m_b \frac{P_b}{\rho_b} \nabla_a W_{ab}. \quad (25)$$

However this SPH form of force can not conserve the linear momentum exactly. It is clear that the force on particle a exerted by particle b is not equal and

opposite to the force on particle a due to particle b , namely,

$$\frac{m_a m_b P_b}{\rho_a \rho_b} \nabla_a W_{ab} \neq -\frac{m_a m_b P_a}{\rho_a \rho_b} \nabla_b W_{ab}, \quad (26)$$

$$\nabla_a W_{ab} = -\nabla_b W_{ab}. \quad (27)$$

From the equation (24), owing to $P_a \neq P_b$, they are not equal. And from the equation (25), the direction is not opposite. In order to conserve the linear momentum and be consistent with the Newton's third law, a new SPH formulation of the equation of motion was proposed by Gingold and Monaghan [36]. By virtue of the identity,

$$\frac{\nabla P}{\rho} = \nabla\left(\frac{P}{\rho}\right) + \frac{P}{\rho^2} \nabla \rho \quad (28)$$

and following the SPH interpolation rules,

$$\frac{d\vec{v}_a}{dt} = -\sum_b m_b \left(\frac{P_a}{\rho_a^2} + \frac{P_b}{\rho_b^2}\right) \nabla_a W_{ab}. \quad (29)$$

If we write $\nabla_a W_{ab} = \mathbf{r}_{ab} F_{ab}$, in which F_{ab} is a scalar function of $\mathbf{r}_a - \mathbf{r}_b$,

$$m_a m_b \left(\frac{P_a}{\rho_a^2} + \frac{P_b}{\rho_b^2}\right) \mathbf{r}_{ab} F_{ab} = -m_b m_a \left(\frac{P_b}{\rho_b^2} + \frac{P_a}{\rho_a^2}\right) \mathbf{r}_{ba} F_{ba} \quad (30)$$

It is apparent that in this form the momentum is conserved exactly. As a matter of fact, we can also deduct the equation of motion which keeps the momentum conserved from the Lagrangian. The Lagrangian for hydrodynamics is

$$L = \int \left(\frac{1}{2} \rho v^2 - \rho u\right) dV \quad (31)$$

Where u stands for the internal energy per unit mass. In the SPH representation,

$$L = \sum_b m_b \left(\frac{1}{2} v_b^2 - u_b\right). \quad (32)$$

Then the equation of motion can be derived from the Euler-Lagrangian equations

$$\frac{d}{dt} \left(\frac{\partial L}{\partial \mathbf{v}_a}\right) - \frac{\partial L}{\partial \mathbf{r}_a} = 0. \quad (33)$$

where

$$\frac{\partial L}{\partial \mathbf{v}_a} = m_a \mathbf{v}_a, \quad (34)$$

$$\frac{\partial L}{\partial \mathbf{r}_a} = \sum_b m_b \frac{\partial u_b}{\partial \rho_b} \bigg|_s \frac{\partial \rho_b}{\partial \mathbf{r}_a} \quad (35)$$

From the relation of thermodynamics, we have

$$\frac{\partial u_b}{\partial \rho_b} \bigg|_s = \frac{P_b}{\rho_b^2} \quad (36)$$

and according to the definition of density, we can get

$$\frac{\partial \rho_b}{\partial \mathbf{r}_a} = \sum_c m_c \nabla_a W_{bc} (\delta_{ba} - \delta_{ca}) \quad (37)$$

Then

$$\frac{\partial L}{\partial \mathbf{r}_a} = \sum_b m_b \frac{P_b}{\rho_b^2} \sum_c m_c \nabla_a W_{bc} (\delta_{ba} - \delta_{ca}), \quad (38)$$

$$\frac{\partial L}{\partial \mathbf{r}_a} = m_a \frac{P_a}{\rho_a^2} \sum_c m_c \nabla_a W_{ac} - \sum_b m_b \frac{P_b}{\rho_b^2} m_a \nabla_a W_{ba}, \quad (39)$$

$$\frac{\partial L}{\partial \mathbf{r}_a} = m_a \frac{P_a}{\rho_a^2} \sum_b m_b \nabla_a W_{ab} - \sum_b m_b \frac{P_b}{\rho_b^2} m_a \nabla_a W_{ba}, \quad (40)$$

$$\frac{\partial L}{\partial \mathbf{r}_a} = \sum_b m_a m_b \left(\frac{P_a}{\rho_a^2} + \frac{P_b}{\rho_b^2} \right) \nabla_a W_{ab}. \quad (41)$$

Finally we can get the equation of motion which is the same as equation (29).

To describe the motion of viscous fluid flow, the Navier-Stokes equations have the form

$$\frac{D\rho}{Dt} = -\rho \frac{\partial \mathbf{v}^\beta}{\partial \mathbf{x}^\beta}, \quad (42)$$

$$\frac{D\mathbf{v}^\alpha}{Dt} = \frac{1}{\rho} \frac{\partial \sigma^{\alpha\beta}}{\partial \mathbf{x}^\beta} + F, \quad (43)$$

$$\frac{De}{Dt} = \frac{\sigma^{\alpha\beta}}{\rho} \frac{\partial \mathbf{v}^\alpha}{\partial \mathbf{x}^\beta}. \quad (44)$$

where the superscripts α, β stand for the coordinate directions, F is the external force, the summation is taken over repeated indices. The total derivative $\frac{D}{Dt}$ is taken in the moving Lagrangian frame. The density ρ , velocity \mathbf{v}^α , the internal energy e and the total stress tensor $\sigma^{\alpha\beta}$ are related each other, only the coordinate \mathbf{x}^β and time t are independent. For the total stress tensor, it consists of two parts. One part is the isotropic pressure P and the other part is the viscous stress $\tau^{\alpha\beta}$

$$\sigma^{\alpha\beta} = -P\delta^{\alpha\beta} + \tau^{\alpha\beta}, \quad (45)$$

$$\tau^{\alpha\beta} = \mu \varepsilon^{\alpha\beta}, \quad (46)$$

$$\varepsilon^{\alpha\beta} = \frac{\partial \mathbf{v}^\beta}{\partial \mathbf{x}^\alpha} + \frac{\partial \mathbf{v}^\alpha}{\partial \mathbf{x}^\beta} - \frac{2}{3} (\nabla \cdot \mathbf{v}) \delta^{\alpha\beta}. \quad (47)$$

Applying the SPH interpolation to function and its derivative to N-S equations,

$$\frac{D\rho_i}{Dt} = \sum_j m_j \mathbf{v}_{ij}^\beta \frac{\partial W_{ij}}{\partial \mathbf{x}_i^\beta}, \quad (48)$$

$$\frac{D\mathbf{v}_i^\alpha}{Dt} = - \sum_j m_j \left(\frac{\sigma_i^{\alpha\beta}}{\rho_i^2} + \frac{\sigma_j^{\alpha\beta}}{\rho_j^2} \right) \frac{\partial W_{ij}}{\partial \mathbf{x}_i^\beta} + F_i, \quad (49)$$

$$\frac{De_i}{Dt} = \frac{1}{2} \sum_j m_j \left(\frac{P_i}{\rho_i^2} + \frac{P_j}{\rho_j^2} \right) \mathbf{v}_{ij}^\beta \frac{\partial W_{ij}}{\partial \mathbf{x}_i^\beta} + \frac{\mu_i}{2\rho_i} \varepsilon_i^{\alpha\beta} \varepsilon_i^{\alpha\beta}. \quad (50)$$

where \mathbf{v}_{ij} equals $\mathbf{v}_i - \mathbf{v}_j$.

Since the kernel function appears in both the kernel approximation and particle approximation, it is essential to spare some effort to investigate the kernel function and show some details of it. We have talked about some properties of the smoothing kernel function as mentioned before, including the normalization and tendency to Dirac delta function when smoothing length becomes zero. However, there exists more requirements for the kernel function in order to keep a good accuracy for the approximation.

1.6 Kernel function

In this section, some basic properties of kernel function are discussed. These contain the requirements of function which are to be kernel functions, the general form of kernel functions and the smoothing length h . Much of work are following the literature reviews [8,36].

1.6.1 Kernel properties

To be a smoothing kernel function, some requirements must be satisfied. Firstly, the kernel function is normalized over the support domain, which is displayed by equation (4). Secondly, it should have compact support, which means that the kernel function has a cut-off distance. Mathematically it can be expressed as

$$W(x - x', h) = 0, |x - x'| > \kappa h \quad (51)$$

where κ determines the range of the specified kernel function and the support domain at point x is $|x - x'| \leq \kappa h$. With this requirement it can save the computation effort and improve the efficiency. Thirdly, the kernel function should be non-negative over the support domain, because it ensures the physical meaning of some quantities. For example, as the density interpolation is defined by equation (16), a negative kernel function may lead to a negative density which is not desirable in physics. Fourthly, the kernel function value for a particle should monotonically decrease as the distance between two particles increase. This is natural because it reflects the general physics picture that the neighbouring particles make greater contribution than the distant particles. Finally, if the smoothing length h tends to zero, the kernel function equals the

Dirac delta function. In this case, the approximation of function value reproduce the original function exactly, namely, $\langle f(x) \rangle = f(x)$.

1.6.2 Kernel general forms

A natural choice that satisfies all of the above properties is the Gaussian kernel function,

$$W(\mathbf{r} - \mathbf{r}', h) = \frac{\sigma}{h^d} \exp \left[-\frac{(\mathbf{r} - \mathbf{r}')^2}{h^2} \right] \quad (52)$$

where d denotes the number of spatial dimensions and σ is a normalization factor given by $\pi^{-\frac{1}{2}}, \pi^{-1}, \pi^{-\frac{3}{2}}$ in one, two, and three dimensions. Owing to the derivative of the Gaussian kernel function is smooth even at higher order, there exists good stability property. However although the contribution from neighbouring particle rapidly decrease with the increasing distance, it spans the whole spatial domain, which requires a lot of computation cost. As a matter of fact, a kernel function with compact support is required in numerical simulation. A set of kernel functions which are similar to the Gaussian kernel function but have compact support are proposed. One of the most commonly used is the cubic spline kernel function which is given by Monaghan [36],

$$W(q) = \begin{cases} \sigma \left[1 - \frac{3}{2}q^2(1 - \frac{q}{2}) \right], & 0 \leq q < 1 \\ \frac{\sigma}{4}(2 - q)^3, & 1 \leq q < 2 \\ 0, & q > 2 \end{cases} \quad (53)$$

where σ is a dimensional normalizing factor given by

$$\sigma = \frac{2}{3h^1}, \dim = 1, \quad (54)$$

$$\sigma = \frac{10}{7\pi h^2}, \dim = 2, \quad (55)$$

$$\sigma = \frac{1}{\pi h^3}, \dim = 3. \quad (56)$$

, $q = \frac{|\mathbf{r} - \mathbf{r}'|}{h}$ and h^1, h^2, h^3 stands for the smoothing length in different dimensions. From the definition the cubic spline is truncated at $2h$, therefore it has compact support of size $2h$. It has smooth first derivative but the second derivative is a piece wise function. In order to obtain smoother kernels and increase the compact support domain, the higher order interpolation kernel functions have been invented. For the quartic spline function,

$$w(q) = \sigma \begin{cases} (2.5 - q)^4 - 5(1.5 - q)^4 + 10(0.5 - q)^4, & 0 \leq q < 0.5 \\ (2.5 - q)^4 - 5(1.5 - q)^4, & 0.5 \leq q < 1.5 \\ (2.5 - q)^4, & 1.5 \leq q < 2.5 \\ 0. & q \geq 2.5 \end{cases} \quad (57)$$

with normalization factor $\sigma = \frac{1}{24}, \frac{96}{1199\pi}, \frac{1}{20\pi}$ and quintic kernel spline function

$$w(q) = \sigma \begin{cases} (3-q)^5 - 6(2-q)^5 + 15(1-q)^5, & 0 \leq q < 1 \\ (3-q)^5 - 6(2-q)^5, & 1 \leq q < 2 \\ (3-q)^5, & 2 \leq q < 3 \\ 0. & q \geq 3 \end{cases} \quad (58)$$

with normalization factor $\sigma = \frac{1}{120}, \frac{7}{478\pi}, \frac{1}{120\pi}$. These higher order spline kernel functions lead to smoother derivatives and contain bigger size of support domain, which can reduce the sensitivity of kernel to particle disorder distribution.

1.6.3 Kernel smoothing length

The smoothing length h determines the resolution and the number of neighbor particles that contribute to the property at a particle. For this reason, it is crucial that has large influence on the efficiency and accuracy of SPH algorithm. For instance, a smaller h means a smaller number of particles summation. However, how to choose an appropriate value of smoothing length becomes a problem. One one hand, if the smoothing length is too small, then few particles are contributed to the interpolation. Large fluctuations will take place because it is not smoothing enough and the SPH algorithm will only model the single particle motion instead of the fluid flow. On the other hand, if the smoothing length is selected too big, then details will be smoothed out which reduces the accuracy.

The smoothing length has changed a lot in the process of developments through many literatures. The basic form of smoothing length h is selected in the beginning and kept constant in the calculations. The magnitude of it is usually comparable to the particle spacing. However this is not always desirable. Therefore the varying forms of smoothing length appears. First, it can change with every time step. As a matter of fact, this form is similar to the basic form and not large modification need to be made. It is able to be expressed as

$$h = \frac{1}{\langle \rho \rangle^{1/d}}, \langle \rho \rangle = \frac{1}{N} \sum_b \rho_b \quad (59)$$

where d is the number of dimensions and N is the number of particles by Monaghan [37].

Second, it varies for every particle. This is due to the fact that h is too large for the areas where particles are highly focused and h is too small for other areas in which particles are extremely sparse. So that h varying for each particle is proposed, yielding h_i for particle i . In this case, how to keep the momentum conservation requires to be considered. In order to guarantee this condition, the symmetric kernel is suggested. One way is to replace the h in the standard kernels by a symmetric combination of the two smoothing lengths of the two particles.

$$W(u, h) = W(u, \frac{h_i + h_j}{2}) \quad (60)$$

The alternative way is to make use of the average of two kernels which have smoothing lengths h_a and h_b respectively.

$$W(u, h) = \frac{W(u, h_i) + W(u, h_j)}{2} \quad (61)$$

There are some important aspects involved in the SPH method, including the accuracy, efficiency, stability and consistency. First of all, we are going to talk about the numerical instability such as tensile instability which usually appears in the solid dynamics. In mathematical numerical analysis, numerical stability is a generally desirable property of numerical algorithms. Usually the definition of it depends on the context concerned. One is numerical linear algebra and the other involves the solution for ordinary and partial differential equations by discrete approximation. The latter is exactly our interest.

1.7 Tensile instability

Let us refer to the example given by Price [37], such a equation of motion as

$$\frac{d\mathbf{v}_a}{dt} = - \sum_b m_b \left(\frac{P_a - P_0}{\rho_a^2} + \frac{P_b - P_0}{\rho_b^2} \right) \nabla_a W_{ab}. \quad (62)$$

Taking into account the case in one dimension, the kernel derivative with respect to the coordinate is

$$\begin{cases} \frac{\partial W_{ab}}{\partial x_a} > 0, & x_a > x_b \\ \frac{\partial W_{ab}}{\partial x_a} < 0, & x_a < x_b \end{cases} \quad (63)$$

When $P_0 > P$ the particles will move towards each other and clump together. We can call this phenomenon as "tensile instability".

For the measurement of tensile instability, Swegle et al. proposed the following criterion [39],

$$W_{\alpha\alpha} \sigma^{\alpha\alpha} > 0 \quad (64)$$

where $W_{\alpha\alpha}$ is the second derivative of kernel function, and $\sigma_{\alpha\alpha}$ is the stress tensor. For example, the derivative of the cubic spline function is always positive when the $\frac{\tau}{h}$ is from 1 to 2. During this support domain, the $W_{\alpha\alpha} \sigma^{\alpha\alpha}$ will always be positive and the tensile instability shows up. In order to illustrate this kind of physical phenomenon caused by tensile instability, a simple test have been given. In a two dimensional space, the boundary particles are fixed and the particles inside are free to move with the external perturbation. Theoretically it will take a long time for a particle moving over a single particle spacing. However for the SPH formulation of system under tensile stress with the use of cubic kernel function, the interior particles will clumped together and form a void, which means that the system demonstrates a numerical instability. This phenomenon can be shown clearly in Fig. 22 in the work by Swegle [38],

In order to overcome the tensile instability, Chen and his co-workers proposed the corrective smoothed particle method (CSPM) [39]. Here one of the examples

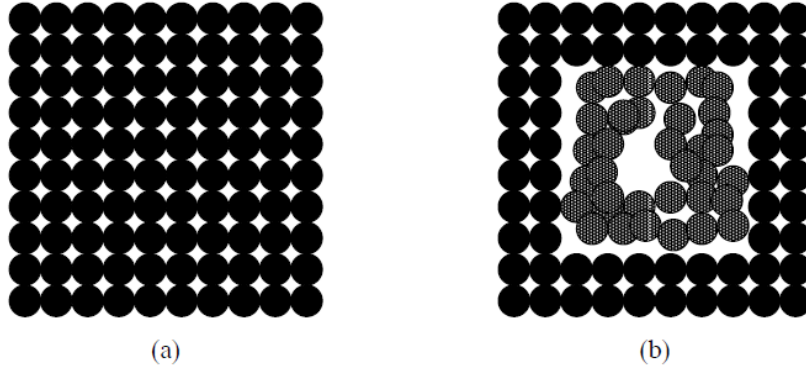


Figure 1: In a two dimensional space, the plot (a) shows the initial particle distribution, the plot (b) displays the particle distribution after some time steps under the effect of tensile instability. The plot is excerpted from the reference [38].

is introduced to illustrate how does the CSPM work. Taking into account an initially stressed bar perturbed by a velocity at the central particle. For the conventional SPH, the perturbation grew exponentially for those with initial tensile stress. Under the method of CSPM, the displace of the perturbed particle is making comparison with the results of finite element method, which is shown by the Fig. 2

Morris advised making use of particular smoothing kernel function owing to the fact that the tensile instability is closely related to the second order derivative of it [40]. In recent years, an artificial force has been proposed by Monaghan and his colleagues to stabilize the computation [41,42].

In the notes written by M.B Liu [43], he attributed the tensile instability to the fact that the particle approximation are carried out only over the particles that represent the whole system, which can cause not enough "sampling" points for setting up equations then lead to numerical instability problem.

We have pointed out the SPH method is suited to deal with a system which is not a continuum. For example, for the interaction of two stars, these material properties such as mass, energy and momentum can be transported accurately by the SPH particles when the stars move through space. However, for the traditional grid based method like finite difference method, its calculation will introduce errors owing to the advection through the grid. Moreover, it needs a large number of cells to cover the space where the stars are moving. In the following, we will introduce some applications of SPH to discrete system.

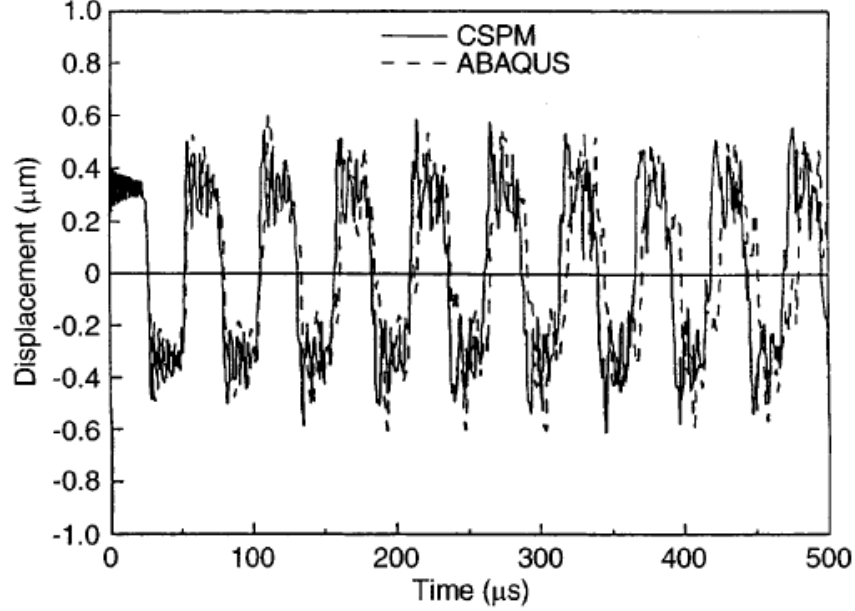


Figure 2: Displacement history of the perturbed particle for the bar under initial tensile stress. The plot is excerpted from the reference [39].

1.8 SPH for discrete system

As pointed by Volker Springel [44], the SPH method allows an intuitive and simple formulation of hydrodynamics which has good conservation properties and is capable of being coupled to self-gravity easily and highly accurately. The Lagrangian feature of SPH method makes it adjust its resolution to the clumping of matter, which makes it ideal for many problems in astrophysics. Here we are going to talk about some detailed examples which the SPH method has been applied successfully.

The first example is mass exchanging white-dwarf binaries studied by Benz [45]. It is well-known that white dwarfs are the end stage of stars evolution for low mass stars. The typical mass density is about $10^6 g/cm^3$. With this large density quantum effects are considered and the pressure is mainly from degenerate electrons.

From the equation of state, we know that the pressure is independent of the temperature and we can get the mass radius relation for the star

$$R = cM^{-\alpha}, \alpha = \alpha(M) > 0, c = const. \quad (65)$$

So that if the star has bigger mass then it has smaller radius. Now making the assumption that there are two stars coming close enough owing to the gravi-

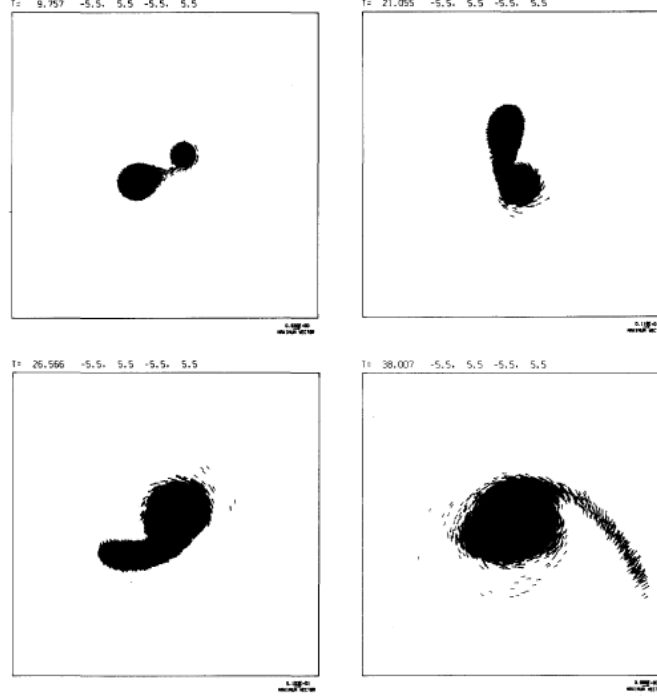


Figure 3: Evolution of a double white dwarf binary system consisting of 1.2 and 0.9 solar masses. The plot is excerpted from the reference [45].

tational radiation. Subsequently the less massive star would lose mass to the primary and its radius would increase. However the total angular momentum of the system is conserved, the secondary will move outside along with the exchange of mass, which eventually causes a decrease in the amount of mass transferred. To illustrate the evolution of two stars mass exchange, setting up two systems, one with a primary star of 1.2 solar mass and a secondary of 0.9 solar mass, and another with a secondary of 0.4 solar mass with the same primary. In the SPH method, the primary star has been simulated by 3000 particles and the secondary with 4000 particles. And the velocity of all the particles has been projected into the orbital plane, as shown by Fig.1 and Fig.2 in this paper [45]. From these two plots, the overflow begins at slow rate but the end points of the two systems are clearly different. In the case of a bigger mass of the secondary the whole star is disrupted and spread out in a form of disk-like structure around the primary. However, for the smaller mass of the secondary, the mass exchange goes on at a slow rate and eventually stop which are not shown here.

Another example is about the collision stripping of Mercury's mantle [45].

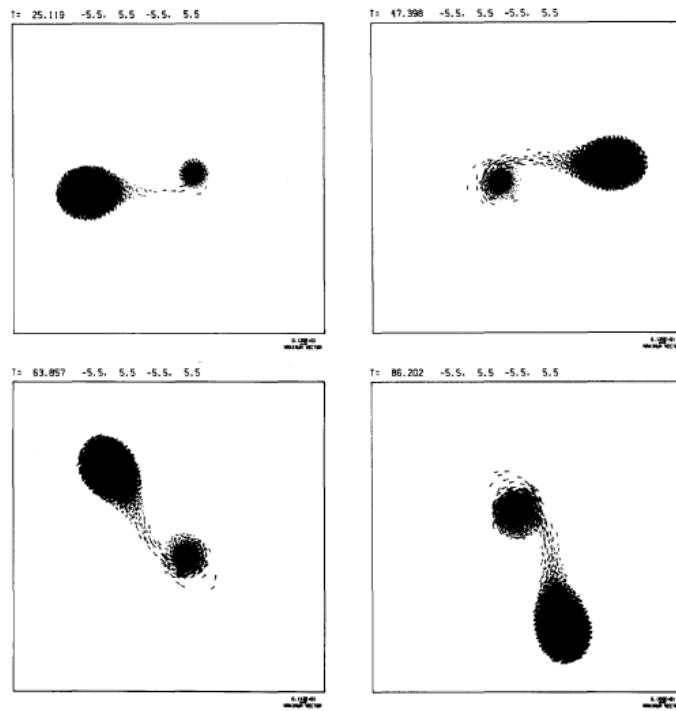


Figure 4: Evolution of a double white dwarf binary system consisting of 1.2 and 0.4 solar masses. The plot is excerpted from the reference [45].

It is well known that the mean density of the earth is around $4.5g/cm^3$ and that of Mercury is about $5.3g/cm^3$ which is anomalously high. For this high mean density, Mercury must have an high ratio between iron and silicate. A lot of hypotheses have been suggested and a particular one is that one or more collisions with Mercury cause plenty of silicate blowing off from the original Mercury proto planet. Why do people think in this way? Because the escape velocity from Mercury is very low and relative velocities between colliding objects are rather high, so that one collision can result in plenty of material loss. Here a check whether one can obtain a selective loss of material was conducted, where the silicate mantle is prior to the iron core for the loss, by running these simulations. In their work, the equation of state CHART D/CSQANEOS was used, and tables of equation of state data by requiring the specific internal energy was built as one entry in code. Considering a head-on collision at $20km/s$ between a proto mercury of 2.25 times the mass of present Mercury and an impact of 1/6 its mass, which was displayed in FIG.3. Moreover an off-axis collision is also shown, in which the collision velocity is increased to $35km/s$ in order to produce the same amount of damage to the planet shown in Fig. 4. In these snapshots, 4000 SPH particles are used and 1000 of them are for the impactor. The collision clearly leads to the disruption of the planet and most of the material loss spread out in a plane which is perpendicular to the collision axis. By comparison with the off-axis collision, shocks are greater in the head-on collisions. The results were in good agreement with theory.

Considering the SPH method as a numerical algorithm, its efficiency should be studied and discussed. Numerical efficiency is usually related to the computational resource usage. For maximum efficiency, resource usage tends to be minimized such as high speed, minimum memory usage. An algorithm is taken into account efficient if its resource consumption is at or below some acceptable level, which means that it will run in a reasonable amount of time on an available computer.

1.9 Efficiency of SPH

Now we are going to talk about the efficiency of the SPH method. First of all let us focus on the SPH simulation of free surface flow. As we all know, free surface flow is common and important in industry and environment, however it is not easy to be tackled owing to the arbitrary moving surface. For the modeling of boundary, SPH shows great adaptivity and flexibility comparing with the grid based numerical approaches. In the work done by Monaghan [46], the boundary was modeled by SPH particles and the results for dealing with the free surface flow are better which are compared with those of MAC method.

We know that the real boundaries are made of atoms or molecules. For the boundary condition that the velocity normal to the boundary becomes zero at the boundary, it can be replaced by a boundary force in the equation of motion. There exists a short range of atomic dimensions for real boundary force, therefore correspondingly a range close to the resolution length of the calculation appear in the artificial force. And the boundary particles are able

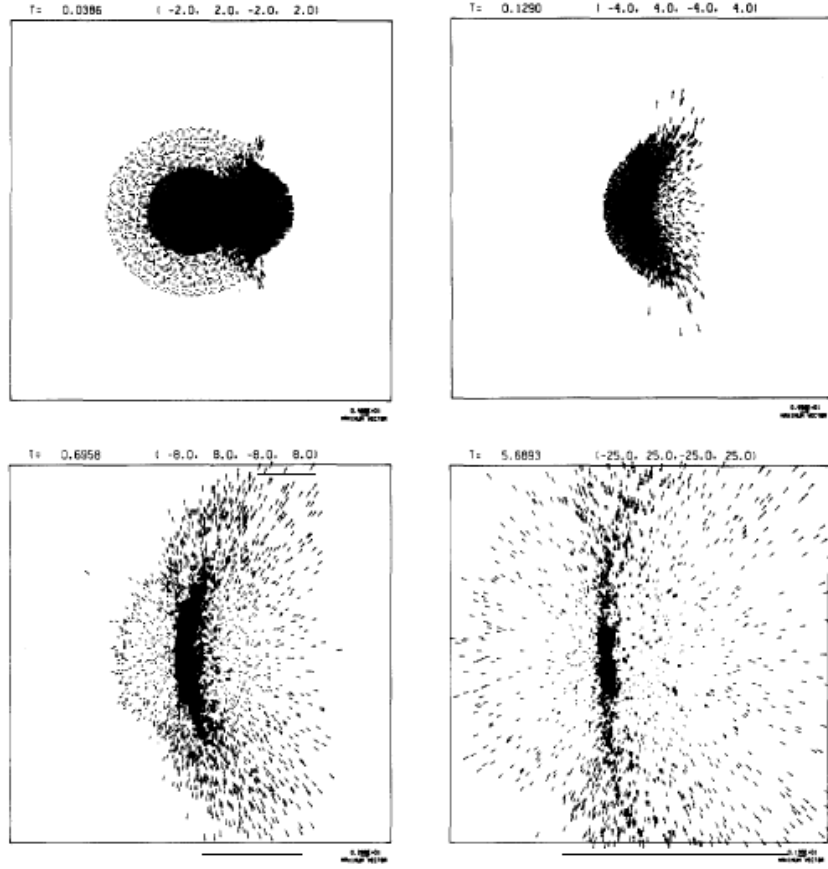
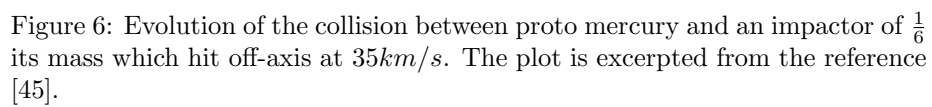


Figure 5: Evolution of the collision between proto mercury and impactor of $\frac{1}{6}$ its mass which hit head-on at $20km/s$. The plot is excerpted from the reference [45].



to be established to follow any fixed or moving boundary. Here it is taken into account that these boundary particles exert central force on fluid particles and the form of force was following the molecules forces. For example, if the boundary and fluid particle are separated by a distance r the force per unit mass $f(r)$ has the form

$$f(r) = D \left[\left(\frac{r_0}{r} \right)^{p1} - \left(\frac{r_0}{r} \right)^{p2} \right] \frac{\vec{r}}{r^2}. \quad (66)$$

where if $r > r_0$ it vanishes and the constant $p1$ is always bigger than $p2$ to make sure the force is purely repulsive. The length scale r_0 is taken as the initial spacing between the particles and the coefficient D was selected by taking count of the physical configuration.

There are some tests like breaking dam, a bore, the simulation of a wave maker and the propagation of waves towards a beach. Here the flow of an elliptical drop in two dimensions is illustrated. The SPH simulation results are shown by Fig. 1 of this article, here shown as Fig. 7.

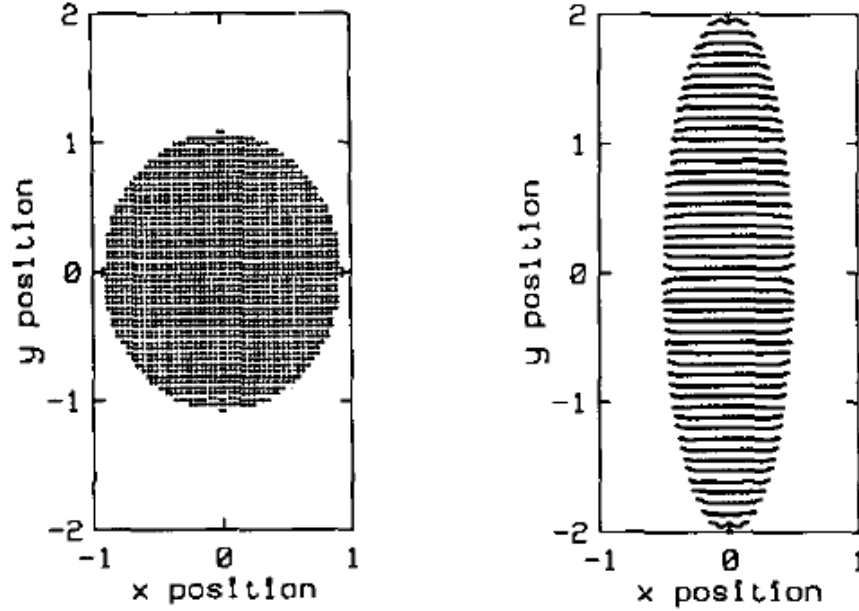


Figure 7: The particle positions for the evolution of an elliptical drop at two instants $t = 0.0008$ and $t = 0.0082$, which shows the system evolves from a circle to a narrow ellipse. The plot is excerpted from the reference [46].

The results display that SPH method is capable to be used to simulate the free surface flows and the approximation of boundaries by boundary particles is

satisfactory. The MAC method makes use of the particles to define the surface and finite differences to solve the hydrodynamic equations, which is a robust numerical methods. However, it is still complicated to program. The SPH method overcomes this difficulty, which is easy to carry out and simulate.

The application to the fluid flow is just a simple test, and many aspects about shocks and shock tube phenomena have been investigated by pioneers. In physics, a shock wave is a kind of propagation disturbance. It is formed when a wave moves faster than the local speed of sound in a fluid. A shock wave carries energy and is able to propagate through a medium, but there exists an abrupt, discontinuous change in pressure, temperature and density of the medium.

After the discussion of efficiency, the accuracy and precision of the SPH algorithm are essential to be addressed. For the definition of accuracy, it is usually taken as a measure of statistical bias, which is a difference between the result and a “true” value. And the precision is a description of random errors and a measure of statistical variability. The analysis and discussion of accuracy and precision shows great significance particularly for a numerical algorithm.

1.10 different kernel leads to distinct accuracy

As follows, some examples which involves the accuracy and precision of the SPH method are given. We have read the work done by Monaghan and Gingold 1983 [47]. In their work, the particle method SPH was applied to one dimensional shock tube problems by including an artificial viscosity into the equations of motion. They talked about the standard artificial viscosity and proposed a new term of viscosity, and they also used the gaussian interpolating kernel and super gaussian kernel in SPH method to compare with the results which were obtained by finite difference methods.

An artificial viscosity described by viscous pressure q is able to be incorporated into the equations of motion by replacing p by $p+q$. For the viscous pressure, two forms of it have been represented, which are the Von Neumann-Richtmyer viscous pressure and bulk viscosity.

For the one dimensional shock tube problem for a perfect gas, the interpolating gaussian kernel and super gaussian are used respectively. Following the equation of motion and combining with the equation of state, the numerical results are shown by Fig.1 from the paper, here as shown in Fig. 8.

It is seen that the numerical results agrees well with the exact solution for pressure and density, but for velocity profile it appears oscillations. So why does this phenomenon take place? The reason has been discussed in detail in the introduction of this paper. Because the artificial viscosity in usual way can not dampen the irregular motion on the scale of the particle separation since the scale is smaller than the resolution of the interpolating kernel function.

So a new form of artificial viscosity was proposed to improve the situation. With this new viscous pressure, the numerical results are displayed by Fig.2 and Fig.3 in the paper by using the Gaussian and super Gaussian kernel functions, here demonstrated by Fig. 9 and Fig. 10. The form of Gaussian and super

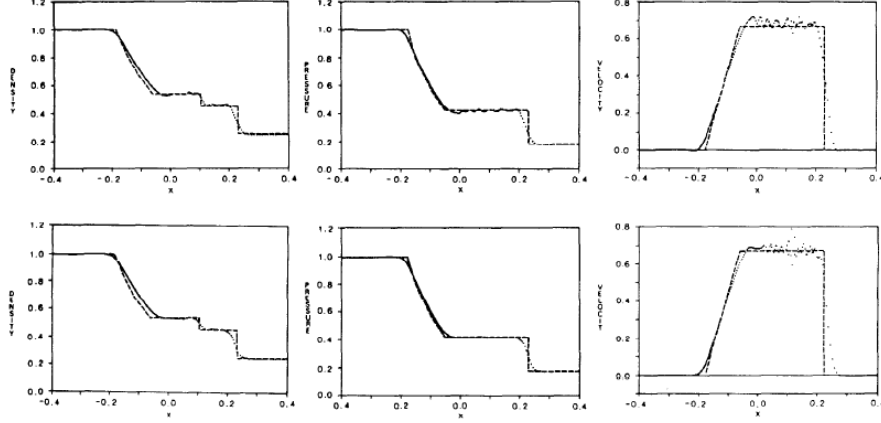


Figure 8: Pressure, density and velocity profiles for the shock tube problem. The upper frames are for the Von Neumann-Richtmyer viscosity, the lower frames are for the bulk viscosity. The exact results are shown by - - -, which the SPH results are shown by dots and full lines. The plot is excerpted from the reference [47].

Gaussian kernel functions are

$$W(u, h) = \frac{1}{h\sqrt{\pi}} \exp^{-u^2/h^2} \quad (67)$$

and

$$W(u, h) = \frac{1}{h\sqrt{\pi}} \exp^{-u^2/h^2} \left(\frac{3}{2} - u^2/h^2 \right) \quad (68)$$

Therefore it is easy to find that for the velocity the oscillation vanishes and the results show good agreement with the exact solution. From this paper, we can make sure that the SPH method can be applied to deal with the shock tube problem successfully and it has the advantage that it is easy to carry out and be generalized to more than one dimension conditions. By comparing the Fig. 2 and Fig. 3, it is clear that the results of standard gaussian kernel are inferior to those of super gaussian. These results are expected because the standard gaussian kernel interpolation with lower accuracy than the super gaussian kernel.

1.11 SPH extension to three dimensional condition

In the past, simple tests have only been limited to one dimension condition. However, SPH is an algorithm easy to carry out and simulate. It is significant to extend it to solve problems involving multi dimensional circumstances. Here

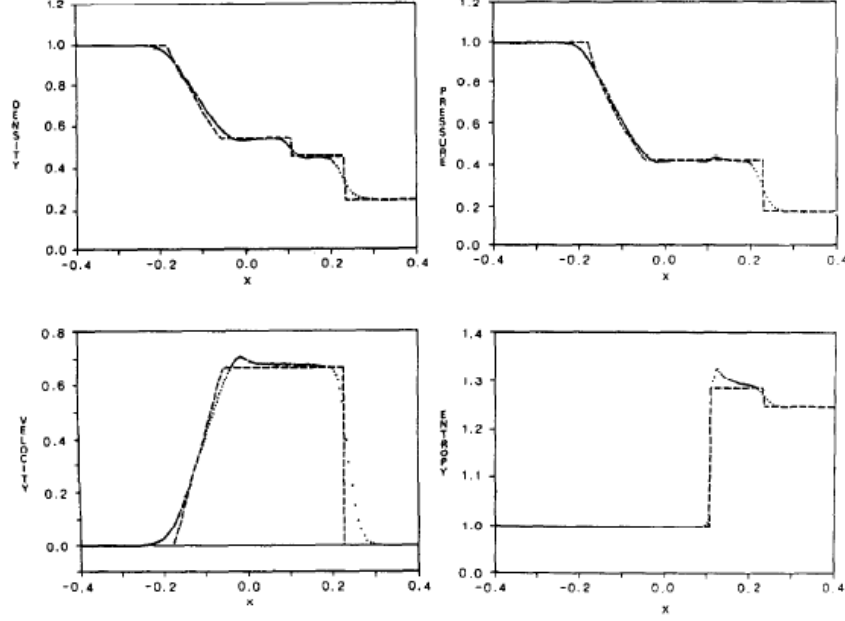


Figure 9: Density, pressure, velocity and entropy profiles for the shock tube problem. The exact results are shown by - - -, which the SPH results are shown by dots and full lines. The kernel is Gaussian. The plot is excerpted from the reference [47].

we are going to talk about wave structure interaction which has been studied in detail by Crespo AJC, Gomez-Gesteira M, and Dalrymple RA [48]. It is a three dimensional numerical simulation of large waves mitigation with a dike. The force and moment exerted on the structure are analyzed in terms of the dike height and the distance between the dike and the structure.

First of all, let us see some SPH validations which describe the wave profiles, velocities and forces exerted by the waves on the structures, which are shown by Fig. 1, Fig. 2 and Fig. 3 in this article, here illustrate by Fig. 11, Fig. 12 and Fig. 13

From these diagrams, we know that the SPH method is applied successfully to multi dimensional condition and satisfactory to handle wave structure interaction. and we can also see the wave colliding with the dike by Fig. 10 in their paper [48], here shown by Fig. 14.

SPH is a pure lagrangian method which permits the study of discontinuities in the flow without limitations comparing with the presence of a grid. In above examples, the formation of a jet over a dike and its interaction with the fluid surrounding the dike can be treated naturally. Additionally the SPH model can

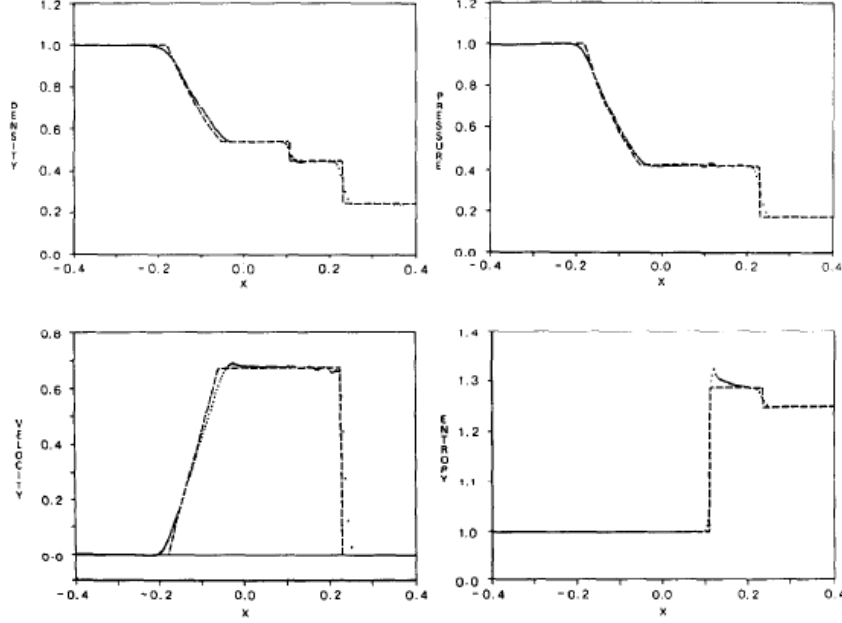


Figure 10: Density, pressure, velocity and entropy profiles for the shock tube problem. The exact results are shown by ---, which the SPH results are shown by dots and full lines. The kernel is super Gaussian. The plot is excerpted from the reference [47].

track the origin of water at certain location inside the medium. On the other hand, for the investigation of wave structure interaction, the flow information can be provided, which is able to predict the damage when wave colliding the dike and correspondingly make some measures to mitigate the impacts.

1.12 SPH application to solid

Over the past few years, SPH for the simulation of solids has been developed which can be found in the work [49-51]. Here we are going to briefly introduce a recent work which deals with the specific solid problem fracture [52]. As we all know, fracture is dependent on the whole stress history of a given piece of material. For a Lagrangian approach, where the frame of reference is attached to the material, it is a natural framework for dealing with these equations of such phenomenon. Euler method shows large difficulties of following accurately stress history and the development of cracks. However, conventional Lagrangian approach is unable to solve large material deformations because deformation of the grid severely affects the accuracy of derivatives. Given any spatial distribu-

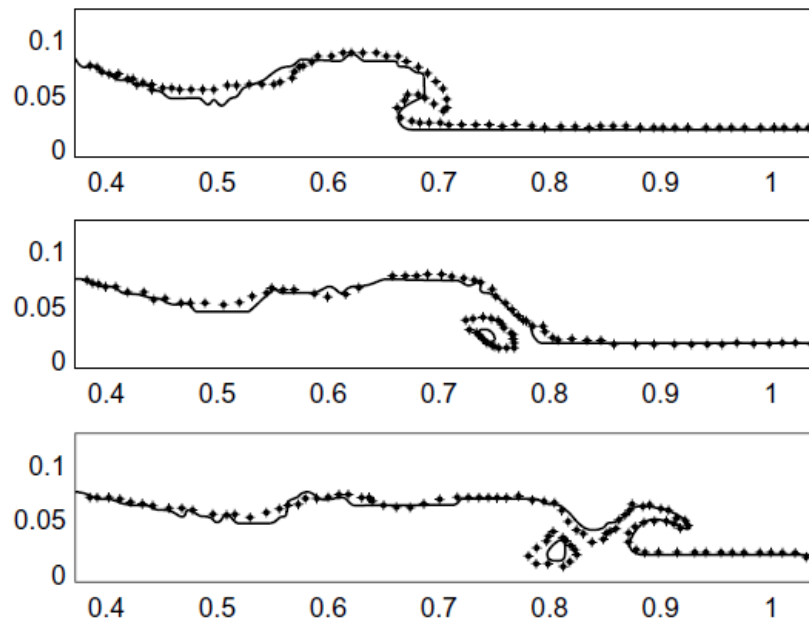


Figure 11: The comparison for 2D validation between numerical (solid line) and experimental (dots) wave profiles. The plot is excerpted from the reference [48].

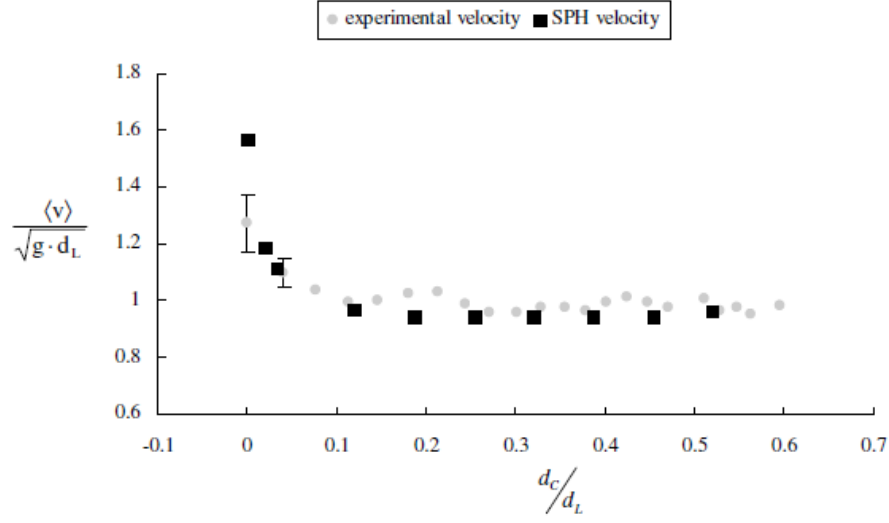


Figure 12: The comparison for 2D validation between numerical (dark squares) and experimental (light dots) wave velocities profile which are averaged during the first 3m of the tank. The plot is excerpted from the reference [48].

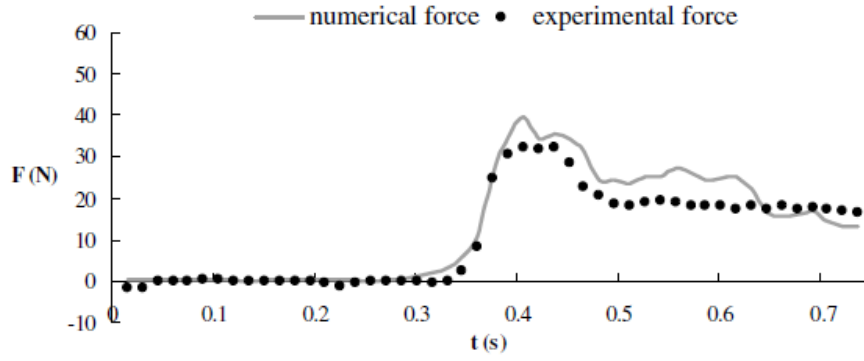


Figure 13: The comparison for 3D validation between numerical (solid line) and experimental (dark circles) forces profiles which are exerted by the incoming wave on the structure. The plot is excerpted from the reference [48].

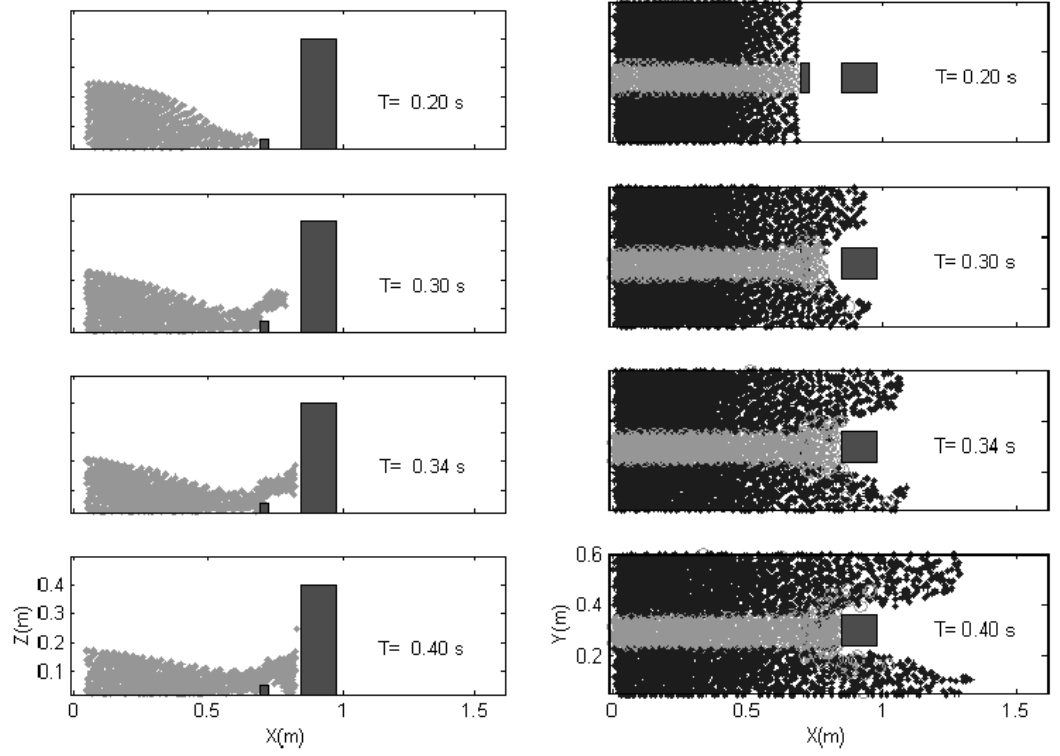


Figure 14: The collision between water and disk from the lateral and top view. The plot is excerpted from the reference [48].

tion of these points, the SPH technique is able to carry out the computation of spatial derivatives without grids. Once the spatial derivatives have been evaluated and the forces have been determined, time integration can be done subsequently in the usual way. Thus, SPH offers an interesting alternative to traditional grid-based methods.

In their work a new fracture model is developed which is based on the nucleation of earliest flaws. The number density of it is given by a Weibull distribution. The detailed implementation of equations into the SPH framework has been discussed. In order to show the success of SPH method and also the strengths and weaknesses of the new model, a comprehensive tests have been done. These tests include a tensile rod, laboratory impact experiments on basalt spheres and laboratory crater experiments. The detailed numerical results have been shown by figures one to five in the paper [52].

As a matter of fact, the SPH method simulation involves a lot of aspects. During their work, these implementation include the discovery of equilibrium solutions of deformed solid beams, the check for the correct propagation of elastic waves and simulation of the bouncing of tennis balls. Anyway the new model shows great power in handling the propagation of a single crack in a simple tensile rod. On the other hand, it demonstrates the SPH method can be successfully applied to fracture problems. Subsequently a important kind of problem appearing in engineering is the high explosive detonation. And the underwater explosion as one of this typical phenomenon will be discussed in the following.

1.13 SPH application to underwater explosion

The underwater explosion is from high explosive detonation which involves a sequence of complicated energetic processes. Due to its large deformations, large inhomogeneities and moving interface, it is difficult to use the traditional grid-based numerical methods like finite difference method and finite volume method. Owing to the mesh free nature of SPH method, it overcomes the difficulties and can be successfully applied to this physical phenomenon. The work done by M.B.Liu and G.R.Liu [53] has been focused on the detonation of the high explosive, the interaction of the explosive gas with the surrounding water, and the propagation of the underwater shock.

The underwater explosion are considered as two parts, one is the detonation process from the high explosive, another is the interaction process between the produced gas and the surrounding water. For the detonation process, it can be taken as the propagation of the reactive wave which passes through the explosive with uniform detonation velocity. If the intense heat and pressure are initiated, the detonation process is sufficient to be maintained. In underwater explosions, the produced gas and the water can be regarded as inviscid and compressible and the explosive process is adiabatic. With these assumptions, Euler equation coupled with related equation of state can be used to model the

explosive process,

$$\frac{d\rho}{dt} = -\rho \nabla \cdot \mathbf{v}, \quad (69)$$

$$\frac{d\mathbf{v}}{dt} = -\frac{\nabla P}{\rho}, \quad (70)$$

$$\frac{du}{dt} = -\frac{P}{\rho} \nabla \cdot \mathbf{v}, \quad (71)$$

$$P = P(\rho, u). \quad (72)$$

where \mathbf{v}, u, ρ, P and t are velocity, internal energy, density, pressure and time respectively. The first three equations are demonstrating the conservation of mass, momentum and energy. And the last equation is the equation of state. Here the standard Jones-Wilkins-Lee equation of state is used,

$$P = A(1 - \frac{\omega\eta}{R_1})e^{-\frac{R_1}{\eta}} + B(1 - \frac{\omega\eta}{R_e})e^{-\frac{R_2}{\eta}} + \omega\eta\rho_0 E \quad (73)$$

Where η is ration of the detonation products density to the initial density of the original explosive, E is the specific internal energy per unit mass and A, B, R_1, R_2, ω are coefficients. By virtue of the kernel and particle approximation of SPH, the equations above can be written as

$$\frac{d\rho_i}{dt} = \sum_j m_j (\mathbf{v}_i - \mathbf{v}_j) \cdot \nabla_i W_{ij}, \quad (74)$$

$$\frac{d\mathbf{v}_i}{dt} = -\sum_j m_j \left(\frac{P_i}{\rho_i^2} + \frac{P_j}{\rho_j^2} + \Pi_{ij} \right) \nabla_i W_{ij}, \quad (75)$$

$$\frac{du_i}{dt} = \frac{1}{2} \sum_j m_j \left(\frac{P_i}{\rho_i^2} + \frac{P_j}{\rho_j^2} + \Pi_{ij} \right) (\mathbf{v}_i - \mathbf{v}_j) \cdot \nabla_i W_{ij}, \quad (76)$$

$$\frac{dx_i}{dt} = \mathbf{v}_i. \quad (77)$$

Now there are some tests shown in this paper. First it is about the one dimensional TNT slab detonation, where a 0.1 long TNT slab detonates at one end of the TNT slab. The density, pressure and velocity transients along the TNT slab are

$$P = \frac{16}{27} \frac{\rho_0}{D} \left(\frac{\mathbf{x}}{2t} + \frac{D}{4} \right)^3 \quad (78)$$

$$\rho = \frac{16}{9} \frac{\rho_0}{D} \left(\frac{\mathbf{x}}{2t} + \frac{D}{4} \right) \quad (79)$$

$$\mathbf{v} = \frac{\mathbf{x}}{2t} - \frac{D}{4} \quad (80)$$

where the parameter D is taken as 10^5 and ρ_0 is the initial density of the high explosive TNT.

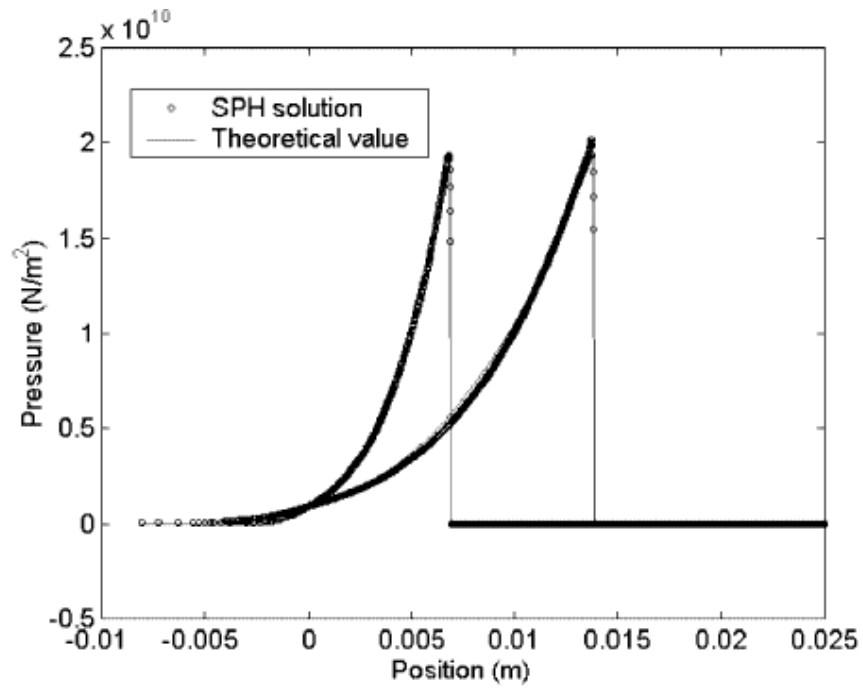


Figure 15: Pressure profiles along the TNT slab during the detonation process. The plot is excerpted from the reference [53].

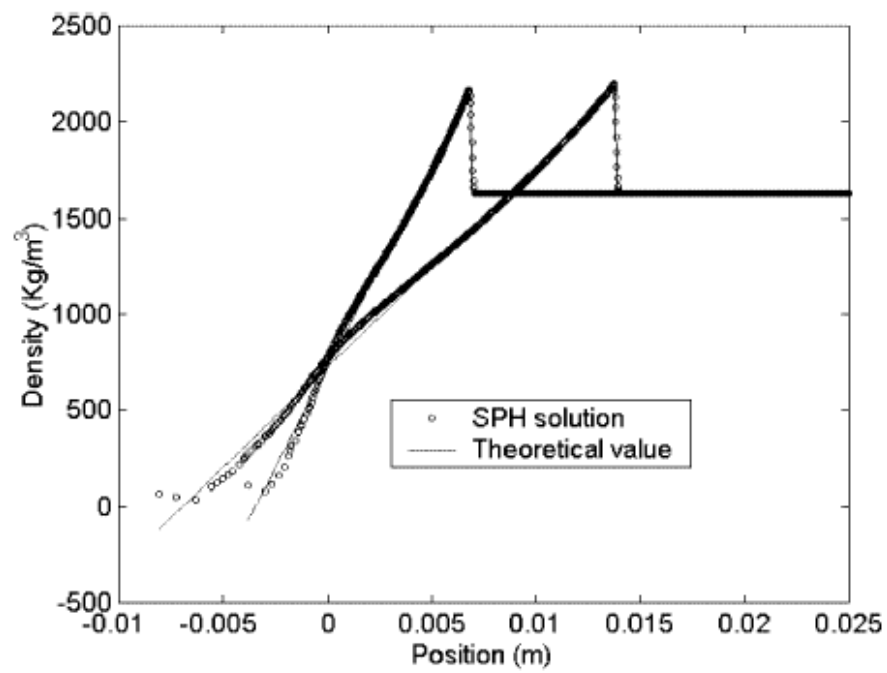


Figure 16: Pressure transients at 1 and $2\mu s$. The plot is excerpted from the reference [53].

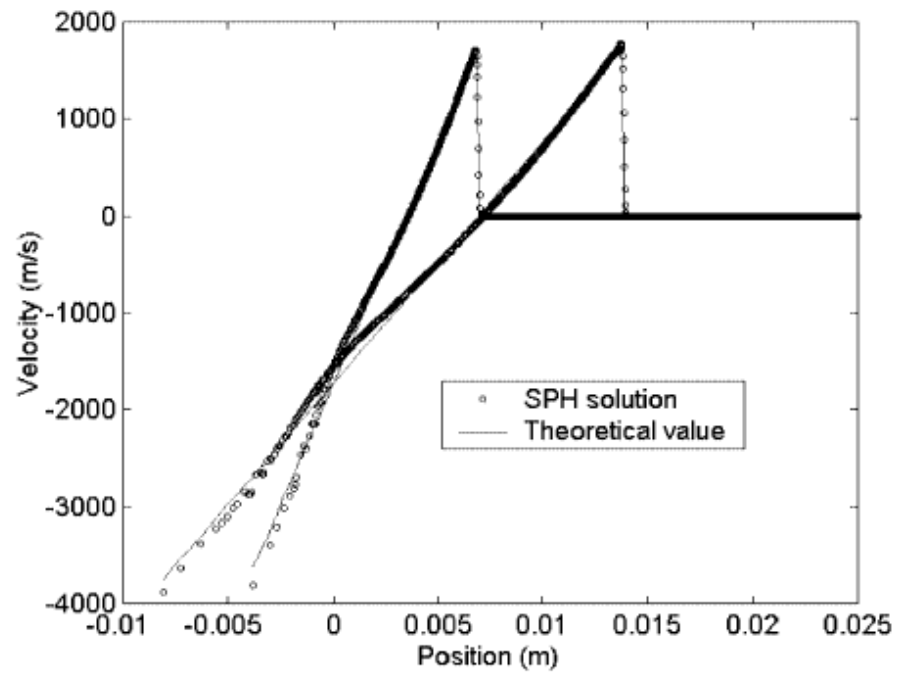


Figure 17: Density transients at 1 and $2\mu s$. The plot is excerpted from the reference [53].

The comparisons of pressure, density and velocity between theoretical values and SPH numerical results are shown in Fig. 4, Fig. 5 and Fig. 6 in this paper, here as shown by Fig. 15, Fig. 16 and Fig. 17.

From these figures, it is apparent that SPH method achieves great success in dealing with one dimensional detonation problems.

The second example is about the underwater explosion in free space, in which a cylindrical TNT charge is surrounded by water and then explodes inside it. The radius of the explosive charge is 0.1m, and the evaluation range is 0.5m. The boundary is treated as a free surface and it moves with the propagation of the shock wave. The pressure transients in the gas and corresponding density and velocity are displayed by Fig. 7, Fig. 8 and Fig. 9 respectively, which are displayed here by Fig. 18, Fig. 19, Fig. 20.

The SPH method can deal with difficulties appearing in large deformations, inhomogeneities and discontinuities as well as material interface. From this work, we know that the SPH method can apply to the underwater explosion shocks quite well.

1.14 Consistency

As proved in the previous context, the kernel approximation of the SPH method has the second accuracy for both the function and its derivative. However this is not definitely the fact, in that the kernel function would be not an even function and its normalization condition would not be satisfied since it may be truncated when approaching the boundary regions. So that the concept of the consistency can be taken as an analysis of truncation error. In the SPH method, the function approximation and derivative approximation are involved, so the truncation error of them would be discussed.

For a constant function $f(x) = c$ where c is a constant, to be reproduced by the kernel approximation, we have

$$f(x) = \int f(x')W(x-x',h)dx' = \int cW(x-x',h)dx' = c \quad (81)$$

so that

$$\int W(x-x',h)dx' = 1 \quad (82)$$

which is exactly the normalization condition of kernel function.

For the first order polynomial, $f(x) = a + bx$, where a and b are constants, to be recreated, we have

$$f(x) = \int (a + bx')W(x-x',h)dx' = a + bx \quad (83)$$

so that

$$\int x'W(x-x',h)dx' = x \quad (84)$$

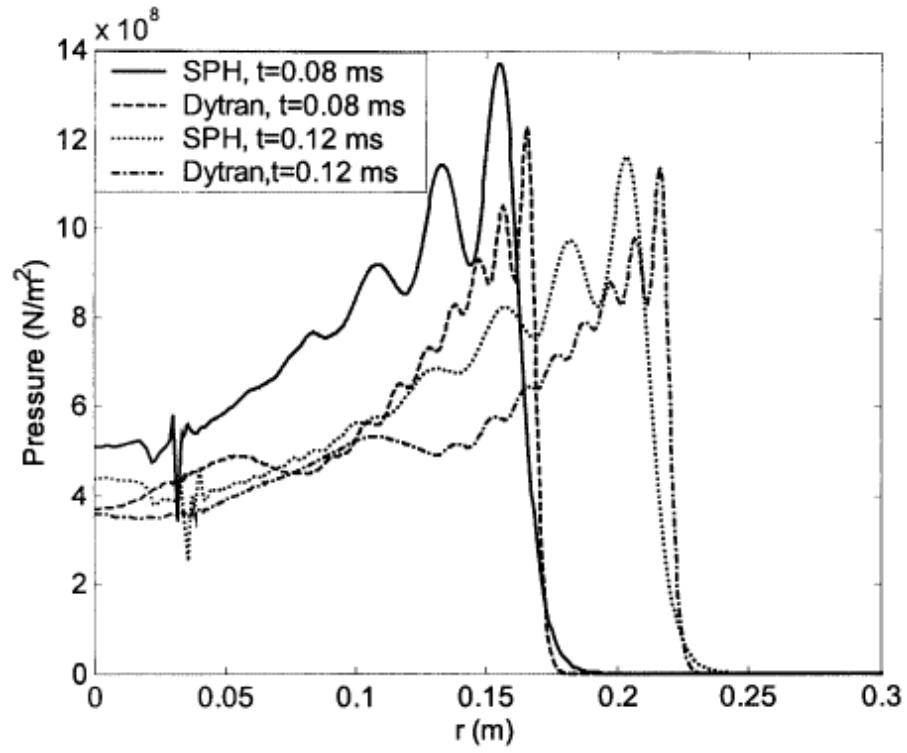


Figure 18: Pressure transients in the explosive gas and water as well as the shock waves at $t = 0.8ms$ and $t = 0.12ms$. The plot is excerpted from the reference [53].

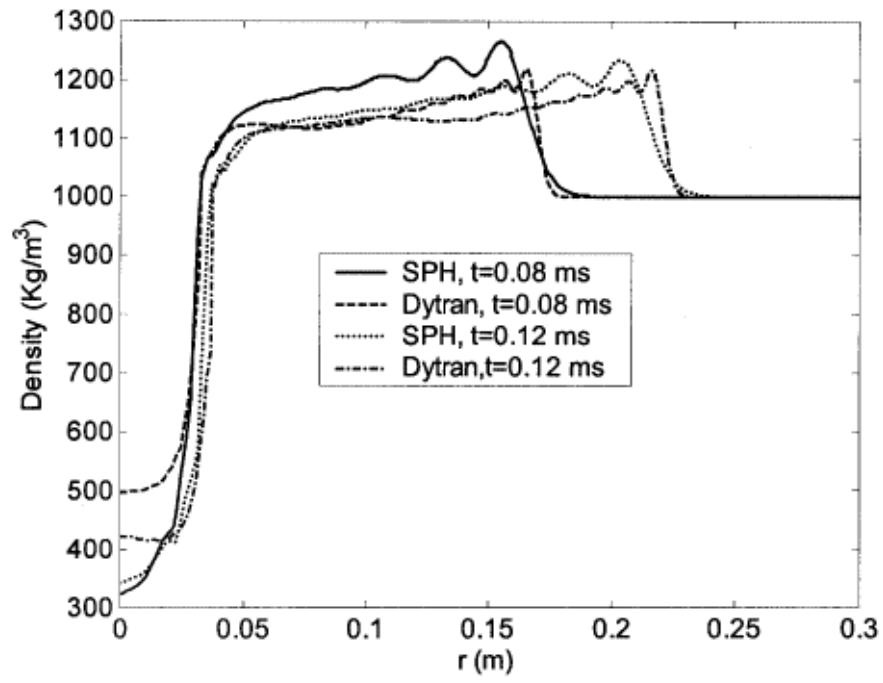


Figure 19: Density profiles in the explosive gas and water at $t = 0.8ms$ and $t = 0.12ms$. The plot is excerpted from the reference [53].

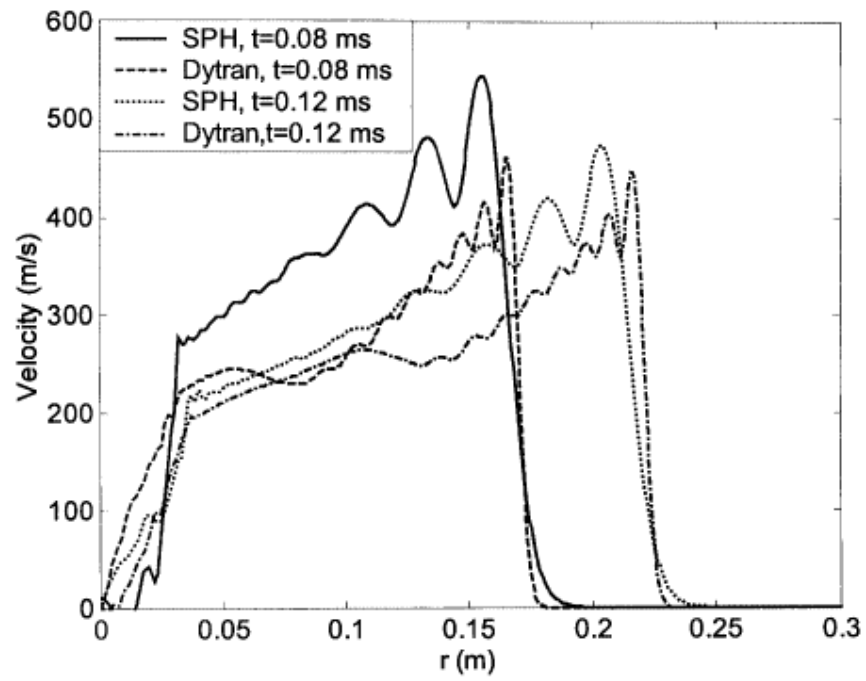


Figure 20: Velocity profiles in the explosive gas and water at $t = 0.8ms$ and $t = 0.12ms$. The plot is excerpted from the reference [53].

Multiplying x to both side of equation (82), we have

$$\int xW(x-x',h)dx' = x \quad (85)$$

then subtracting equation (84) from equation (85), we obtain

$$\int (x-x')W(x-x',h)dx' = 0 \quad (86)$$

which is naturally satisfied because of the kernel function is an even function.

However we should note that the constant and linear functions are not able to be reproduced exactly because the equations (82) and (86) are not satisfied if the kernel approximation is carried out for the boundary regions. In this case, we can conclude that the conventional SPH method has up to the first order consistency for interior regions but even does not have zero order consistency for boundary regions.

As mentioned before the high order accuracy kernel approximation does not guarantee the high accuracy of the SPH approach. Even though the kernel consistency conditions are satisfied, the SPH method will not have such consistency because consistency can be distorted by the particle approximation. So that the consistency of particle approximation is crucial and consistency analysis should be conducted in the particle approximation process.

The constant and linear consistency conditions in equations (82) and (88) can be expressed in discrete form as

$$\sum_{j=1}^N W(x-x_j,h)\Delta V_j = 1 \quad (87)$$

and

$$\sum_{j=1}^N (x-x_j)W(x-x_j,h)\Delta V_j = 0 \quad (88)$$

where ΔV_j is the volume element for particle indexed by j .

For boundary regions, it has been proved by pioneers that even for uniform particle distribution the left hand side of equation (87) is smaller than one and the right hand side of equation (88) is not zero. And along with irregular particle distribution for the interior regions the consistency conditions for constant and linear functions in discrete forms are not exactly satisfied. Therefore the conventional SPH method even does not have zero order particle consistency for both interior and boundary regions.

In summary, the inconsistency conditions lead to inaccuracy of solution in the conventional SPH. And such inconsistency are originated from the difference between the SPH kernel approximation and particle approximation. In order to restore the inconsistency and improve the accuracy of SPH method, some approaches for restoring consistency would be reviewed.

First of all, a corrective smoothed particle method (CSPM) which is proposed by Chen et al [54] is worth to be addressed. This method is based on the Taylor series expansion during the process of the SPH approximation of a function. The process of CSPM can be described as follows.

For a smooth function $f(x)$, conducting Taylor series expansion at a point x_i , we have

$$f(x) = f_i + (x - x_i)f_{i,x} + \frac{(x - x_i)^2}{2!}f_{i,xx} + \dots \quad (89)$$

where $f_i, f_{i,x}, f_{i,xx}$ stand for the function, its first order derivative and its second order derivative at point x_i .

Multiplying both sides of equation (89) by the kernel function and integrating over the whole computational domain, we obtain

$$\int f(x)W_i(x)dx = f_i \int W_i(x)dx + f_{i,x} \int (x - x_i)W_i(x)dx + \frac{f_{i,xx}}{2!} \int (x - x_i)^2 W_i(x)dx + \dots \quad (90)$$

Neglecting the derivative terms, it yields a corrective kernel approximation for function $f(x)$ at point x_i

$$f_i = \frac{\int f(x)W_i(x)dx}{\int W_i(x)dx}. \quad (91)$$

It is apparent that the second term at the right hand side of equation (91) for interior region will vanish and is not zero for boundary region. So the corrective kernel approximation shown by equation (91) keeps the second order consistency for interior region and first order consistency for boundary region.

The corresponding particle approximation for equation (91) can be written as

$$f_i = \frac{\sum_{j=1}^N f_j W_{ij} \Delta V_j}{\sum_{j=1}^N W_{ij} \Delta V_j} \quad (92)$$

We should note that even for interior regions the particle approximation of the second term in equation (90) is not exactly zero owing to the irregular distribution of particles. Only the uniform distribution of particles causes this term disappear. Therefore the particle approximation expressed by equation (92) guarantees the zero order consistency for interior and boundary region with irregular particle distribution, while keeps the first order consistency for the uniform particle distribution.

Replacing the kernel function $W_i(x)$ in equation (82) with its derivative $W_{i,x}$ and neglecting the second and higher order derivatives, then a corrective kernel approximation for smoothing function derivative is

$$f_{i,x} = \frac{\int (f(x) - f(x_i))W_{i,x}dx}{\int (x - x_i)W_{i,x}dx} \quad (93)$$

The particle approximation for the above equation is

$$f_{i,x} = \frac{\sum_{j=1}^N (f_j - f_i)W_{i,x} \Delta V_j}{\sum_{j=1}^N (x_j - x_i)W_{i,x} \Delta V_j} \quad (94)$$

From the equation (94), the CSPM kernel approximations for the function derivative in uniformly distributed particles are of first order consistency for interior regions and of zero order consistency for boundary regions. Otherwise the CSPM kernel approximations are of zero order consistency for both interior and boundary regions.

From the above discussions the CSPM has better accuracy than the conventional SPH method in that it improves the SPH simulations at boundary regions. However this method is based on the Taylor series expansion. It is well known that the function ought to be smooth if the Taylor series analysis is carried out. For problems involving discontinuities such as hydrodynamic problems which create shock waves, the CSPM method is not desirable. To resolve the discontinuity problems, Liu and his co-workers suggested a method called discontinuous SPH (DSPH) [55].

The present report is organized as follows. In the next section, we will introduce the idea of SPH algorithm and we are going to focus on the SPH algorithm called finite particle method (FPM). In the section III, we will spare effort to discuss the hydrodynamical equations of motion, including the classical Euler equation and the relativistic equation of motion. Some detail derivation of them will be shown. In the section IV, we will reproduce the entropy density distribution with time evolution in laboratory system about one dimensional Landau model and compare these numerical results with the exact Khalatnikov analytic solution accompanying with simple rarefied wave solution. In the section V, we will reproduce the temperature profile of a cylindrically symmetric flow with longitudinally scaling expansion. In the section VI, we show a new equation of motion based on the new SPH algorithm. Some concluding remarks and outlook will be given in section VII.

2 Finite particle method

As discussed in previous chapter, consistency is one of important numerical properties of the SPH method. In order to restore it many approaches have been proposed. Liu MB and Liu GR proposed an approach called Finite Particle Method (FPM) to restore the particle consistency [2]. This approach maintains the conventional non-negative smoothing function rather than to construct new smoothing function. Here we will spare efforts to address it because it is closely related to the Taylor SPH algorithm devised by Philippe Mota [1]. First of all, the FPM method would be discussed. Then the work done by Philippe Mota about SPH schemes would be addressed in the following.

For a sufficiently smooth function $f(\mathbf{x})$ at spatial place $\mathbf{x} = x, y, z$, by performing Taylor series expansion at a surrounding point $\mathbf{x}_j = x_j, y_j, z_j$ and only retaining the second order derivatives, it can be written as

$$f(\mathbf{x}) = f_j + (\mathbf{x}^\alpha - \mathbf{x}_j^\alpha) f_{j,\alpha} + \frac{(\mathbf{x}^\alpha - \mathbf{x}_j^\alpha)(\mathbf{x}^\beta - \mathbf{x}_j^\beta)}{2!} f_{j,\alpha\beta} + r((\mathbf{x} - \mathbf{x}_j)^3) \quad (95)$$

where α, β are the indices of dimension ranging from x to z . $r((\mathbf{x} - \mathbf{x}_j)^3)$ is the

remainder of the expansion. Here f_j , $f_{j,\alpha}$ and $f_{j,\alpha\beta}$ have the form

$$f_j = f(\mathbf{x}_j), \quad (96)$$

$$f_{j,\alpha} = f_\alpha(\mathbf{x}_j) = (\partial f / \partial \mathbf{x}^\alpha)_j, \quad (97)$$

$$f_{j,\alpha\beta} = f_{\alpha\beta}(\mathbf{x}_j) = (\partial^2 f / \partial \mathbf{x}^\alpha \partial \mathbf{x}^\beta)_j \quad (98)$$

Now multiplying a function $\psi(\mathbf{x} - \mathbf{x}_j)$ at both sides of equation (99) and making integration over the whole space Ω yield

$$\begin{aligned} \int_{\Omega} f(\mathbf{x}) \psi(\mathbf{x} - \mathbf{x}_j) d\mathbf{x} &= f_j \int_{\Omega} \psi(\mathbf{x} - \mathbf{x}_j) d\mathbf{x} + f_{j,\alpha} \int_{\Omega} (\mathbf{x}^\alpha - \mathbf{x}_j^\alpha) \psi(\mathbf{x} - \mathbf{x}_j) d\mathbf{x} \\ &+ \frac{f_{j,\alpha\beta}}{2!} \int_{\Omega} (\mathbf{x}^\alpha - \mathbf{x}_j^\alpha) (\mathbf{x}^\beta - \mathbf{x}_j^\beta) \psi(\mathbf{x} - \mathbf{x}_j) d\mathbf{x} + r((\mathbf{x} - \mathbf{x}_j)^3) \end{aligned} \quad (99)$$

From the above equation, the integration is conducted over the whole space which is quite time consuming. Usually one assumption is made that a variable at point \mathbf{x}_j is affected by the variables at nearby points and the influence from variables at points far away from point \mathbf{x}_j is very small and therefore is able to be ignored. In this case, the global integration is converted into a local integration. The support domain for point \mathbf{x}_j can be defined where the variables at nearby points are determined. It is convenient to regard the shape of the support domain as sphere in three dimensions and circle in two dimensions with the radius of κh , where κ is a constant factor and h is smoothing length characterising the support domain. So that the function $\psi(\mathbf{x} - \mathbf{x}_j)$ has limitation of the support domain and therefore can be written as $\psi(\mathbf{x} - \mathbf{x}_j, h)$.

Due to the fact that the points in the space are particles, each of them has own volume, the equation (99) can be represented by summation over the particles near point \mathbf{x}_j

$$\begin{aligned} \sum_{i=1}^N f(\mathbf{x}_i) \psi(\mathbf{x}_i - \mathbf{x}_j, h) \Delta V_i &= f_j \sum_{i=1}^N \psi(\mathbf{x}_i - \mathbf{x}_j, h) \Delta V_i + f_{j,\alpha} \sum_{i=1}^N (\mathbf{x}_i^\alpha - \mathbf{x}_j^\alpha) \psi(\mathbf{x}_i - \mathbf{x}_j, h) \Delta V_i \\ &+ \frac{f_{j,\alpha\beta}}{2!} \sum_{i=1}^N (\mathbf{x}_i^\alpha - \mathbf{x}_j^\alpha) (\mathbf{x}_i^\beta - \mathbf{x}_j^\beta) \psi(\mathbf{x}_i - \mathbf{x}_j, h) \Delta V_i \end{aligned} \quad (100)$$

where N denotes the number of particles within the support domain of particle i . Here the term $r((\mathbf{x} - \mathbf{x}_j)^3)$ appearing in equation (99) has been omitted.

For the above equation, further simplification can be made as the following equation

$$G_{1j} = H_{1kj}^T F_{kj} \quad (101)$$

where

$$\begin{aligned} F_{kj} &= [f_j \quad f_{j,\alpha} \quad f_{j,\alpha\beta}]^T, \\ G_{1j} &= \sum_{i=1}^N f(\mathbf{x}_i) \psi(\mathbf{x}_i - \mathbf{x}_j, h) \Delta V_i \end{aligned} \quad (102)$$

$$H_{1kj} = \begin{bmatrix} \sum_{i=1}^N \psi(\mathbf{x}_i - \mathbf{x}_j, h) \Delta V_i \\ \sum_{i=1}^N (\mathbf{x}_i^\alpha - \mathbf{x}_j^\alpha) \psi(\mathbf{x}_i - \mathbf{x}_j, h) \Delta V_i \\ \frac{1}{2!} \sum_{i=1}^N (\mathbf{x}_i^\alpha - \mathbf{x}_j^\alpha)(\mathbf{x}_i^\beta - \mathbf{x}_j^\beta) \psi(\mathbf{x}_i - \mathbf{x}_j, h) \Delta V_i \end{bmatrix}.$$

For the one, two, and three dimensions, there are one function value, one, two and three first derivatives and one, three and six second order derivatives correspondingly. The k is three, six and ten corresponding to one, two and three dimensional cases. It is clear that in 1, 2 and 3 dimensions, in total 3, 6 and 10 functions $\psi_M(\mathbf{x} - \mathbf{x}_j, h)$ are needed in order to calculate the function value, its first derivative and second derivative. These functions $\psi_M(\mathbf{x} - \mathbf{x}_j, h)$ form a set of basis functions.

It is natural to summarize that to multiply a body of basis functions at both sides of equation (99) and integrate over the whole problem space, sum over the nearest particles in the local support domain of particle i , a set of matrix equations can be created to evaluate the function value, the first and second derivatives at particle i . The matrix equation at particle i has the form

$$G_{Mj} = H_{Mkj}^T F_{kj} \quad (103)$$

where

$$G_{Mj} = \sum_i^N f(\mathbf{x}_i) \psi_M(\mathbf{x}_i - \mathbf{x}_j, h) \Delta V_i \quad (104)$$

$$H_{Mkj} = \begin{bmatrix} \sum_{i=1}^N \psi_M(\mathbf{x}_i - \mathbf{x}_j, h) \Delta V_i \\ \sum_{i=1}^N (\mathbf{x}_i^\alpha - \mathbf{x}_j^\alpha) \psi_M(\mathbf{x}_i - \mathbf{x}_j, h) \Delta V_i \\ \frac{1}{2!} \sum_{i=1}^N (\mathbf{x}_i^\alpha - \mathbf{x}_j^\alpha)(\mathbf{x}_i^\beta - \mathbf{x}_j^\beta) \psi_M(\mathbf{x}_i - \mathbf{x}_j, h) \Delta V_i \end{bmatrix}.$$

This is the basic idea of the FPM method. Only if the coefficients of matrix H is not singular, can these M equations determine the M unknowns in vector G . By solving these matrix equations, the function value as well as its first derivative and second derivative can be approximated. Here only second order terms are retained as the Taylor series expansion is carried out. For problems involve higher order terms, the same procedure can be conducted. In that case, more unknowns are required to be solved and more basis equations are included.

After introducing the FPM method, the Taylor SPH algorithm is going to be addressed. We named the new algorithm as Taylor SPH algorithm, because it actually is related to the Taylor series expansion for the function and its derivative. And there are many kinds of SPH schemes and detailed discussion about Taylor SPH algorithm in the note of Philippe Mota [1]. Now we introduce the idea of interpolation for Taylor SPH algorithm. From the Taylor series expansion we have

$$f(x) = \sum_n \frac{(x - r_a)_i^n}{n!} (\partial_i^n f)_{r_a}. \quad (105)$$

where the index i expresses the position component and index n means the derivative order. Now we multiply both sides by $W(x - r_a)$ and integrate over

x

$$\int dx f(x) W(x - r_a) = \sum_n \frac{(\partial_i^n f)_{r_a}}{n!} \int dx (x - r_a)_i^n W(x - r_a). \quad (106)$$

and simultaneously we also multiply both sides by the gradient of kernel function $W(x - r_a)$,

$$\int dx f(x) \frac{x - r_a}{|x - r_a|} W'(x - r_a) = \sum_n \frac{(\partial_i^n f)_{r_a}}{n!} \int dx (x - r_a)_i^n \frac{x - r_a}{|x - r_a|} W'(x - r_a). \quad (107)$$

By virtue of neglecting the second and higher order derivatives in Taylor series expansion (106) and (107), we obtain a linear system in function and its first derivative.

$$\int dx f(x) W(x - r_a) = f_a \int dx W(x - r_a) + \partial_j f_a \int dx (x - r_a)_j W(x - r_a). \quad (108)$$

$$\int dx f(x) \frac{(x - r_a)_i}{|x - r_a|} W'(x - r_a) = f_a \int dx \frac{(x - r_a)_i}{|x - r_a|} W'(x - r_a) + \partial_j f_a \int dx (x - r_a)_j \frac{(x - r_a)_i}{|x - r_a|} W'(x - r_a). \quad (109)$$

Using particle approximation and written in the form of matrix,

$$AF = B. \quad (110)$$

$$A = \begin{bmatrix} \sum_b \frac{\nu_b}{\rho_b} W(r_b - r_a) & \sum_b \frac{\nu_b}{\rho_b} (r_b - r_a)_j W(r_b - r_a) \\ \sum_b \frac{\nu_b}{\rho_b} \frac{(r_b - r_a)_i}{|r_b - r_a|} W'(r_b - r_a) & \sum_b \frac{\nu_b}{\rho_b} (r_b - r_a)_j \frac{(r_b - r_a)_i}{|r_b - r_a|} W'(r_b - r_a) \end{bmatrix},$$

$$F = \begin{bmatrix} f_a \\ \partial_j f_a \end{bmatrix},$$

$$B = \begin{bmatrix} \sum_b \frac{\nu_b f_b}{\rho_b} W(r_b - r_a) \\ \sum_b \frac{\nu_b f_b}{\rho_b} \frac{(r_b - r_a)_i}{|r_b - r_a|} W'(r_b - r_a) \end{bmatrix}.$$

where ρ_b is the reference density, ν_b is the weight carried by every SPH particle which is located at r_b . It easily comes out

$$F = A^{-1} B. \quad (111)$$

Generally speaking, the above expressions are obtained by expanding the interpolation up to the first order terms in Taylor series. In this context, the standard SPH algorithm can be equivalently viewed as the zeroth order approximation of the present scheme.

By reviewing the previous FPM method, it is easy to find that the Taylor SPH algorithm is an special case of FPM. If the smoothing kernel function and its first and second derivatives are selected as the basis functions, then Taylor SPH algorithm is equivalent to the FPM.

To compare the standard SPH and Taylor SPH in interpolation, let's apply them to some given test functions. The results are shown in detail by Sibilla [56]

and we can know that if a uniform particle distribution is used, the functions and their derivatives are reproduced correctly, except for the region near the boundaries. Here we show an ordinary function which is a superposition of Gaussian function under a random particle distribution. From the graphs below, the Taylor SPH algorithm performs better in function and its derivative.

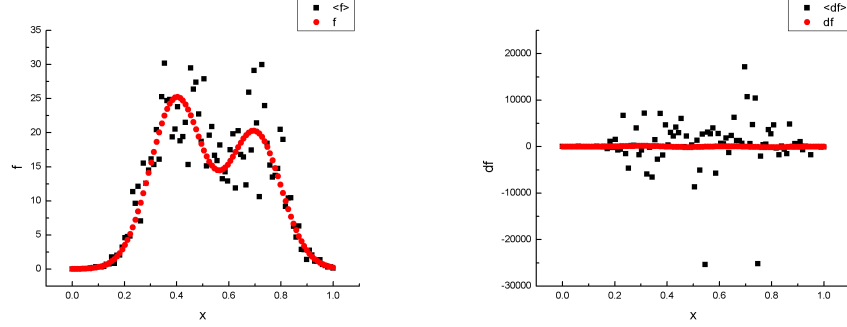


Figure 21: Standard SPH, f is original function value and $\langle f \rangle$ is interpolated value, df is original function derivative value and $\langle df \rangle$ is interpolated value

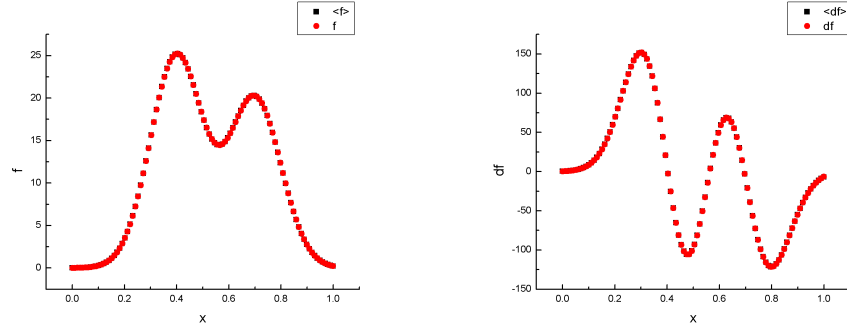


Figure 22: Taylor SPH, f is original function value and $\langle f \rangle$ is interpolated value, df is original function derivative value and $\langle df \rangle$ is interpolated value

So that we can make conclusion that the standard SPH shows great deficiency in interpolation when the particles are not distributed uniformly however the Taylor SPH algorithm overcomes this problem. This is attributed to the particle consistency restoring.

3 Introduction of hydrodynamical equations of motion

It is well known that hydrodynamics is a subdisciplines of fluid dynamics. It mainly focuses on the study of liquids motion. The foundational theorems of it are the conservation laws, like mass conservation, momentum conservation and energy conservation. In the following, the dominant equation of motion named Navier-Stokes equations will be discussed. Euler's equations as one of the special case will also be addressed. Then the topic will be transited to the relativistic circumstances along with the derivation of relativistic Euler equation of motion. Most of what we have discussed here is based on the book written by G.R. Liu and M.B. Liu [57].

3.1 Navier-Stokes equations in Lagrangian form

We have known that the basic governing equations of fluid dynamics are based upon three fundamental physical laws of conservation. However different forms of equations can be used to describe the fluid flow, which depend on the specific conditions. There exist two approaches named Euler description and Lagrangian description. The coordinate system is fixed in Euler description and usually it moves with fluid in Lagrangian description. The total time derivative is employed in the Lagrangian description and the SPH method is actually a Lagrangian meshfree method. To appeal the Lagrangian nature of the SPH method, the governing equations in Lagrangian form will be addressed. And the equations of motion will be deducted based upon these equations.

3.1.1 The continuity equation

The continuity equation is originated from the conservation of mass. Considering an infinitesimal element with volume of δV , the mass belonging to this volume is

$$\delta m = \rho \delta V \quad (112)$$

where ρ and m are density and mass respectively.

Because the mass is conserved in the element, the time rate of mass change is zero.

$$\frac{D\delta m}{Dt} = \frac{D(\rho\delta V)}{Dt} = \delta V \frac{D\rho}{Dt} + \rho \frac{D(\delta V)}{Dt} = 0 \quad (113)$$

The above equation can be written as

$$\frac{D\rho}{Dt} + \rho \frac{1}{\delta V} \frac{D(\delta V)}{Dt} = 0 \quad (114)$$

Here the time rate of volume change is involved. It is clear that the volume change ΔV due to the movement of surface dS over a time interval Δt is

$$\Delta V = \mathbf{v} \cdot \mathbf{n} \Delta t dS \quad (115)$$

where \mathbf{n} denotes the unit perpendicular to the surface dS . Then the total volume change equals the integral over the surface S

$$\Delta V = \oint_S \mathbf{v} \delta t \cdot \mathbf{n} dS \quad (116)$$

Therefore it is easy to obtain

$$\frac{\Delta V}{\Delta t} = \oint_s \mathbf{v} \cdot \mathbf{n} dS = \int_V \nabla \cdot \mathbf{v} dV \quad (117)$$

Where ∇ is the gradient operator and the divergence theorem has been employed. For an infinitesimal element with volume of δV ,

$$\frac{\Delta(\delta V)}{\Delta t} = (\nabla \cdot \mathbf{v}) \int d(\delta V) = (\nabla \cdot \mathbf{v}) \delta V \quad (118)$$

So that the time change rate of the infinitesimal volume is

$$\frac{D(\delta V)}{Dt} = (\nabla \cdot \mathbf{v}) \delta V \quad (119)$$

then the velocity divergence has the form

$$\nabla \cdot \mathbf{v} = \frac{1}{\delta V} \frac{D(\delta V)}{Dt} \quad (120)$$

Substituting into the continuity of equation (114) yields

$$\frac{D\rho}{Dt} = -\rho \nabla \cdot \mathbf{v} \quad (121)$$

3.1.2 The momentum equation

The momentum equation is established according to Newton's second law, which states that the net force on a Lagrangian fluid element equals to its mass multiplying its acceleration. For example, in the x acceleration, all the forces including the body forces and surface forces exerting on the infinitesimal element are

$$\begin{aligned} & -\left[\left(p + \frac{\partial p}{\partial x} dx\right) - p\right] dydz + \\ & \left[\left(\tau_{xx} + \frac{\partial \tau_{xx}}{\partial x} dx\right) - \tau_{xx}\right] dydz + \\ & \left[\left(\tau_{yx} + \frac{\partial \tau_{yx}}{\partial y} dy\right) - \tau_{yx}\right] dx dz + \\ & \left[\left(\tau_{zx} + \frac{\partial \tau_{zx}}{\partial z} dz\right) - \tau_{zx}\right] dx dy \\ & = -\frac{\partial p}{\partial x} dx dy dz + \frac{\partial \tau_{xx}}{\partial x} dx dy dz + \frac{\partial \tau_{yx}}{\partial y} dx dy dz + \frac{\partial \tau_{zx}}{\partial z} dx dy dz \end{aligned} \quad (122)$$

where p is the pressure and τ_{ij} is the stress in the j direction exerted on the plane perpendicular to the i axis. Assuming the body force in the x direction per unit mass is F_x , we have

$$m \frac{dv_x}{dt} = \rho dx dy dz \frac{dv_x}{dt} = -\frac{\partial p}{\partial x} dx dy dz + \frac{\partial \tau_{xx}}{\partial x} dx dy dz + \frac{\partial \tau_{yx}}{\partial y} dx dy dz + \frac{\partial \tau_{zx}}{\partial z} dx dy dz + F_x \rho dx dy dz \quad (123)$$

Finally the momentum equation in the x direction has the form

$$\rho \frac{Dv_x}{Dt} = -\frac{\partial p}{\partial x} + \frac{\partial \tau_{xx}}{\partial x} + \frac{\partial \tau_{yx}}{\partial y} + \frac{\partial \tau_{zx}}{\partial z} + \rho F_x \quad (124)$$

The same procedure can be done in the y and z directions yielding

$$\rho \frac{Dv_y}{Dt} = -\frac{\partial p}{\partial y} + \frac{\partial \tau_{xy}}{\partial x} + \frac{\partial \tau_{yy}}{\partial y} + \frac{\partial \tau_{zy}}{\partial z} + \rho F_y, \quad (125)$$

$$\rho \frac{Dv_z}{Dt} = -\frac{\partial p}{\partial z} + \frac{\partial \tau_{xz}}{\partial x} + \frac{\partial \tau_{yz}}{\partial y} + \frac{\partial \tau_{zz}}{\partial z} + \rho F_z \quad (126)$$

3.1.3 The energy equation

The energy equation is based on the energy conservation. It is a representation of the first thermodynamics law. It means that the energy time change rate equals the summation of the net heat flux into the fluid element, and time rate of work due to the body forces and surface forces. It can be written as

$$\begin{aligned} \rho \frac{De}{Dt} = & -p \left(\frac{\partial v_x}{\partial x} + \frac{\partial v_y}{\partial y} + \frac{\partial v_z}{\partial z} \right) \\ & + \tau_{xx} \frac{\partial v_x}{\partial x} + \tau_{yx} \frac{\partial v_x}{\partial y} + \tau_{zx} \frac{\partial v_x}{\partial z} \\ & + \tau_{xy} \frac{\partial v_y}{\partial x} + \tau_{yy} \frac{\partial v_y}{\partial y} + \tau_{zy} \frac{\partial v_y}{\partial z} \\ & + \tau_{xz} \frac{\partial v_z}{\partial x} + \tau_{yz} \frac{\partial v_z}{\partial y} + \tau_{zz} \frac{\partial v_z}{\partial z} \end{aligned} \quad (127)$$

In summary, the Navier-Stokes equations are a set of partial differential equations in Lagrangian description, which demonstrate the conservation of mass, momentum and energy. If α and β express the coordinate directions, and the summation is taken over repeated indices, the Navier-Stokes equations can be written as the following

$$\frac{D\rho}{Dt} = -\rho \frac{\partial \mathbf{v}^\beta}{\partial \mathbf{x}^\beta} \quad (128)$$

$$\frac{D\mathbf{v}^\alpha}{Dt} = \frac{1}{\rho} \frac{\partial \sigma^\alpha}{\partial \mathbf{x}^\beta} \quad (129)$$

$$\frac{De}{Dt} = \frac{\sigma^{\alpha\beta}}{\rho} \frac{\partial \mathbf{v}^\alpha}{\partial \mathbf{x}^\beta} \quad (130)$$

where $\sigma^{\alpha\beta}$ is the total stress tensor. It consists of two parts, one is the isotropic pressure p and the other is viscous stress τ .

$$\sigma^{\alpha\beta} = -p\delta^{\alpha\beta} + \tau^{\alpha\beta} \quad (131)$$

3.2 Euler's equation

Taking into account some volume in the fluid, it is exerted by the force which equals the integral of the pressure over the surface surrounding the volume $-\oint p d\mathbf{f}$. By virtue of the diverge theorem, we obtain

$$-\oint p d\mathbf{f} = -\int \nabla p d\mathbf{V} \quad (132)$$

From the above equation, it is clear that the unit volume is affected by force $-\nabla p$. In this case, we can write down the acceleration equation:

$$\rho \frac{D\mathbf{v}}{Dt} = -\nabla p \quad (133)$$

Here \mathbf{v} stands for the velocity of a given fluid particle moving about in space, we have

$$\mathbf{v} = \mathbf{v}(t, x, y, z) \quad (134)$$

So the derivative of it can be written as

$$\frac{D\mathbf{v}}{Dt} = \frac{\partial \mathbf{v}}{\partial t} + \mathbf{v} \cdot \nabla \mathbf{v} \quad (135)$$

Finally we obtain

$$\frac{\partial \mathbf{v}}{\partial t} + \mathbf{v} \cdot \nabla \mathbf{v} = -\frac{1}{\rho} \nabla p \quad (136)$$

This is the equation of motion of the fluid, and it is also called Euler's equation.

3.3 SPH representations for equations

After introducing the Navier-Stokes equations and Euler's equation, the SPH formulation for these equations are discussed. First of all, the density approximation is represented. It is crucial because it determines the particle distribution and the smoothing length. There are two approaches approximating the density. One approach is to directly approximate it by virtue of SPH formulation, which is a form of summation

$$\rho_a = \sum_{b=1}^N m_b W_{ab} \quad (137)$$

where N is the number of particles within the support domain of particle a , and m_b is the mass of particle b . W_{ab} is the smoothing kernel function of particle a calculated at particle b .

Another approach to evaluate the density is according to the continuity equation. Taking a look at the equation (128), the SPH approximation can be applied to the velocity divergence, which is

$$\frac{D\rho_a}{Dt} = -\rho_a \sum_{b=1}^N \frac{m_b}{\rho_b} \mathbf{v}_b^\beta \cdot \frac{\partial W_{ab}}{\partial \mathbf{x}_a^\beta} \quad (138)$$

As a matter of fact, there are some other transformations for the velocity divergence. Considering the approximation on the gradient of the unity, we obtain

$$\nabla 1 = \int 1 \nabla W(\mathbf{x} - \mathbf{x}', h) d\mathbf{x}' = \sum_{b=1}^N \frac{m_b}{\rho_b} \frac{\partial W_{ab}}{\partial \mathbf{x}_a^\beta} = 0 \quad (139)$$

Multiplying the term $\rho_a \mathbf{v}_a^\beta$ on both sides of the above equation yields

$$\rho_a \mathbf{v}_a^\beta \left(\sum_{b=1}^N \frac{m_b}{\rho_b} \frac{\partial W_{ab}}{\partial \mathbf{x}_a^\beta} \right) = \rho_a \sum_{b=1}^N \frac{m_b}{\rho_b} \mathbf{v}_a^\beta \frac{\partial W_{ab}}{\partial \mathbf{x}_a^\beta} \quad (140)$$

Finally we add this equation to the continuity of equation, obtaining another form of density approximation equation

$$\frac{D\rho_a}{Dt} = \rho_a \sum_{b=1}^N \frac{m_b}{\rho_b} \mathbf{v}_{ab}^\beta \cdot \frac{\partial W_{ab}}{\partial \mathbf{x}_a^\beta} \quad (141)$$

where

$$\mathbf{v}_{ab}^\beta = \mathbf{v}_a^\beta - \mathbf{v}_b^\beta \quad (142)$$

Here the velocity difference are introduced in the particle approximation, which is preferred in the SPH formulations. It takes into account the relative velocities of particle pairs which in some problems can reduce the error coming from the particle inconsistency.

There exists another form of the density gradient expression by applying the following equation

$$-\rho \frac{\partial \mathbf{v}^\beta}{\partial \mathbf{x}^\beta} = -\left[\frac{\partial(\rho \mathbf{v}^\beta)}{\partial \mathbf{x}^\beta} - \mathbf{v}^\beta \cdot \frac{\partial \rho}{\partial \mathbf{x}^\beta} \right] \quad (143)$$

Therefore with the help of this identity, the continuity equation has the form

$$\frac{D\rho_a}{Dt} = \sum_{b=1}^N m_b \mathbf{v}_{ab}^\beta \cdot \frac{\partial W_{ab}}{\partial \mathbf{x}_a^\beta} \quad (144)$$

For these two approaches, summation density and continuity density approximations, both of them have merits and drawbacks. The density summation can conserve the mass exactly because the integral of the density over the whole problem space is exactly the total mass of the system. But the continuity equation can not guarantee this. However the summation density approach shows

deficiency as it is applied to boundary particles of the fluid domain. This edge effect can be remedied by the continuity equation by using boundary virtual particles. Another comparison is arising from the computational calculation. For the summation density approach, it takes more computational time because the evaluation of density have to be done before other parameters are calculated and the smoothing kernel function also need to be evaluated. However the continuity density method does not require calculating other parameters in the beginning and therefore save a lot of computational efforts.

For the SPH formulation of the equation of momentum, the procedure is very similar to the continuity density approach. And there are many transformations for deriving different forms of momentum approximation equations. Directly applying the SPH particle approximation to the RHS of equation (129) yields

$$\frac{D\mathbf{v}_a^\alpha}{Dt} = \frac{1}{\rho_b} \sum_{b=1}^N m_b \frac{\sigma_b^{\alpha\beta}}{\rho_b} \frac{\partial W_{ab}}{\partial \mathbf{x}_a^\beta} \quad (145)$$

Using the following identity

$$\sum_{b=1}^N m_b \frac{\sigma_a^{\alpha\beta}}{\rho_a \rho_b} \frac{\partial W_{ab}}{\partial \mathbf{x}_a^\beta} = \frac{\sigma_a^{\alpha\beta}}{\rho_a} \left(\sum_{b=1}^N \frac{m_b}{\rho_b} \frac{\partial W_{ab}}{\partial \mathbf{x}_a^\beta} \right) \quad (146)$$

we can obtain a new form of the momentum equation

$$\frac{D\mathbf{v}_a^\alpha}{Dt} = \sum_{b=1}^N m_b \frac{\sigma_a^{\alpha\beta} + \sigma_b^{\alpha\beta}}{\rho_a \rho_b} \frac{\partial W_{ab}}{\partial \mathbf{x}_a^\beta} \quad (147)$$

This above equation is usually used because of its symmetrized form which can reduce error from the particle inconsistency.

If we consider the following identity

$$\frac{1}{\rho} \frac{\partial \sigma^{\alpha\beta}}{\partial \mathbf{x}^\beta} = \frac{\partial}{\partial \mathbf{x}^\beta} \left(\frac{\sigma^{\alpha\beta}}{\rho} \right) + \frac{\sigma^{\alpha\beta}}{\rho^2} \frac{\partial \rho}{\partial \mathbf{x}^\beta} \quad (148)$$

Now applying the SPH particle approximation to the identity and the momentum equation becomes

$$\frac{D\mathbf{v}_a^\alpha}{Dt} = \sum_{b=1}^N \frac{m_b}{\rho_b} \frac{\sigma_b^{\alpha\beta}}{\rho_b} \frac{\partial W_{ab}}{\partial \mathbf{x}_a^\beta} + \frac{\sigma_a^{\alpha\beta}}{\rho_a^2} \sum_{b=1}^N \frac{m_b}{\rho_b} \rho_b \frac{\partial W_{ab}}{\partial \mathbf{x}_a^\beta} \quad (149)$$

Through some rearrangements, finally we can get

$$\frac{D\mathbf{v}_a^\alpha}{Dt} = \sum_{b=1}^N m_b \left(\frac{\sigma_a^{\alpha\beta}}{\rho_a^2} + \frac{\sigma_b^{\alpha\beta}}{\rho_b^2} \right) \frac{\partial W_{ab}}{\partial \mathbf{x}_a^\beta} \quad (150)$$

For the internal energy evolution in equation (128), combination with the equation (131), the viscous shear stress is proportional to the shear strain rate expressed by ε through the dynamic viscosity μ ,

$$\tau^{\alpha\beta} = \mu \varepsilon^{\alpha\beta} \quad (151)$$

where

$$\varepsilon^{\alpha\beta} = \frac{\partial \mathbf{v}^\beta}{\partial \mathbf{x}^\alpha} + \frac{\partial \mathbf{v}^\alpha}{\partial \mathbf{x}^\beta} - \frac{2}{3}(\nabla \cdot \mathbf{v})\delta^{\alpha\beta} \quad (152)$$

Then the energy equation can be rewritten as

$$\frac{De}{Dt} = -\frac{p}{\rho} \frac{\partial \mathbf{v}^\beta}{\partial \mathbf{x}^\beta} + \frac{\mu}{2\rho} \varepsilon^{\alpha\beta} \varepsilon^{\alpha\beta} \quad (153)$$

Taking into account the following relation

$$-\frac{p}{\rho} \frac{\partial \mathbf{v}^\beta}{\partial \mathbf{x}^\beta} = \frac{p}{\rho^2} (-\rho \frac{\partial \mathbf{v}^\beta}{\partial \mathbf{x}^\beta}) = \frac{p}{\rho^2} \frac{D\rho}{Dt} \quad (154)$$

for the pressure work, it can be approximated as

$$-\frac{p}{\rho} \frac{\partial \mathbf{v}_a^\beta}{\partial \mathbf{x}_a^\beta} = \frac{p_a}{\rho_a^2} \sum_{b=1}^N m_b \mathbf{v}_{ab}^\beta \cdot \frac{\partial W_{ab}}{\partial \mathbf{x}_a^\beta} \quad (155)$$

Another way to approximate the pressure work is by using the following identity

$$-\frac{p}{\rho} \frac{\partial \mathbf{v}^\beta}{\partial \mathbf{x}^\beta} = -\frac{\partial}{\partial \mathbf{x}^\beta} \left(\frac{p \mathbf{v}^\beta}{\rho} \right) + \mathbf{v}^\beta \frac{\partial}{\partial \mathbf{x}^\beta} \left(\frac{p}{\rho} \right) \quad (156)$$

so it leads to

$$-\frac{p}{\rho} \frac{\partial \mathbf{v}_a^\beta}{\partial \mathbf{x}_a^\beta} = \sum_{b=1}^N m_b \frac{p_b}{\rho_b^2} \mathbf{v}_{ab}^\beta \cdot \frac{\partial W_{ab}}{\partial \mathbf{x}_a^\beta} \quad (157)$$

By adding equation (155) and equation (157), we can obtain the another form of approximation of the pressure work

$$-\frac{p}{\rho} \frac{\partial \mathbf{v}_a^\beta}{\partial \mathbf{x}_a^\beta} = \frac{1}{2} \sum_{b=1}^N m_b \left(\frac{p_a}{\rho_a^2} + \frac{p_b}{\rho_b^2} \right) \mathbf{v}_{ab}^\beta \frac{\partial W_{ab}}{\partial \mathbf{x}_a^\beta} \quad (158)$$

Using the following transformation

$$-\frac{p}{\rho} \frac{\partial \mathbf{v}^\beta}{\partial \mathbf{x}^\beta} = -\frac{1}{\rho} \left[\frac{\partial}{\partial \mathbf{x}^\beta} (p \mathbf{v}^\beta) - \mathbf{v}^\beta \frac{\partial P}{\partial \mathbf{x}^\beta} \right] \quad (159)$$

another form of SPH approximation for pressure work is got

$$-\frac{p}{\rho} \frac{\partial \mathbf{v}_a^\beta}{\partial \mathbf{x}_a^\beta} = \frac{1}{\rho_a} \sum_{b=1}^N m_b \frac{p_b}{\rho_b} \mathbf{v}_{ab}^\beta \frac{\partial W_{ab}}{\partial \mathbf{x}_a^\beta} \quad (160)$$

Adding the equation (158) and equation (160) together produces another useful form of the pressure work approximation

$$-\frac{p}{\rho} \frac{\partial \mathbf{v}_a^\beta}{\partial \mathbf{x}_a^\beta} = \frac{1}{2} \sum_{b=1}^N m_b \frac{p_a + p_b}{\rho_a \rho_b} \mathbf{v}_{ab}^\beta \cdot \frac{\partial W_{ab}}{\partial \mathbf{x}_a^\beta} \quad (161)$$

As discussed before, there are many kinds of form for the pressure work. However the most frequently used are the following two forms

$$\frac{De_a}{Dt} = \frac{1}{2} \sum_{b=1}^N m_b \left(\frac{p_a}{\rho_a^2} + \frac{p_b}{\rho_b^2} \right) \mathbf{v}_{ab}^\beta \frac{\partial W_{ab}}{\partial \mathbf{x}_a^\beta} + \frac{\mu_a}{2\rho_a} \varepsilon_a^{\alpha\beta} \varepsilon_a^{\alpha\beta} \quad (162)$$

and

$$\frac{De_a}{Dt} = \frac{1}{2} \sum_{b=1}^N m_b \left(\frac{p_a + p_b}{\rho_a \rho_b} \right) \mathbf{v}_{ab}^\beta \frac{\partial W_{ab}}{\partial \mathbf{x}_a^\beta} + \frac{\mu_a}{2\rho_a} \varepsilon_a^{\alpha\beta} \varepsilon_a^{\alpha\beta} \quad (163)$$

The SPH equations for the Navier-Stokes equations for evolving the density, momentum and energy have been discussed in the previous paragraphs. If we ignore the viscous term appearing in the Navier-Stokes equations, then we can obtain the Euler equations. The SPH formulations for Euler equations of evolving density, momentum and energy are listed as follows. First the density approximation has forms

$$\rho_a = \sum_{b=1}^N m_b W_{ab} \quad (164)$$

$$\rho_a = \frac{\sum_{b=1}^N m_b W_{ab}}{\sum_{b=1}^N \left(\frac{m_b}{\rho_b} \right) W_{ab}} \quad (165)$$

$$\frac{D\rho_a}{Dt} = -\rho_a \sum_{b=1}^N \frac{m_b}{\rho_b} \mathbf{v}_b^\beta \cdot \frac{\partial W_{ab}}{\partial \mathbf{x}_a^\beta} \quad (166)$$

$$\frac{D\rho_a}{Dt} = \rho_a \sum_{b=1}^N \frac{m_b}{\rho_b} \mathbf{v}_{ab}^\beta \cdot \frac{\partial W_{ab}}{\partial \mathbf{x}_a^\beta} \quad (167)$$

$$\frac{D\rho_a}{Dt} = \sum_{b=1}^N m_b \mathbf{v}_{ab}^\beta \cdot \frac{\partial W_{ab}}{\partial \mathbf{x}^\beta} \quad (168)$$

the conservation of momentum can be approximated as

$$\frac{D\mathbf{v}_a^\alpha}{Dt} = - \sum_{b=1}^N m_b \frac{p_a + p_b}{\rho_a \rho_b} \frac{\partial W_{ab}}{\partial \mathbf{x}_a^\alpha} \quad (169)$$

$$\frac{D\mathbf{v}_a^\alpha}{Dt} = - \sum_{b=1}^N m_b \left(\frac{p_a}{\rho_a^2} + \frac{p_b}{\rho_b^2} \right) \frac{\partial W_{ab}}{\partial \mathbf{x}_a^\alpha} \quad (170)$$

And the conservation of energy can be expressed as

$$\frac{De_a}{Dt} = \frac{1}{2} \sum_{b=1}^N m_b \frac{p_a + p_b}{\rho_a \rho_b} \mathbf{v}_{ab}^\beta \frac{\partial W_{ab}}{\partial \mathbf{x}_a^\beta} \quad (171)$$

$$\frac{De_a}{Dt} = \frac{1}{2} \sum_{b=1}^N m_b \left(\frac{p_a}{\rho_a^2} + \frac{p_b}{\rho_b^2} \right) \mathbf{v}_{ab}^\beta \frac{\partial W_{ab}}{\partial \mathbf{x}_a^\beta} \quad (172)$$

3.4 Relativistic hydrodynamical equations of motion

As a matter of fact, we can obtain the relativistic hydrodynamic equations of motion from variational approaches. Let us first briefly review this method. We start the action

$$I = \int d^4x (-\varepsilon). \quad (173)$$

where ε is the proper energy density. In the following, we regard the velocity of light as unity $c = 1$. The velocity field of matter is

$$\vec{v} = \vec{v}(\vec{r}, t). \quad (174)$$

and the four-vector velocity has the form

$$u^0 = \gamma, \vec{u} = \gamma \vec{v}. \quad (175)$$

where it satisfies

$$u_\mu u^\mu = 1. \quad (176)$$

In order to help the discussion, we have the assumption that the baryon number is conserved. We write the local density of baryon in comoving frame as n , then we have

$$\partial_\mu (n u^\mu) = 0. \quad (177)$$

now we can define the specific volume V as

$$V = \frac{1}{n}. \quad (178)$$

So that the energy of matter in this volume E equals

$$E = \varepsilon V \quad (179)$$

With the assumption of local equilibrium, we have the thermodynamical relation,

$$\left(\frac{\partial E}{\partial V}\right)_S = -P \quad (180)$$

where S denotes the entropy of the matter in this volume and P is the pressure. According to the energy density and baryon density, we can get

$$\left(\frac{\partial E}{\partial V}\right)_S = \left(\frac{\partial(\varepsilon V)}{\partial V}\right)_S = \varepsilon + V \left(\frac{\partial \varepsilon}{\partial V}\right)_S = \varepsilon + \frac{1}{n} \left(\frac{\partial \varepsilon}{\partial(\frac{1}{n})}\right)_S = -P \quad (181)$$

then

$$\left(\frac{\partial \varepsilon}{\partial n}\right)_S = \frac{\varepsilon + P}{n} \quad (182)$$

From the above discussion, the hydrodynamical equations of motion for the fluid involves the proper energy density ε , the local baryon density n and the

four vector velocity u^μ . In terms of the Lagrangian multipliers method, we can incorporate them into the action,

$$I = \int d^4x \{-\varepsilon + \xi \partial_\mu (nu^\mu) + \frac{1}{2} \zeta (u_\mu u^\mu - 1)\} \quad (183)$$

and use the variational principle

$$\delta I = 0 \quad (184)$$

where ξ and ζ are the Lagrangian multipliers and they are arbitrary functions of x . If we make variations with respect to ξ and ζ , we can get the constraint equations (176) and (177). Doing the integration by parts for the second term in equation (181), we can obtain the effective Lagrangian,

$$L_{eff} = -\varepsilon(n) - nu^\mu \partial_\mu \xi(x) + \frac{1}{2} \zeta(x) (u^\mu u_\mu - 1), \quad (185)$$

$$I = \int d^4x L_{eff} \quad (186)$$

The variations in n and u^μ cause immediately

$$-\mu - u^\mu \partial_\mu \xi = 0, \quad (187)$$

$$-n \partial_\mu \xi - \zeta u_\mu = 0. \quad (188)$$

Multiplying the both sides of equation (186) by u^μ , and by virtue of Eqs. (176, 177), we obtain

$$\zeta = \varepsilon + P \quad (189)$$

We substitute ζ into equation (186) and multiply u_ν ,

$$\zeta u_\mu u_\nu = -nu_\nu \partial_\mu \xi \quad (190)$$

now taking the divergence of it,

$$\partial^\nu (\zeta u_\mu u_\nu) = -nu_\nu \partial^\nu \partial_\mu \xi = n \partial_\mu (u_\nu \partial^\nu \xi) - n \partial^\nu \xi \partial_\mu u_\nu = -n \partial_\mu \mu - n \partial^\nu \xi \partial_\mu u_\nu \quad (191)$$

so that

$$\partial^\nu (\zeta u_\mu u_\nu) = n \partial_\mu \mu + \partial_\mu u_\nu \zeta u^\nu = \partial_\mu P \quad (192)$$

and finally we get the standard form of the relativistic hydrodynamic equation of motion

$$\partial^\nu T_{\mu\nu} = 0 \quad (193)$$

where

$$T_{\mu\nu} = (P + \varepsilon) u_\mu u_\nu - g_{\mu\nu} P \quad (194)$$

is the energy momentum tensor of the fluid.

3.5 Derivation of relativistic Euler's equation

In cartesian coordinate frame,

$$\partial_\mu T^{\mu\nu} = 0, \quad (195)$$

$$T^{\mu\nu} = (\varepsilon + P)u^\mu u^\nu - P g^{\mu\nu}, \quad (196)$$

$$\partial_\mu T^{\mu\nu} = \partial_\mu [(\varepsilon + P)u^\mu u^\nu] - \partial_\mu (P g^{\mu\nu}), \quad (197)$$

$$\partial_\mu T^{\mu\nu} = \partial_\mu [s u^\mu \frac{\varepsilon + P}{s} u^\nu] - g^{\mu\nu} \partial_\mu P, \quad (198)$$

$$\partial_\mu T^{\mu\nu} = s u^\mu \partial_\mu (\frac{\varepsilon + P}{s} u^\nu) - g^{\mu\nu} \partial_\mu P, \quad (199)$$

$$\partial_\mu T^{\mu\nu} = s \gamma \frac{d}{dt} (\frac{\varepsilon + P}{s} u^\nu) - g^{\mu\nu} \partial_\mu P \quad (200)$$

Considering the time part of it,

$$s \gamma \frac{d}{dt} (\frac{\varepsilon + P}{s} u^0) - g^{\mu 0} \partial_\mu P = 0, \quad (201)$$

$$s \gamma \frac{d}{dt} (\frac{\varepsilon + P}{s} \gamma) - g^{00} \partial_0 P = 0, \quad (202)$$

$$s \gamma \frac{d}{dt} (\frac{\varepsilon + P}{s} \gamma) = \frac{\partial P}{\partial t}. \quad (203)$$

Taking into account the spatial part,

$$s \gamma \frac{d}{dt} (\frac{\varepsilon + P}{s} \gamma v^i) - g^{\mu i} \partial_\mu P = 0, \quad (204)$$

$$s \gamma \frac{d}{dt} (\frac{\varepsilon + P}{s} \gamma) v^i + s \gamma (\frac{\varepsilon + P}{s} \gamma) \frac{dv^i}{dt} - g^{\mu i} \partial_\mu P = 0, \quad (205)$$

$$\frac{\partial P}{\partial t} v^i + (\varepsilon + P) \gamma^2 \frac{dv^i}{dt} + \partial_i P = 0. \quad (206)$$

If we write them by the vector form,

$$\frac{d\vec{v}}{dt} = -\frac{1}{(\varepsilon + P) \gamma^2} (\vec{\nabla} P + \vec{v} \frac{\partial P}{\partial t}), \quad (207)$$

$$\frac{\partial \vec{v}}{\partial t} + (\vec{v} \cdot \vec{\nabla}) \vec{v} = -\frac{1 - v^2}{\varepsilon + P} (\vec{\nabla} P + \vec{v} \frac{\partial P}{\partial t}). \quad (208)$$

Here we have made use of the conservation of entropy.

3.6 summary

We have derived the relativistic hydrodynamics equations, now its application to nuclear collisions is going to be discussed. First, we will follow the pioneering work by Landau which investigated the multiple production of particles with the use of hydrodynamic theory. Second, we are going to study the more realistic condition of particle collisions involved with a well known characteristic method.

4 One dimensional Landau Model

In this chapter, one dimensional Landau model will be discussed, which is taken as a test that the SPH can be applied to high energy nuclear collision. The analytic solution of this model will be described in detail and the SPH numerical simulation of the system would be carried out. The obtained results have been compared which show the SPH method achieves success.

From the point view of Landau [58], the qualitative analysis of the high energy collision process can be divided into several stages. First, as two nucleons collision, a new compound system appears and the energy is concentrated in a small volume. The lorentz contraction takes place in the collision direction. A large amount of particles is produced at the moment of collisions and the collision mean free path is small as it compares with the volume of the system. Second, the system expands which is determined by hydrodynamics theory, and the expansion is regarded as motion of ideal fluid. During the evolution of the system, the collision mean free path is still small so that the hydrodynamics equations work. Due to the velocities in the system are comparable with light velocity, the relativistic hydrodynamics is applied. Third, as the system evolves, the interaction decreases and the collision free path increases. When the mean free path is comparable to the system volume, the system will break up into separate particles.

We are mainly interested in the second stage of high energy collisions which make use of the hydrodynamics theory to describe the expansion of the compound system. As a matter of fact, all SPH particles are set static in the foregoing discussion. However the SPH particles should follow the equation of motion and they are not still any more if problems are taken into account in real fluid. Therefore we investigate the one dimensional Landau model, with the application of the FPM algorithm. Since the analytic solution is well known [59], we can compare the SPH numerical results to it. The analytic solution consists of two parts. One part is Riemann simple wave solution, while the other part is Khalatnikov solution. Both the standard SPH and Taylor SPH algorithms are applied to obtain numerical results.

4.1 Analytic solutions

Before we introduce the two parts of analytic solution for one dimensional Landau model, some important physical quantities and notations need to be illustrated, including the energy density ϵ , the velocity v , the energy density logarithm ζ , the flow rapidity y , the hydrodynamical potential χ , the temperature T , the entropy density s and the sound velocity c_s . The relations between

the physical quantities are as follows

$$\zeta = \frac{1}{4} \ln(\epsilon/\epsilon_0) = \ln(T/T_0), \quad (209)$$

$$\epsilon/\epsilon_0 = (T/T_0)^4 = e^{4\zeta}, \quad (210)$$

$$s/s_0 = (\epsilon/\epsilon_0)^{3/4} = (T/T_0)^3 = e^{3\zeta}, \quad (211)$$

$$v = \tanh y. \quad (212)$$

4.1.1 The Riemann simple wave solution

After the relativistic high energy collisions, the system in the center of mass reference frame has a form of a flat slab whose thickness is $2l$. The slab is in contact with the vacuum at the two edge boundaries. The Riemann simple wave could be regarded as the superposition of the propagation of sound wave with the sound speed c_s and the propagation of the fluid element with the flow velocity v , which is originated from the disturbance presenting at edge boundaries. It can be formulated by

$$y = -\frac{\zeta}{c_s}, \quad (213)$$

$$\frac{x}{t} = \frac{\tanh(-\zeta/c_s) - c_s}{1 - \tanh(-\zeta/c_s)c_s}. \quad (214)$$

Considering an initial slab with width $2l$ at rest in the beginning, it has an initial energy density ϵ_0 . The slab contacts the vacuum and the energy density of the slab will decrease from the matter region to the vacuum region. In this case, the early stage evolution of the slab is governed by the Riemann simple wave solution.

Numerically we conduct the equation (213) and equation (214) as follows. For a definite value of time t , which is smaller than l/c_s , we set the value of the rapidity y to zero at beginning and increase it stepwise. If the value of rapidity y is known, then from equation (213), the energy density logarithm ζ can be evaluated. Subsequently the value of x can be calculated. To obtain the next value of rapidity y , same calculation is repeated. The results of the slab evolution at the early stage can be shown from the Fig 1 in this paper [60]. From this figure, the rarefaction wave begins at $z = l$ and propagates inside to $z = 0$ with the speed of sound c_s . It reaches the spatial position $z = 0$ at time $t = l/c_s = \sqrt{3}l$. Second, as the value of rapidity y increases, the value of energy density logarithm ζ gets more and more negative, which corresponds to the energy density ϵ reduction. So that the change of y yields the whole profile of ϵ/ϵ_0 as a function of z/l for every constant time t . The fluid expands outside and the velocity of fluid element increases. However the velocity will be limited by the speed of light as it contacts the vacuum. So that the farthestmost reach of fluid element is corresponding to $z = l + t$.

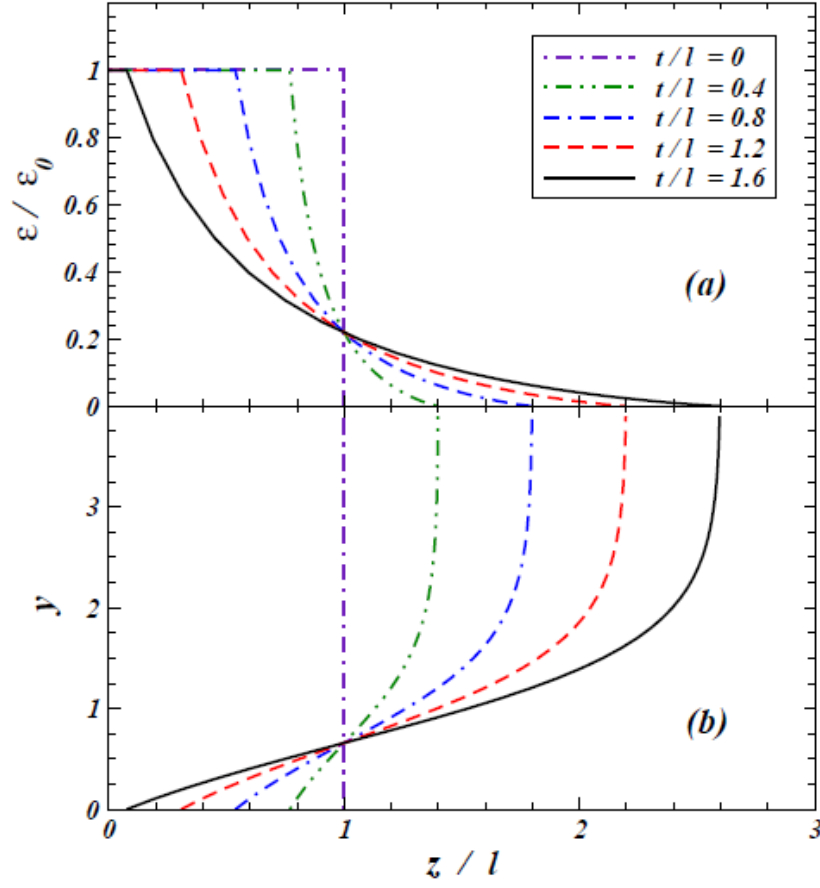


Figure 23: The profile of the energy density ratio ϵ/ϵ_0 and the flow rapidity y as a function of z/l at different values of t/l is achieved by the Riemann simple wave solution. The plot is excerpted from the reference [60].

4.1.2 The Khalatnikov solution

After the time $t \geq l/c_s$, the simple wave that begins at edges and propagates inward reaches the center of slab. Subsequently the fluid expands in the middle region following the Khalatnikov solution. For the Khalatnikov analytic solution,

$$\chi = -l\sqrt{3}e^\zeta \int_{y/\sqrt{3}}^{-\zeta} e^{2\zeta'} I_0 \left[\sqrt{\zeta'^2 - \frac{1}{3}y^2} \right] d\zeta', \quad (215)$$

$$t(\zeta, y) = e^{-\zeta} \left(\frac{\partial \chi}{\partial \zeta} \cosh y - \frac{\partial \chi}{\partial y} \sinh y \right), \quad (216)$$

$$x(\zeta, y) = e^{-\zeta} \left(\frac{\partial \chi}{\partial \zeta} \sinh y - \frac{\partial \chi}{\partial y} \cosh y \right). \quad (217)$$

From the form of the hydrodynamical potential in equation (215), the terms $\frac{\partial \chi}{\partial \zeta}$ and $\frac{\partial \chi}{\partial y}$ can be written as

$$\frac{\partial \chi}{\partial \zeta}(\zeta, y) = \chi + l\sqrt{3}e^{-\zeta} I_0 \left[\sqrt{\zeta^2 - \frac{1}{3}y^2} \right] \quad (218)$$

$$\frac{\partial \chi}{\partial y}(\zeta, y) = -l\sqrt{3}e^\zeta \int_{y/\sqrt{3}}^{-\zeta} e^{2\zeta'} \frac{I_1 \left[\sqrt{\zeta'^2 - \frac{1}{3}y^2} \right]}{\sqrt{\zeta'^2 - \frac{1}{3}y^2}} d\zeta' + le^\zeta e^{2y/\sqrt{3}}. \quad (219)$$

Numerically we want to express (ζ, y) as a function of (z, t) . To achieve this purpose, we consider the value of rapidity y starting from zero and increasing stepwise with a fixed value of time t . From equation (216), for each pair values of (t, y) , the unknown quantity ζ can be calculated. For the evaluation of ζ , we can use the Newton's method by giving a good guess on the value of ζ for a given time t and $y = 0$. Subsequently from the equation (217), the value of x can be defined. The results are shown in the Fig. 2 in this paper,

4.1.3 summary

In this section, we present the analytical solutions of Landau hydrodynamics. The earliest history can be described by the Riemann simple wave solution, and the later evolution stage can be illustrated by the Khalatnikov solution. What's more, the Khalatnikov solution has to be matched to the Riemann simple wave solution at boundary regions. In the following, we are going to introduce the SPH algorithm to deal with the one dimensional Landau model. The equation of motion will be derived and carried out by numerical codes. The numerical results will be represented and compared with the exact analytic solutions.

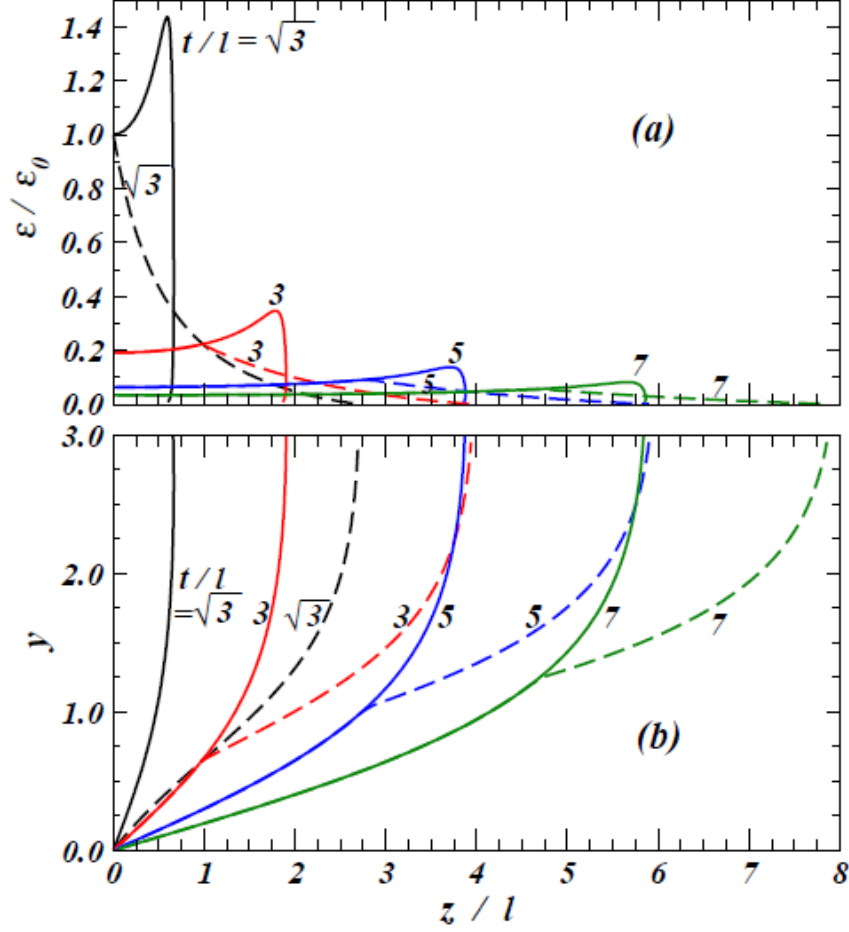


Figure 24: The profile of the energy density ratio ϵ/ϵ_0 and the flow rapidity y as a function of z/l at different values of t/l is achieved by Khalatnikov solution. The solid line give the Khalatnikov solution but it has to match the Riemann simple wave solutions at the boundary regions that are shown as dashed lines. So that a total hydrodynamical solution is made of the Khalatnikov solution for small z/l combining with the matched Riemann solution for large z/l . The plot is excerpted from the reference [60].

4.2 Equation of motion for SPH particles

The equation of motion followed by SPH particles in Cartesian coordinate is written as [61],

$$\frac{d}{dt}(\nu_i \frac{p_i + \varepsilon_i}{s_i} \gamma_i \vec{v}_i) + \sum_j \nu_i \nu_j [\frac{p_i}{s_i^{*2}} + \frac{p_j}{s_j^{*2}}] \nabla_i W(\vec{r}_i - \vec{r}_j; h) = 0. \quad (220)$$

Taking into account a system of one dimensional relativistic massless free baryon gas initially at rest, the equation of state is

$$p = \frac{1}{3} \varepsilon = C s^{\frac{4}{3}}, \quad (221)$$

where

$$C = (\frac{15}{128\pi^2})^{\frac{1}{3}}. \quad (222)$$

The derivation of the equation of motion is as follows:

4.3 Derivation of EOM

The action of the system

$$I = - \int d^4x \varepsilon. \quad (223)$$

and the Lagrangian has the form

$$L = - \int d^3\vec{r} \varepsilon. \quad (224)$$

In the SPH representation, the Lagrangian can be written as

$$L_{SPH}(\vec{r}_i, \vec{v}_i = \frac{d\vec{r}_i}{dt}) = - \sum_i \nu_i (\varepsilon/a^*)_i = - \sum_i (\frac{E}{\gamma})_i \quad (225)$$

where E_i is the rest energy of particle i which equals $\nu_i(\varepsilon/a)_i$ and a^* is the reference density in space-fixed frame. In this case, the action of SPH model is

$$I_{SPH} = - \int dt \sum_i (E/\gamma)_i. \quad (226)$$

then we have

$$\delta I_{SPH} = - \int dt \sum_i (\frac{\delta E \gamma - E \delta \gamma}{\gamma^2})_i \quad (227)$$

where

$$\delta E = -P\delta V, \quad (228)$$

$$\delta\gamma_i = \delta \frac{1}{\sqrt{1-v_i^2}} = \gamma_i^3 \vec{v}_i \cdot \delta \vec{v}_i, \quad (229)$$

$$V_i = \delta \frac{\nu_i}{a_i} = \delta \frac{\gamma \nu_i}{a_i^*}, \quad (230)$$

$$\delta V_i = V_i \left(\frac{\delta\gamma_i}{\gamma_i} - \frac{\delta a_i^*}{a_i^*} \right), \quad (231)$$

$$\delta V_i = -\frac{\nu_i}{a_i} (-\gamma_i^2 \vec{v}_i \cdot \delta \vec{v}_i + \frac{1}{a_i^*} \sum_j \nu_j (\delta \vec{r}_i - \delta \vec{r}_j) \cdot \nabla_i W_{ij}). \quad (232)$$

then we can write the variation of action like

$$\begin{aligned} \delta I_{SPH} = - \int dt \sum_i \{ P_i \frac{\nu_i}{\gamma_i a_i} (-\gamma_i^2 \vec{v}_i \cdot \vec{v}_i + \frac{1}{a_i^*} \sum_j \nu_j (\delta \vec{r}_i - \delta \vec{r}_j) \cdot \nabla_i W_{ij}) \\ - \frac{E_i}{\gamma_i^2} \gamma_i^3 \vec{v}_i \cdot \delta \vec{v}_i \}. \end{aligned} \quad (233)$$

Subsequently,

$$\begin{aligned} \delta I_{SPH} = - \int dt \sum_i -\frac{\nu_i}{a_i} (P + \varepsilon)_i \gamma_i \vec{v}_i \cdot \delta \vec{v}_i - \\ \int dt \sum_i \frac{P_i \nu_i}{a_i^{*2}} \sum_j \nu_j (\delta \vec{r}_i - \delta \vec{r}_j) \cdot \nabla_i W_{ij} \end{aligned} \quad (234)$$

For the equation (234), the first term can be simplified by using the integration by parts, for example,

$$A \delta \vec{v}_i = A \delta \frac{d\vec{r}_i}{dt} = A \frac{d}{dt} \delta \vec{r}_i = \frac{d}{dt} (A \delta \vec{r}_i) - \frac{dA}{dt} \delta \vec{r}_i. \quad (235)$$

then the equation (234) can be written like

$$\begin{aligned} \delta I_{SPH} = - \int dt \sum_i \delta \vec{r}_i \frac{d}{dt} [\nu_i (\frac{P + \varepsilon}{a})_i \gamma_i \vec{v}_i] \\ - \int dt \sum_i \frac{P_i \nu_i}{a_i^{*2}} \sum_j \nu_j (\delta \vec{r}_i - \delta \vec{r}_j) \cdot \nabla_i W_{ij} \end{aligned} \quad (236)$$

and finally

$$\frac{d}{dt} [\nu_i (\frac{P + \varepsilon}{a})_i \gamma_i \vec{v}_i] = - \sum_j [\frac{\nu_i \nu_j}{\gamma_i^2} \frac{P}{a_i^2} + \frac{\nu_i \nu_j}{\gamma_j^2} \frac{P}{a_j^2}] \nabla_i W_{ij} \quad (237)$$

From this equation, it is clear that it conserves the momentum of system.

4.4 numerical results for entropy density in laboratory frame

Now according to the equation of motion of SPH particles combining with the equation of state, numerical implementation can be carried out. Some important parameters related to the evaluation are: the number of SPH particles is 1000 and the number of fixed spatial points is 200. The initial SPH particle is uniformly set in $[-1.0, 1.0]$, while the fixed points are distributed equally in $[-12.0, 12.0]$. The entropy density distribution at fixed spatial points for $t=0.0, 2.0, 4.0, 6.0, 8.0, 10.0$ is shown as follows.

There exists a essential difference when we implement the numerical calculation making use of standard algorithm and Taylor SPH algorithm. For standard SPH algorithm, the entropy density in space-fixed frame has the form

$$s_i^* = \sum_j \nu_j W_{ij}. \quad (238)$$

while for the Taylor SPH algorithm, it can be written as

$$s_j^* = \frac{\sum_i \frac{\nu_i}{s_i^*} (r_i - r_j) \vec{\nabla}_j W_{ji} \cdot \sum_k \nu_k W_{jk} - \sum_i \frac{\nu_i}{s_i^*} (r_i - r_j) W_{ji} \cdot \sum_k \nu_k \vec{\nabla}_j W_{jk}}{\sum_i \frac{\nu_i}{s_i^*} W_{ji} \cdot \sum_k \frac{\nu_k}{s_k^*} (r_k - r_j) \vec{\nabla}_j W_{jk} - \sum_i \frac{\nu_i}{s_i^*} \vec{\nabla}_j W_{ji} \cdot \sum_k \frac{\nu_k}{s_k^*} (r_k - r_j) W_{jk}}, \quad (239)$$

$$s_i^* = \sum_k \nu_k W_{ik}. \quad (240)$$

where the laboratory entropy density s_i^* in equation(239) should be substituted by equation(240).

From Fig. 3 and Fig. 4, We can see that entropy density distribution reproduced with the use of Taylor SPH algorithm is as satisfactory as the application of standard SPH algorithm, which at lease illustrates that the new algorithm Taylor SPH is useful and applicable at present.

5 Transverse expansion on longitudinal scaling expansion

In this chapter, a three dimensional hydrodynamic evolution has been taken into consideration. The transverse expansion of a cylindrically symmetric homogeneous massless pion gas, which undergoes a longitudinally scaling expansion, has been investigated. Compared with one dimensional Landau model, this system is more closer to the realistic condition. It shows the SPH ability to deal with multi-dimensional problems appearing in heavy ion collisions. Most of the context is based on the work by Y. Hama and F.W.Pottag [62]. From this chapter a good understanding of SPH application to complex high dimensional problems can be formed

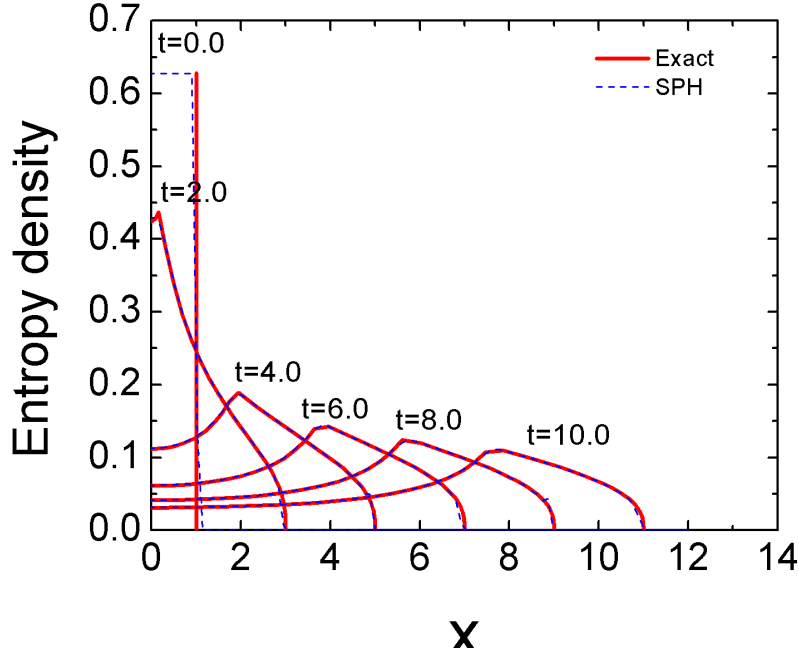


Figure 25: Entropy density for different values of t applying standard SPH, the exact results are given by broken curves, the SPH solution is shown by full curves.

5.1 Resolution of transverse expansion analytically

Considering the transverse expansion of a flat disc, which has the uniform thickness $2l$ and its radius $R \gg l$, its initial temperature T_0 is constant and $T_0 \gg T_d$, where T_d is the breaking up temperature. As discussed before, the equations of relativistic hydrodynamics are

$$\partial_\mu T^{\mu\nu} = 0 \quad (241)$$

where the energy momentum tensor $T^{\mu\nu}$ and the pressure p have the form

$$T^{\mu\nu} = (\varepsilon + p)u^\mu u^\nu - pg^{\mu\nu} \quad (242)$$

$$p = c_0^2 \varepsilon \quad (243)$$

and here c_0 is the sound velocity. The equations have been resolved by Khalatnikov in the case of one dimensional evolution. Define the temperature ratio y and denote flow rapidity by α , giving the conditions

$$y^2 - c_0^2 \alpha^2 \gg 1 \quad (244)$$

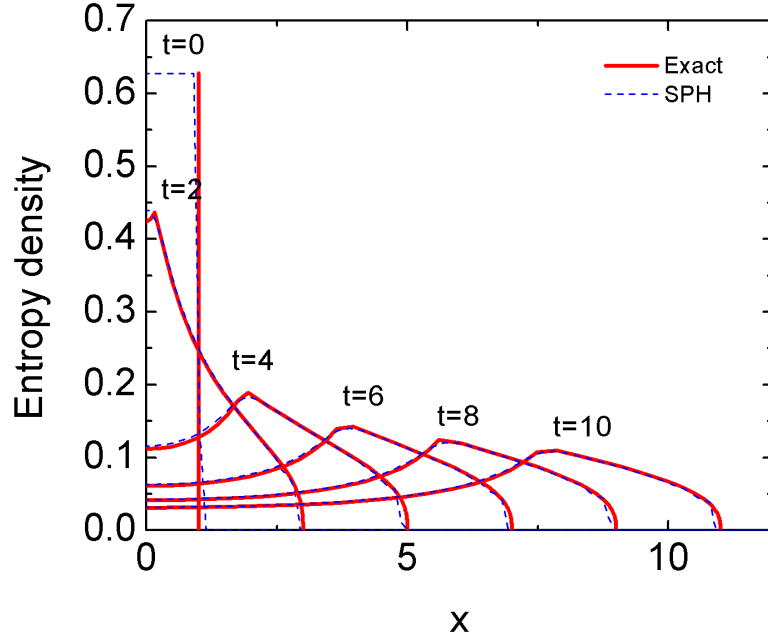


Figure 26: Entropy density for different values of t using Taylor SPH, the exact results are given by broken curves, the SPH solution is shown by full curves.

$$y^2 \gg \alpha^2 \quad (245)$$

where

$$y = \ln \frac{T}{T_0} \quad (246)$$

Under these circumstances, his solution can be written as

$$\alpha = \frac{1}{2} \ln \frac{t+x}{t-x} \quad (247)$$

$$y = -\frac{1+c_0^2}{4} \ln \frac{t^2-x^2}{\Delta^2} + \frac{1-c_0^2}{4} [\ln^2 \frac{t^2-x^2}{\Delta^2} - \ln^2 \frac{t+x}{t-x}]^{1/2} \quad (248)$$

where

$$\Delta = \sqrt{\frac{1-c_0^2}{\pi}} l \quad (249)$$

If $\alpha \ll \ln \frac{\sqrt{t^2-x^2}}{\Delta}$, we can simply y as

$$y = -c_0^2 \ln \frac{\sqrt{t^2-x^2}}{\Delta} \quad (250)$$

In summary, the equation (247) and equation (250) appear as the solutions of the relativistic hydrodynamical equations in one dimension.

Now to investigate the transverse flow expansion, new coordinate system needs to be established. The coordinate system is introduced as follows

$$\tau = \sqrt{t^2 - x^2}, \quad (251)$$

$$\alpha_0 = \tanh^{-1} \frac{x}{t}, \quad (252)$$

$$r = \sqrt{y^2 + z^2}, \quad (253)$$

$$\phi = \tan^{-1} \frac{z}{y}. \quad (254)$$

according to the above relations we have

$$t = \tau \cosh \alpha_0, \quad (255)$$

$$x = \tau \sinh \alpha_0, \quad (256)$$

$$y = r \cos \phi, \quad (257)$$

$$z = r \sin \phi. \quad (258)$$

So that it is easy to get the metric tensor $g^{\mu\nu}$ and $g_{\mu\nu}$ in this new coordinate system

$$g^{00} = 1, \quad (259)$$

$$g^{11} = -\frac{1}{\tau^2}, \quad (260)$$

$$g^{22} = -1, \quad (261)$$

$$g^{33} = -\frac{1}{r^2}. \quad (262)$$

and $g^{\mu\nu} = 0$ for $\mu \neq \nu$.

$$g_{00} = 1, \quad (263)$$

$$g_{11} = -\tau^2, \quad (264)$$

$$g_{22} = -1, \quad (265)$$

$$g_{33} = -r^2. \quad (266)$$

and $g_{\mu\nu} = 0$ for $\mu \neq \nu$.

In the new coordinate system, the four velocity can be rewritten as

$$u^\mu(x) = (\cosh(\alpha - \alpha_0) \cosh \xi, \frac{\sinh(\alpha - \alpha_0)}{\tau} \cosh \xi, \sinh \xi, 0), \quad (267)$$

$$u_\mu(x) = (\cosh(\alpha - \alpha_0) \cosh \xi, -\tau \sinh(\alpha - \alpha_0) \cosh \xi, -\sinh \xi, 0) \quad (268)$$

where ξ is the transverse rapidity.

The relativistic hydrodynamical equation can be generalized as

$$\frac{1}{\sqrt{-g}} \frac{\partial(\sqrt{-g} T_\nu^\mu)}{\partial x^\mu} - \frac{1}{2} \frac{\partial g_{\mu\nu}}{\partial x^\nu} T^{\mu\nu} = 0 \quad (269)$$

According to the form of energy momentum tensor and pressure, by virtue of the thermodynamical relations, it can be simplified as

$$\frac{\partial y}{\partial x^\nu} = -\frac{c_0^2 u_\nu}{\sqrt{-g}} \frac{\partial}{\partial x^\mu} [\sqrt{-g} u^\mu] + u^\mu \frac{\partial u_\nu}{\partial x^\mu} - \frac{u^\mu u^\nabla}{2} \frac{\partial g_{\mu\nabla}}{\partial x^\nu} \quad (270)$$

and now making the assumption that

$$\alpha = \alpha_0 \quad (271)$$

which yields

$$\begin{aligned} \frac{\partial y}{\partial \tau} = & -\frac{c_0^2 \cosh^2 \xi}{\tau} - \frac{c_0^2 \sinh \xi \cosh \xi}{r} + (1 - c_0^2) \sinh \xi \cosh \xi \frac{\partial \xi}{\partial \tau} \\ & + (\sinh^2 \xi - c_0^2 \cosh^2 \xi) \frac{\partial \xi}{\partial r} \end{aligned} \quad (272)$$

$$\frac{\partial y}{\partial \alpha_0} = 0 \quad (273)$$

$$\begin{aligned} \frac{\partial y}{\partial r} = & \frac{c_0^2 \sinh \xi \cosh \xi}{r} + \frac{c_0^2 \sinh^2 \xi}{r} - (\cosh^2 \xi - c_0^2 \sinh^2 \xi) \frac{\partial \xi}{\partial \tau} \\ & - (1 - c_0^2) \sinh \xi \cosh \xi \frac{\partial \xi}{\partial r} \end{aligned} \quad (274)$$

$$\frac{\partial y}{\partial \varphi} = 0 \quad (275)$$

Here we can see that there are two unknown functions y and ξ , and there exist two independent variables τ and r . To solve this system, the boundary conditions require to be specified.

Physically for the central region of the disc and for $t \leq R$, the Khalatnikov one dimensional solution is good for describing the phenomena. However to explain the system expansion at the boundary, the deviation appears with this solution. As a matter of fact, the fluid in three dimensional flow has such boundary conditions. It will be bounded by the surface

$$r = R + \tau \quad (276)$$

one the vacuum side and would relate the one dimensional flow region on

$$r = R - c_0 \tau \quad (277)$$

and when $r = R + \tau$,

$$\xi = \infty, \quad (278)$$

$$y = -\infty \quad (279)$$

and when $r = R - c_0 \tau$

$$\xi = 0, \quad (280)$$

$$y = -c_0^2 \ln \frac{\tau}{\Delta} \quad (281)$$

Along the axis and for $\tau \geq \frac{R}{c_0}$,

$$\xi = 0 \quad (282)$$

which implies

$$\frac{\partial y}{\partial r} = 0 \quad (283)$$

After figuring out these boundary conditions, the equation (272) to equation (275) can be solved. These equations are going to be resolved by characteristic method.

5.2 Characteristic method

Mathematically the method of characteristics is a technique to solve the partial differential equations. It can reduce a partial differential equation to a family of ordinary differential equations. For example, let us see how it works for first order partial differential equation. Considering a function z of two independent variables x and y , it satisfies the following relation

$$a(x, y, z) \frac{\partial z}{\partial x} + b(x, y, z) \frac{\partial z}{\partial y} = c(x, y, z) \quad (284)$$

From this partial differential equation, a normal vector to the surface $z = z(x, y)$ is

$$\mathbf{N} = \left(\frac{\partial z}{\partial x}(x, y), \frac{\partial z}{\partial y}(x, y), -1 \right) \quad (285)$$

In this case, we can regard the partial differential equation as the vector field \mathbf{D}

$$\mathbf{D} = (a(x, y, z), b(x, y, z), c(x, y, z)) \quad (286)$$

tangent to the surface $z = z(x, y)$. Because for every point at the surface, the dot product of vector field \mathbf{D} with the normal vector \mathbf{N} is zero. Therefore the solution can be considered as a set of integral curves of the vector field. These integral curves can be expressed by

$$\frac{dx}{a(x, y, z)} = \frac{dy}{b(x, y, z)} = \frac{dz}{c(x, y, z)} \quad (287)$$

Finally assuming the parameter t of the curves is fixed, we can obtain

$$\frac{dx}{dt} = a(x, y, z), \quad (288)$$

$$\frac{dy}{dt} = b(x, y, z), \quad (289)$$

$$\frac{dz}{dt} = c(x, y, z). \quad (290)$$

We call these equations as characteristic equations for the original system.

Now applying the characteristic method to the transverse flow expansion, we have

$$y = y_t - c_0^2 \ln \frac{\tau}{\Delta} \quad (291)$$

where y_t denotes the transverse contribution which separates from the longitudinal contribution $-c_0^2 \ln \frac{\tau}{\Delta}$. It should note that the new variable y_t satisfies the boundary condition

$$y_t = 0 \quad (292)$$

at $r = R - c_0\tau$ which is equivalent to the equations (280) and (281). For the rapidity variables y_t and ξ , introducing the variables ψ and φ , they have such relations

$$\psi = y_t + c_0\xi, \quad (293)$$

$$\varphi = y_t - c_0\xi. \quad (294)$$

so that it is easy to obtain the reverse relations

$$y_t = \frac{1}{2}(\psi + \varphi), \quad (295)$$

$$\xi = \frac{1}{2c_0}(\psi - \varphi) \quad (296)$$

With the help of these transformations, the equations we need to calculate become

$$\frac{\partial\psi}{\partial\tau} + \frac{v_t + c_0}{1 + c_0v_t} \frac{\partial\varphi}{\partial r} + \frac{c_0^2v_t}{1 + c_0v_t} \left[\frac{1}{r} - \frac{c_0}{\tau} \right] = 0, \quad (297)$$

$$\frac{\partial\varphi}{\partial\tau} + \frac{v_t - c_0}{1 - c_0v_t} \frac{\partial\varphi}{\partial r} + \frac{c_0^2v_t}{1 - c_0v_t} \left[\frac{1}{r} + \frac{c_0}{\tau} \right] = 0. \quad (298)$$

where

$$v_t = \tanh \frac{\psi - \varphi}{2c_0} \quad (299)$$

From the above quasi-linear equations, the following characteristics curves are obtained

$$\frac{dr}{d\tau} = \frac{v_t + c_0}{1 + c_0v_t}, \quad (300)$$

$$\frac{dr}{d\tau} = \frac{v_t - c_0}{1 - c_0v_t} \quad (301)$$

Along the curve expressed by equation (300), we have

$$d\psi = \frac{c_0^2v_t}{1 + c_0v_t} \left[\frac{c_0}{\tau} - \frac{1}{r} \right] d\tau \quad (302)$$

and along the curve illustrated by equation (301), we obtain

$$d\varphi = -\frac{c_0^2v_t}{1 - c_0v_t} \left[\frac{c_0}{\tau} + \frac{1}{r} \right] d\tau \quad (303)$$

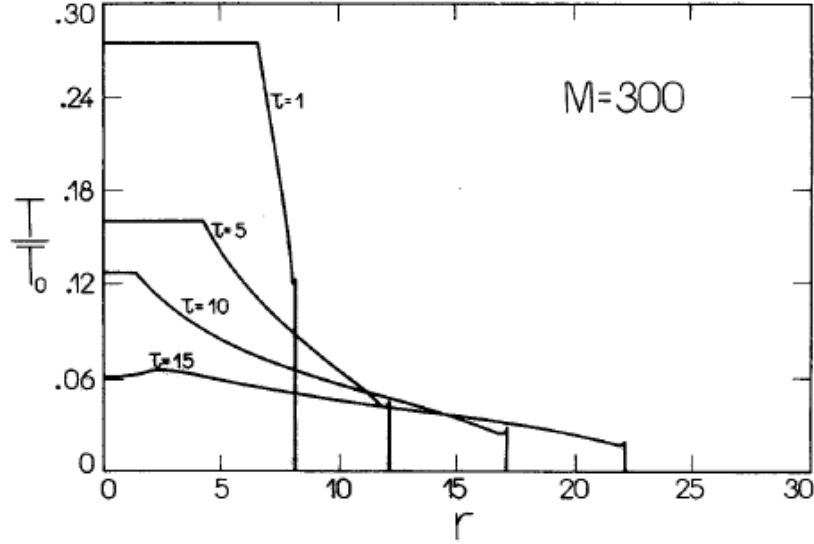


Figure 27: Radial distribution of T/T_0 at different instants $\tau = 1.0, 5.0, 10.0, 15.0$. The plot is excerpted from the reference [63].

In summary, to solve the transverse part of hydrodynamical equations, the procedure is to integrate the equations (302) and (303) along the curves (300) and (301) with the help of the boundary conditions as discussed before.

The discussion of how to solve the hydrodynamical equations of transverse flow expansion is over which is based on the work done by Yogi Hama and Pottag [63]. Here we want to show the temperature evolution at the radial direction which is display at Fig. 6 in their work.

5.3 SPH formulation and evaluation for the transverse expansion

Here we emphasis on the numerical resolution by using SPH method. We are going to introduce the general coordinate because it is very important when we take into account realistic initial conditions for simulations of RHIC processes. It is well known that during a relativistic heavy ion collisions, the initial state of the system is a cold and quantum nuclear matter. After the process of collisions, the hadronic matter will stay at an off-shell state and the process of materialization takes place only after $\sim 1 fm/c$ in the proper time. In this case, the local thermodynamical state occurs not for the global space-fixed time but for local proper time. So that it is significant to choose specific coordinate system to describe the relativistic heavy ion collisions. Therefore the hyperbolic

time and longitudinal coordinates will be addressed subsequently.

5.3.1 General coordinate system

Taking into account a general coordinate system,

$$ds^2 = g_{\mu\nu} dx^\mu dx^\nu \quad (304)$$

Here the time-time coordinate is orthogonal to the space-time coordinates in order to define the conserved quantity without any doubts,

$$g_{\mu 0} = 0 \quad (305)$$

And the variation of the action for the relativistic fluid has the form

$$\delta I = -\delta \int d^4x \sqrt{-g} \varepsilon = 0 \quad (306)$$

The total entropy of the system is conserved due to the adiabatic approximation, which can be expressed by

$$\frac{1}{\sqrt{-g}} \partial_\mu (\sqrt{-g} s u^\mu) = 0 \quad (307)$$

$$\frac{1}{\sqrt{-g}} \partial_\tau (\sqrt{-g} s \gamma) + \frac{1}{\sqrt{-g}} \sum_{i=1}^3 \partial_i (\sqrt{-g} s \gamma v^i) = 0 \quad (308)$$

where

$$v^i = \frac{u^i}{u^0} \quad (309)$$

There are some notations going to be used,

$$\tau = x^0, \quad (310)$$

$$\gamma = u^0 \quad (311)$$

and the general gamma factor can be derived by virtue of the identity

$$u_\mu u^\mu = 1 \quad (312)$$

therefore it has the following form

$$\gamma = \frac{1}{\sqrt{g_{00} - \mathbf{v}^T \mathbf{g} \mathbf{v}}} \quad (313)$$

Now the SPH formulation for the action principle will be addressed. Before talking about this, the SPH representation for the entropy density is important and essential. As a matter of fact, there are two ways to define the entropy density,

$$\sqrt{-g} s \gamma = s^* \quad (314)$$

or

$$s\gamma = s^* \quad (315)$$

Since the total entropy is written as

$$S = \int d^3\mathbf{r} \sqrt{-g} s\gamma = \sum_i \nu_i \quad (316)$$

therefore for the parametrization equation (314), the normalization of kernel function W is

$$\int d^3\mathbf{r} W(\mathbf{r} - \mathbf{r}') = 1 \quad (317)$$

and for the parametrization equation (315), it should be taken as

$$\int d^3\mathbf{r} \sqrt{-g} W(\mathbf{r} - \mathbf{r}') = 1 \quad (318)$$

It should be noted that the $-\mathbf{g}$ is the three by three space part of the general metric tensor $g_{\mu\nu}$ which is dependent on space time. In the usual calculation, it is not desirable for the kernel function to depend on space time. So that the expression of entropy density is taken as the form of equation (314).

After making sure of the approximation of the entropy density, the SPH action is given by

$$I_{SPH} = - \int d^4x \sqrt{-g} \varepsilon = - \int d\tau \int d^3\mathbf{r} \sqrt{-g} \varepsilon, \quad (319)$$

$$I_{SPH} = - \int d\tau \int d^3\mathbf{r} \sum_i \nu_i \left(\frac{\sqrt{-g} \varepsilon}{\sqrt{-g} s \gamma} \right)_i W(\mathbf{r} - \mathbf{r}_i), \quad (320)$$

$$I_{SPH} = - \int d\tau \sum_i \left(\frac{\varepsilon}{s \gamma} \right)_i \quad (321)$$

Using the above form of action and applying the variational principle, the following equation of motion is obtained,

$$\begin{aligned} \frac{d\pi_i}{d\tau} = & - \sum_j \nu_i \nu_j \left[\frac{1}{\sqrt{-g_i} \gamma_i^2} \frac{p_i}{s_i^2} + \frac{1}{\sqrt{-g_j} \gamma_j^2} \frac{p_j}{s_j^2} \right] \nabla_i W_{ij} \\ & + \frac{\nu_i p_i}{\gamma_i s_i} \left(\frac{1}{\sqrt{-g}} \nabla \sqrt{-g} \right)_i \\ & + \frac{\nu_i \gamma_i}{2} \left(\frac{p + \varepsilon}{s} \right)_i (\nabla g_{00} - \mathbf{v}^T \nabla \mathbf{g} \mathbf{v})_i \end{aligned} \quad (322)$$

where the momentum π_i has the form

$$\pi_i = \gamma_i \nu_i \left(\frac{p + \varepsilon}{s} \right)_i \mathbf{g} \mathbf{v}_i \quad (323)$$

The detailed deduction of the above equation of motion is going to be addressed as follows. The Lagrangian of the system has the form

$$L = - \sum_i \nu_i \left(\frac{\varepsilon}{s \gamma} \right)_i = - \sum_i \left(\frac{E}{\gamma} \right)_i \quad (324)$$

where E_i denotes the rest energy of the particle i . The variation of the Lagrangian is written as

$$\delta L = - \sum_i \delta \left(\frac{E}{\gamma} \right)_i = \sum_i \frac{p_i}{\gamma_i} \delta V_i + \sum_i \frac{\varepsilon_i \nu_i}{s_i \gamma_i^2} \delta \gamma_i \quad (325)$$

where the variation of E_i equaling $p \delta V_i$ has been used. Now it is necessary to obtain the variation of gamma factor $\delta \gamma_i$ and the volume δV_i .

$$\begin{aligned} \delta \gamma_i &= \delta [g_{00} - v^{\mu 2} g_{\mu\mu}]_i^{-\frac{1}{2}} \\ &= -\frac{1}{2} [g_{00} - v^{\mu 2} g_{\mu\mu}]_i^{-\frac{3}{2}} (-2) (v^1 g_{11} \delta v^1 + v^2 g_{22} \delta v^2 + v^3 g_{33} \delta v^3)_i \\ &\quad - \frac{1}{2} [g_{00} - v^{\mu 2} g_{\mu\mu}]_i^{-\frac{3}{2}} (\nabla g_{00} - v^{\mu 2} \nabla g_{\mu\mu})_i \delta \mathbf{r}_i \\ &= \gamma_i^3 \mathbf{v}_i^T g_i \delta V_i - \frac{1}{2} \gamma_i^3 (\nabla g_{00} - v^T \nabla g v)_i \delta \mathbf{r}_i \end{aligned} \quad (326)$$

and the volume has the form

$$V_i = \frac{\nu_i}{s_i} = \frac{\nu_i \gamma_i \sqrt{-g_i}}{s_i^*} \quad (327)$$

therefore

$$\begin{aligned} \delta V_i &= V_i \left(\frac{\delta \gamma_i}{\gamma_i} - \frac{\delta s_i^*}{s_i^*} \right) + \frac{\nu_i \gamma_i}{s_i^*} \delta(\sqrt{-g_i}) \\ &= \frac{\nu_i}{s_i} \left[\gamma_i^2 \mathbf{v}_i^T g_i \delta V_i - \frac{1}{2} \gamma_i^2 (\nabla g_{00} - \mathbf{v}^T \nabla g v)_i \delta \gamma_i \right] \\ &\quad - \frac{\nu_i}{\sqrt{-g_i} s_i^2 \gamma_i} \sum_j \nu_j \nabla_i W_{ij} (\delta \mathbf{r}_i - \delta \mathbf{r}_j) + \frac{\nu_i \gamma_i}{s_i^*} \delta(\sqrt{-g_i}) \end{aligned} \quad (328)$$

Now the two key terms $\delta \gamma_i$ and δV_i are obtained, so that the variation of La-

grangian can be expressed as

$$\begin{aligned}
\delta L &= \sum_i \frac{p_i \nu_i}{\gamma_i s_i} [\gamma_i^2 \mathbf{v}_i^T g_i \delta v_i - \frac{1}{2} \gamma_i^2 (\nabla g_{00} - \mathbf{v}^T \nabla g v)_i \delta \gamma_i] \\
&\quad - \sum_i \sum_j \frac{p_i}{\gamma_i} \frac{\nu_i \nu_j}{\sqrt{-g_i} s_i^2 \gamma_i} \nabla_i W_{ij} (\delta \mathbf{r}_i - \delta \mathbf{r}_j) + \sum_i \frac{p_i}{\nu_i} \frac{\nu_i \gamma_i}{s_i^*} \nabla \sqrt{-g_i} \delta \gamma_i \\
&\quad + \sum_i \frac{\varepsilon_i \nu_i}{s_i \gamma_i^2} \gamma_i^3 \mathbf{v}_i^T g_i \delta V_i - \frac{1}{2} \sum_i \frac{\varepsilon_i \nu_i}{s_i \gamma_i^2} \gamma_i^3 (\nabla g_{00} - \mathbf{v}^T \nabla g v)_i \delta \gamma_i \\
&= \sum_i \left(\frac{p_i \nu_i}{s_i} \gamma_i \mathbf{v}_i^T g_i + \frac{\varepsilon_i \nu_i}{s_i} \gamma_i \mathbf{v}_i^T g_i \right) \delta V_i \\
&\quad - \frac{1}{2} \sum_i \frac{p_i \nu_i}{s_i} \gamma_i (\nabla g_{00} - \mathbf{v}^T \nabla g v)_i \delta \mathbf{r}_i \\
&\quad - \sum_i \sum_j \nu_i \nu_j \left(\frac{p_i}{\sqrt{-g_i} s_i^2 \gamma_i^2} + \frac{p_j}{\sqrt{-g_j} s_j^2 \gamma_j^2} \right) \nabla_i W_{ij} \delta \mathbf{r}_i \\
&\quad - \frac{1}{2} \sum_i \frac{\varepsilon_i \nu_i}{s_i} \gamma_i (\nabla g_{00} - \mathbf{v}^T \nabla g v)_i \delta \mathbf{r}_i \tag{329} \\
&\quad + \sum_i \frac{p_i \nu_i}{s_i^*} \nabla \sqrt{-g_i} \delta \gamma_i \\
&= \sum_i \frac{d}{dt} \left[\frac{(p_i + \varepsilon_i) \nu_i}{s_i} \nu_i \mathbf{v}_i^T g_i \delta \mathbf{r}_i \right] \\
&\quad - \sum_i \frac{d}{dt} \left[\frac{p_i + \varepsilon_i}{s_i} \nu_i \gamma_i \mathbf{v}_i^T g_i \right] \delta \mathbf{r}_i \\
&\quad - \frac{1}{2} \sum_i \frac{p_i + \varepsilon_i}{s_i} \nu_i \gamma_i (\nabla g_{00} - \mathbf{v}^T \nabla g v)_i \delta \mathbf{r}_i \\
&\quad - \sum_i \sum_j \nu_i \nu_j \left(\frac{p_i}{\sqrt{-g_i} s_i^2 \gamma_i^2} + \frac{p_j}{\sqrt{-g_j} s_j^2 \gamma_j^2} \right) \nabla_i W_{ij} \delta \mathbf{r}_i \\
&\quad + \sum_i \frac{p_i \nu_i}{s_i \gamma_i \sqrt{-g_i}} \nabla \sqrt{-g_i} \delta \mathbf{r}_i
\end{aligned}$$

5.3.2 Hyperbolic coordinate system

For the hyperbolic coordinate, which is related to the Cartesian coordinate by

$$\tau = \sqrt{t^2 - z^2}, \tag{330}$$

$$x = x, \tag{331}$$

$$y = y, \tag{332}$$

$$\eta = \frac{1}{2} \ln \frac{t+z}{t-z}. \tag{333}$$

Where the τ is not exactly the proper time of matter but the time-like coordinate in hyperbolic coordinate. From the relation between coordinates, the metric

tensor is given by

$$g_{00} = 1, g_{11} = -1, g_{22} = -1, g_{33} = -\tau^2, \quad (334)$$

$$g_{\mu\nu} = 0, \mu \neq \nu. \quad (335)$$

Deriving from the conservation of energy momentum tensor and only consider the spatial part,

$$\partial^\mu (\tau T_{\mu i}) = 0. \quad (336)$$

where the energy momentum tensor has the form $T_{\mu i} = (\varepsilon + P)u_\mu u_i - g_{\mu i}P, i = 1, 2, 3$. And finally we can obtain the equation of motion:

$$\frac{d}{d\tau} \left(\frac{\varepsilon + P}{s} g_{ij} u^j \right) = \frac{1}{s\gamma} \partial_i P. \quad (337)$$

If we consider the system evolution in the cartesian coordinate, from the equations (185) to (188), we can have the relation

$$\begin{pmatrix} d\tau \\ dx \\ dy \\ d\eta \end{pmatrix} = \begin{pmatrix} \cosh \eta & 0 & 0 & -\sinh \eta \\ 0 & 1 & 0 & 0 \\ 0 & 0 & 1 & 0 \\ -\frac{\sinh \eta}{\tau} & 0 & 0 & \frac{\cosh \eta}{\tau} \end{pmatrix} \begin{pmatrix} dt \\ dx \\ dy \\ dz \end{pmatrix} \quad (338)$$

Divided by the proper time on both sides, we will have

$$\begin{pmatrix} \gamma' \\ u'_x \\ u'_y \\ u'_\eta \end{pmatrix} = \begin{pmatrix} \cosh \eta & 0 & 0 & -\sinh \eta \\ 0 & 1 & 0 & 0 \\ 0 & 0 & 1 & 0 \\ -\frac{\sinh \eta}{\tau} & 0 & 0 & \frac{\cosh \eta}{\tau} \end{pmatrix} \begin{pmatrix} \gamma \\ u_x \\ u_y \\ u_z \end{pmatrix} \quad (339)$$

where γ' denotes the lorentz factor in the hyperbolic coordinate and γ is the one in cartesian coordinate frame. Now the relation between velocity in both frames is clear,

$$\gamma' = \gamma(\cosh \eta - \sinh \eta v_z), \quad (340)$$

$$v'_x = \frac{v_x}{\cosh \eta - \sinh \eta v_z}, \quad (341)$$

$$v'_y = \frac{v_y}{\cosh \eta - \sinh \eta v_z}, \quad (342)$$

$$v'_\eta = \frac{-\sinh \eta + \cosh \eta v_z}{\tau(\cosh \eta - \sinh \eta v_z)}. \quad (343)$$

For example, for the equation of motion at z direction,

$$\frac{dv_z}{dt} = -\frac{1}{(\varepsilon + P)\gamma^2} (\partial_z P + v_z \frac{\partial P}{\partial t}) \quad (344)$$

where

$$\frac{d}{dt} = \cosh \eta \frac{d}{d\tau} - \frac{\sinh \eta}{\tau} \frac{d}{d\eta}, \quad (345)$$

$$v_z = \frac{\tau v_\eta \cosh \eta + \sinh \eta}{\tau v_\eta \sinh \eta + \cosh \eta}, \quad (346)$$

$$\partial_z P = -\sinh \eta \frac{\partial P}{\partial \tau} + \frac{\cosh \eta}{\tau} \frac{\partial P}{\partial \eta}, \quad (347)$$

$$\frac{\partial P}{\partial t} = \cosh \eta \frac{\partial P}{\partial \tau} - \frac{\sinh \eta}{\tau} \frac{\partial P}{\partial \eta}. \quad (348)$$

as a test, if $v_\eta = 0$ and the pressure P is not the function of η , then

$$v_z = \frac{\sinh \eta}{\cosh \eta}, \quad (349)$$

$$\frac{\partial P}{\partial \eta} = 0, \quad (350)$$

$$\partial_z P + v_z \frac{\partial P}{\partial t} = -\sinh \eta \frac{\partial P}{\partial \tau} + \frac{\sinh \eta}{\cosh \eta} \cosh \eta \frac{\partial P}{\partial t} = 0, \quad (351)$$

$$\frac{dv_z}{dt} = \frac{d(\tanh \eta)}{dt} = 0. \quad (352)$$

In the previous section, the SPH representation of equation of motion has been deducted in general coordinate system. Here the hyperbolic coordinate system as one specific coordinate, the equation of motion can be written as

$$\frac{d}{d\tau} \left(\frac{\varepsilon + P}{s} \gamma v_x \right) = -\frac{1}{\tau} \sum_j \nu_j \left[\frac{p_i}{\gamma_i^2 s_i^2} + \frac{p_j}{\gamma_j^2 s_j^2} \right] \partial_x W_{ij}, \quad (353)$$

$$\frac{d}{d\tau} \left(\frac{\varepsilon + P}{s} \gamma v_y \right) = -\frac{1}{\tau} \sum_j \nu_j \left[\frac{p_i}{\gamma_i^2 s_i^2} + \frac{p_j}{\gamma_j^2 s_j^2} \right] \partial_y W_{ij}, \quad (354)$$

$$\frac{d}{d\tau} \left(\frac{\varepsilon + P}{s} \gamma \tau^2 v_\eta \right) = -\frac{1}{\tau} \sum_j \nu_j \left[\frac{p_i}{\gamma_i^2 s_i^2} + \frac{p_j}{\gamma_j^2 s_j^2} \right] \partial_\eta W_{ij}. \quad (355)$$

where the lorentz factor

$$\gamma = \frac{1}{\sqrt{1 - v_x^2 - v_y^2 - \tau^2 v_\eta^2}}. \quad (356)$$

The analytic solution has been addressed before. Now applying the SPH formulations of equation of motion to obtain the temperature evolution in radial direction which is in order to make comparisons with the analytic results. The work has been done by Yogi, et. al. [62] which is presently in his review paper by Fig. 10, here is shown by Fig. 28.

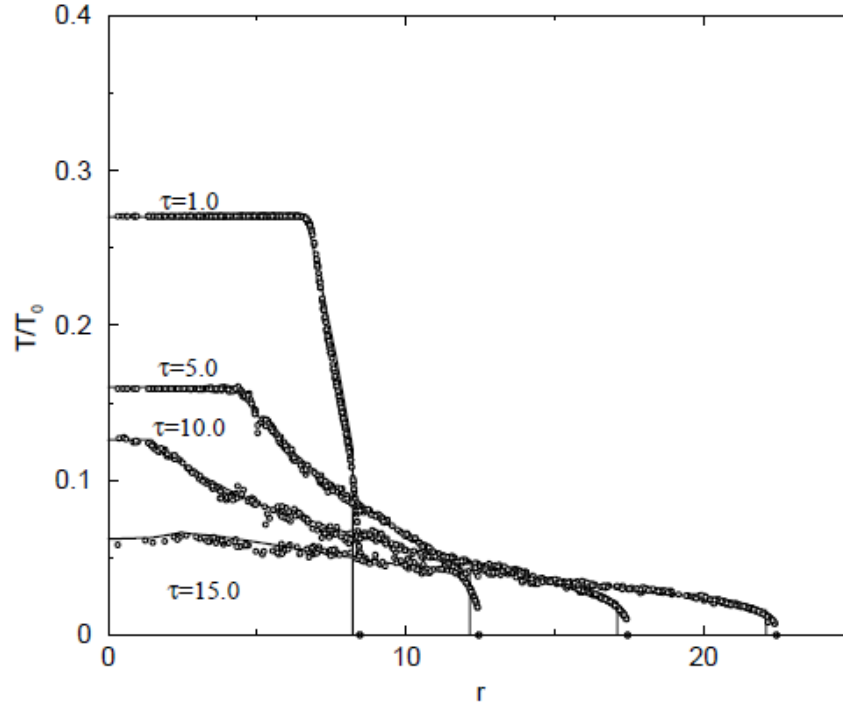


Figure 28: Radial distribution of T/T_0 at different instants $\tau = 1.0, 5.0, 10.0, 15.0$, the SPH results at $\eta = 0$ shown by circles are compared with the numerical solution by using characteristic method. The plot is excerpted from the reference [62].

5.4 Conclusions

In summary, the transverse expansion of a cylindrically symmetric homogeneous massless pion gas, which is undergoing a longitudinal scaling expansion and stay at rest initially in transverse directions has been discussed. This test is closer to a realistic situation comparing with the one dimensional Landau model. The detailed analytic solution by virtue of the characteristic method and SPH numerical results have been presented. The SPH simulations of temperature evolution at transverse direction is compared with those of analytic solution, which is satisfactory.

The SPH simulations have achieved success in dealing with the problems of realistic heavy ion collision process. During these implementations, the standard SPH scheme is employed. However, as discussed before, the FPM method restores the particle consistency which may improve the accuracy of the numerical results. So that we are interested in investigating the FPM method and apply it to realistic problems. The first thing is to derive a new equation of motion based on the FPM method.

6 Hydrodynamic equation of motion in FPM

In this chapter, a hydrodynamic equation of motion in FPM is derived. As mentioned in the previous paragraphs, the FPM method keeps good particle consistency, which can lead to better numerical results. Although the form of equation of motion in FPM is more complex than that in standard SPH, it is still meaningful. The detailed derivation of equation of motion will be given.

The standard SPH presents some inherent problems which cause low numerical accuracy under certain circumstances. The particle consistency is one of the notable problems that reflects the difference between the discrete form summation over particles and the corresponding continuous form involving the kernel function integral. The particle inconsistency in standard SPH is illustrated since it is unable to reproduce a constant function. This is result from the particle approximation which is closely related to the boundary particles, irregular particle distribution and the smoothing length. The FPM method, as discussed before, is proposed to restore particle consistency. The basic idea of this method is performing the Taylor series expansion of a function and multiplying both sides of equation by basis functions and integrating over the whole problem space. It has been demonstrated that the particle consistency is associated to the order of the expansion terms, which is independent of the specific form of these basis functions and the particle distribution.

In usual SPH calculations to the partial differential equations, the gradient terms are usually symmetrized or asymmetric based upon some rules. For the equation of motion, the pressure gradient is symmetrized in order to obey the Newton's third law. The pair of forces exerting on the two particles should be equal in size but opposite in direction. As mentioned before, the equation of motion can be derived from the conservation of energy momentum tensor

or variational principle. The satisfaction of Newton's third law is guaranteed if one deduces the hydrodynamic equations making use of the variational principle. For system of event by event fluctuating initial conditions, although the SPH particles distribution is set uniformly at the initial moment, it will be irregular as the system evolves in time. In this case, the FPM approach is desirable to deal with such physical system. The momentum conservation is very crucial for small systems produced in the relativistic heavy ion collisions, so that a model which exactly and explicitly guarantee the conservation of momentum need to be developed. However as shown in chapter two, the form of FPM is not straightforward to keep the momentum conservation just by symmetrizing some certain physical quantities. To apply the FPM method to relativistic heavy ion collisions, like the one dimensional Landau model and the transverse expansion flow, we need to use the variational principle combining with the FPM approach to obtain the corresponding equation of motion. How to obtain the new equation of motion by virtue of the FPM method is the main goal of this section.

The relativistic hydrodynamic equation for ideal fluid has been deduced in previous context,

$$\frac{d}{d\tau}(\frac{\varepsilon + p}{s}\gamma g_{ij}v^j) - \frac{1}{s\gamma}\partial_i P = 0 \quad (357)$$

where ε, p, s are the energy density, pressure and entropy density in the lagrangian frame. γ, v^j are the gamma factor, three velocity of the fluid element, the g_{ij} denotes the metric in Minkowski space.

For the standard SPH, the gradient of pressure has been symmetrized which is given by

$$(\partial P)_i = \sum_j \nu_j s_i^* (\frac{P_i}{s_i^{*2}} + \frac{P_j}{s_j^{*2}}) \nabla_i W(\mathbf{r}_i - \mathbf{r}_j, h) \quad (358)$$

together with the expression of entropy density

$$s_i^* = \sum_j \nu_j W(\mathbf{r}_i - \mathbf{r}_j, h) \quad (359)$$

so that the hydrodynamic equation in SPH representation is

$$\frac{d}{dt}(\nu_i \frac{p_i + \varepsilon_i}{s_i} \gamma_i \mathbf{v}_i) = - \sum_j \nu_i \nu_j [\frac{P_i}{s_i^{*2}} + \frac{P_j}{s_j^{*2}}] \nabla_i W(\mathbf{r}_i - \mathbf{r}_j, h) \quad (360)$$

the R.H.S of equation (360) can be written as

$$\sum_j \mathbf{f}_{ij} \quad (361)$$

with

$$\mathbf{f}_{ij} = -\nu_i \nu_j \frac{P_i}{s_i^{*2}} \nabla_i W(x_i - x_j; h) \quad (362)$$

Because the kernel function W is an even function, it is clear that

$$\mathbf{f}_{ij} = -\mathbf{f}_{ji} \quad (363)$$

This exactly reflects the Newton's third law.

One method to get the new equation of motion is directly approximation the entropy density and the gradient of pressure by FPM method,

$$s_i^* = \frac{\langle \Delta x \rangle_{i,x} \langle s \rangle_i - \langle \Delta x \rangle_i \langle s \rangle_{i,x}}{\langle 1 \rangle_i \langle \Delta x \rangle_{i,x} - \langle 1 \rangle_{i,x} \langle \Delta x \rangle_i} \quad (364)$$

$$(\partial p)_i = \frac{\langle 1 \rangle_i \langle P \rangle_{i,x} - \langle 1 \rangle_{i,x} \langle p \rangle_i}{\langle 1 \rangle_i \langle \Delta x \rangle_{i,x} - \langle 1 \rangle_{i,x} \langle \Delta x \rangle_i} \quad (365)$$

where the term $\langle p \rangle_i, \langle p \rangle_{i,x}$ can be written as

$$\langle p \rangle_i = \sum_j \frac{\nu_j p_j}{\rho_j} W_{ij}, \quad (366)$$

$$\langle p \rangle_{i,x} = \sum_j \frac{\nu_j p_j}{\rho_j} \nabla_i W_{ij} \quad (367)$$

If we follow this idea to write down the hydrodynamic equation of motion, it is easy to find that this obtained hydrodynamic equation does not take into account the momentum conservation.

As the equation of motion derived in one dimensional Landau Model, we have

$$\delta I_{SPH} = - \int dt \sum_i \delta \vec{r}_i \frac{d}{dt} [\nu_i (\frac{P + \varepsilon}{a})_i \gamma_i \vec{v}_i] - \int dt \sum_i \frac{P_i \nu_i}{a_i^{*2}} \delta a_i^* \quad (368)$$

Now using the new algorithm, choosing the entropy density as the reference density. Before making variation with respect to s_i^* , we consider the general variation for arbitrary quantity a_i and b_i , which has the form

$$a_i = g_i \sum_j t_j W^{(e)}(x_i - x_j; h), \quad (369)$$

$$b_i = h_i \sum_j u_j W^{(o)}(x_i - x_j; h). \quad (370)$$

where $W^{(e)}(x_i - x_j; h)$ is any even kernel function and $W^{(o)}(x_i - x_j; h)$ is any

odd kernel function. In this case, it is easy to find

$$\begin{aligned}
\delta(\sum_i a_i) &= \delta \sum_i g_i \sum_j t_j W^{(e)}(x_i - x_j; h) \\
&= \delta \sum_i \sum_j g_i t_j W^{(e)}(x_i - x_j; h) \\
&= \sum_i \sum_j g_i t_j \delta W^{(e)}(x_i - x_j; h) \\
&= \sum_i \sum_j g_i t_j W_i^{(e)}(\delta \mathbf{r}_i - \delta \mathbf{r}_j) \\
&= \sum_i \sum_j g_i t_j W_i^{(e)} \delta x_i - \sum_i \sum_j g_i t_j W_i^{(e)} \delta x_j.
\end{aligned} \tag{371}$$

For the second term on the r.h.s of equation (371), exchanging the index i and j yields

$$\delta(\sum_i a_i) = \sum_i \sum_j g_i t_j W_i^{(e)} \delta x_i - \sum_j \sum_i g_j t_i W_j^{(e)} \delta x_i \tag{372}$$

For the even function $W^{(e)}(x_i - x_j; h)$, the derivative to the spatial coordinate x_i and x_j has the relation

$$\begin{aligned}
W_j^{(e)}(x_i - x_j; h) &= \frac{\partial W^{(e)}}{\partial x_j}(x_i - x_j; h) \\
&= -\frac{\partial W^{(e)}}{\partial x_i}(x_i - x_j; h)
\end{aligned} \tag{373}$$

Therefore

$$\begin{aligned}
\delta(\sum_i a_i) &= \sum_i \sum_j g_i t_j W_i^{(e)} \delta x_i + \sum_j \sum_i g_j t_i W_i^{(e)} \delta x_i \\
&= \sum_{ij} (g_i t_j + g_j t_i) W_i^{(e)}(x_i - x_j; h) \delta x_i
\end{aligned} \tag{374}$$

The same procedure can be done for the variation of summation of b ,

$$\begin{aligned}
\delta(\sum_i b_i) &= \delta \sum_i h_i \sum_j \mu_j W^{(o)}(x_i - x_j; h) \\
&= \delta \sum_i \sum_j h_i \mu_j W^{(o)}(x_i - x_j; h) \\
&= \sum_i \sum_j h_i \mu_j \delta W^{(o)}(x_i - x_j; h) \\
&= \sum_i \sum_j h_i \mu_j W_i^{(o)}(\delta \mathbf{r}_i - \delta \mathbf{r}_j) \\
&= \sum_i \sum_j h_i \mu_j W_i^{(o)} \delta x_i - \sum_i \sum_j h_i \mu_j W_i^{(o)} \delta x_j.
\end{aligned} \tag{375}$$

For the second term on the r.h.s of equation (375), exchanging the index i and j yields

$$\delta(\sum_i b_i) = \sum_i \sum_j h_i \mu_j W_i^{(o)} \delta x_i - \sum_j \sum_i h_j \mu_i W_j^{(o)} \delta x_i \quad (376)$$

For the odd function $W^{(o)}(x_i - x_j; h)$, the derivative to the spatial coordinate x_i and x_j has the relation

$$\begin{aligned} W_j^{(o)}(x_i - x_j; h) &= \frac{\partial W^{(o)}}{\partial x_j}(x_i - x_j; h) \\ &= \frac{\partial W^{(o)}}{\partial x_i}(x_i - x_j; h) \end{aligned} \quad (377)$$

So that

$$\begin{aligned} \delta(\sum_i a_i) &= \sum_i \sum_j g_i t_j W_i^{(e)} \delta \mathbf{r}_i + \sum_j \sum_i g_j t_i W_i^{(e)} \delta \mathbf{r}_i \\ &= \sum_{ij} (g_i t_j + g_j t_i) W_i^{(e)}(x_i - x_j; h) \delta x_i \end{aligned} \quad (378)$$

In summary,

$$\begin{aligned} \delta(\sum_i a_i) &= \sum_{ij} (g_i t_j + g_j t_i) W^{(e)'}(x_i - x_j; h) \delta x_i \\ &= \sum_j (f_{ij}^{(e)} + f_{ji}^{(e)}) \delta x_i \end{aligned} \quad (379)$$

$$\begin{aligned} \delta(\sum_i b_i) &= \sum_{ij} (h_i u_j + h_j u_i) W^{(o)'}(x_i - x_j; h) \delta x_i \\ &= \sum_j (f_{ij}^{(o)} + f_{ji}^{(o)}) \delta x_i. \end{aligned} \quad (380)$$

where

$$f_{ij}^{(e)} = \sum_i g_i t_j W^{(e)'}(x_i - x_j; h), \quad (381)$$

$$f_{ji}^{(e)} = \sum_i g_j t_i W^{(e)'}(x_i - x_j; h), \quad (382)$$

$$f_{ij}^{(o)} = \sum_i h_i \mu_j W^{(o)'}(x_i - x_j; h), \quad (383)$$

$$f_{ji}^{(o)} = \sum_i h_j \mu_i W^{(o)'}(x_i - x_j; h). \quad (384)$$

In both cases, $f_{ij}^{(e,o)} = -f_{ji}^{(e,o)}$. And the hydrodynamic equation is as follows

$$\frac{d}{dt}(\nu_i \frac{P_i + \varepsilon_i}{s_i} \gamma_i v_i) = \sum_j f_{ij}^{(n)}, \quad (385)$$

where

$$f_{ij}^{(n)} = -[l_i^{(n)} m_j^{(n)} + (-1)^{k(n)} l_j^{(n)} m_i^{(n)}] W^{(n)'}(x_i - x_j; h) \quad (386)$$

with

$$k_i^{(1,3,6,8)} = 1, \quad (387)$$

$$k_i^{(2,4,5,7)} = 2, \quad (388)$$

$$l_i^{(1)} = \frac{D_i \langle s \rangle_i}{B_i}, \quad (389)$$

$$l_i^{(2)} = \frac{D_i \langle \Delta x \rangle_{i,x}}{B_i}, \quad (390)$$

$$l_i^{(3)} = -\frac{D_i \langle s \rangle_{i,x}}{B_i}, \quad (391)$$

$$l_i^{(4)} = -\frac{D_i \langle \Delta x \rangle_i}{B_i}, \quad (392)$$

$$l_i^{(5)} = -\frac{C_i D_i \langle \Delta x \rangle_{i,x}}{B_i^2}, \quad (393)$$

$$l_i^{(6)} = -\frac{C_i D_i \langle 1 \rangle_i}{B_i^2}, \quad (394)$$

$$l_i^{(7)} = \frac{C_i D_i \langle \Delta x \rangle_i}{B_i^2}, \quad (395)$$

$$l_i^{(8)} = \frac{C_i D_i \langle 1 \rangle_{i,x}}{B_i^2}, \quad (396)$$

$$m_i^{(1,3,5,6,7,8)} = \frac{\nu_i}{\rho_i}, \quad (397)$$

$$m^{(2,4)} = \nu_i, \quad (398)$$

$$W^{(1,6)}(x_i - x_j; h) = \frac{x_{ij}^2}{|x_{ij}|} W'(x_i - x_j; h), \quad (399)$$

$$W^{(2,5)}(x_i - x_j; h) = W(x_i - x_j; h), \quad (400)$$

$$W^{(3,8)}(x_i - x_j; h) = x_{ij} W(x_i - x_j; h), \quad (401)$$

$$W^{(4,7)}(x_i - x_j; h) = \frac{x_{ij}}{|x_{ij}|} W'(x_i - x_j; h), \quad (402)$$

$$B_i = \langle 1 \rangle_i \langle \Delta x \rangle_{i,x} - \langle 1 \rangle_{i,x} \langle \Delta x \rangle_i, \quad (403)$$

$$C_i = \langle s \rangle_i \langle \Delta x \rangle_{i,x} - \langle s \rangle_{i,x} \langle \Delta x \rangle_i, \quad (404)$$

$$D_i = \frac{\nu_i P_i}{s_i^{*2}}. \quad (405)$$

As a test, the new form of force in equation of motion should be reduced to the one in standard form. By comparison of equation (385) and equation (360), it is not difficult to see that equation (360) is corresponding to the specific term $f_{ij}^{(2)}$ in one dimensional case when one assumes $\langle 1 \rangle_i \rightarrow 1$ and $\langle 1 \rangle_{i,x} \rightarrow 0$.

In this section, we mainly try to study the implementation of FPM into the entropy-based SPH hydrodynamic model. And the equation of motion derived from the variational principle guarantees the momentum conservation which plays a important role in small systems dynamics arising from relativistic heavy ion collisions. The new equation of motion keeps the conservation of momentum in another way. It says that not a pair of forces between two particles are equal in size and opposite in direction but the total force summation over all particles are zero. This idea is creative and the derived equation of motion can reduce to the standard SPH form as a limit.

Owing to the observation of the “ridge” effect in two-particle correlation in relativistic heavy ion collision, the fluctuating initial conditions play an increasingly important role in the hydrodynamical description of nuclear collisions. The improvement of particle consistency brought by the FPM, therefore, can be significant in the context of precision and efficiency of the numerical approach. It is interesting to implement the obtained equation of motion for realistic collision simulations, which will be carried out in our subsequent study.

7 Discussion and Outlook

The results throughout this dissertation will be summarized and commented. The goal of this chapter is to make summary of the work as a whole and the future research direction are going to be addressed. The work is based on a lot of literatures written by many pioneers in this field. By reading and learning plenty of their work, more and more understanding of the SPH numerical method is achieved.

In the section of introduction, the history and development of the SPH method are reviewed. As a new numerical method to handle the partial differential equations, it is compared with the state of art numerical methods like FVM, FEM and FDM. Through the comparisons, its merits and drawbacks are present. As a numerical method, some important numerical properties like stability and consistency are required to be discussed. The whole dissertation can be broken into two main categories. One is to review some important numerical properties of SPH and the other is to make implementation of SPH. For the most part of the chapter one focus on the numerical properties of SPH and the other parts including chapter four and chapter five discuss the SPH implementation. Every chapter in the dissertation will now be reviewed according to the above discussion.

7.1 Numerical Properties of SPH

In chapter one section seven, the tensile stability is discussed. As a common instability phenomena appearing in material strength problems, it is well addressed. And some approaches to avoid such instability have been addressed.

Chapter one section nine focuses on the efficiency of SPH implementation. The efficiency of a numerical technique usually refers to its speed and resource

usage. The SPH method shows great efficiency in dealing with problems of free surface flow due to its inherent properties without the use of grids or meshes.

Chapter one section ten concentrate on the accuracy of SPH method. It is meant to illustrate the selection of smoothing kernel function in different problems is significant and it may affect the accuracy of numerical results simulated by SPH approach.

In chapter one section twelve concentrates on consistency. It begins with a detailed derivation of the kernel approximation and the particle approximation for a function and its derivative. Then a discussion of how to maintain the kernel consistency and particle consistency are performed. The detailed method includes the CSPM, DSPH and the FPM method.

7.2 The kernel function

Chapter one section six focus on the SPH kernel. The kernel function is included in the SPH interpolations so that it is essential to talk about it in detail. The kernel properties, specific form and the smoothing length inherent to it have been addressed. Although in usual SPH implementations, the cubic spline kernel is used. However corresponding to different problems and different requirements, other kernel functions would be chosen. Since it appears in kernel approximation and particle approximation, it has a great influence on the numerical properties like consistency and stability.

7.3 The SPH implementation

In the discussion about the numerical properties of SPH method, it is unavoidable to involve the SPH implementation both in physical and engineering problems. To compare with the SPH method and the FPM method, the interpolation of an arbitrary function is performed firstly. For the SPH implementation in the relativistic heavy ion collisions, the one dimensional Landau model and the transverse flow expansion with longitudinally scaling expansion are applied.

7.4 Future research directions

Actually predicting the future development direction of SPH is very difficult. However based on the work in this dissertation, there are some possible paths. Maybe it is not complete and mature, but it is worthwhile to discuss.

First of all, the numerical properties like consistency, stability and accuracy should be investigated more deeply. Stability is the investigation of error propagation in numerical methods. As a matter of fact, there are some approaches to analyze the error for the stability problems, like the linear stability analysis and total variation stability analysis.

Secondly further study into the effects of a variable smoothing length. This contains the effects on consistency, stability and accuracy.

Thirdly the SPH applications to astrophysics and engineering are enormous. It should enlarge its application into relativistic heavy ion collisions like dealing with shock wave, viscosity fluid and turbulence phenomena.

Fourthly the new derived equation of motion based upon the FPM method should be tested. Theoretically it is consistent but detailed test has not been performed.

8 Publications

This work has been published in Commun. Theor. Phys. 68 (2017) 382. The arXiv number of the work is 1704.06165.

References

- [1] Private communications from Dr. Philipe Mota.
- [2] Liu MB, Liu GR. Restoring particle consistency in smoothed particle hydrodynamics. *Appl Numer Mat* 2006;56:19C36.
- [3] Chung TJ (2002) *Computational fluid dynamics*. Cambridge University Press.
- [4] Anderson JD (2002) *Computational fluid dynamics: the basics with applications*. McGraw Hill, New York.
- [5] Zienkiewicz OC, Taylor RL (2000) *The finite element method*. Butterworth-Heinemann.
- [6] Liu GR (2002) *Meshfree methods: moving beyond the finite element method*. CRC Press.
- [7] Hirsch C (1988) *Numerical computation of internal and external flows: fundamentals of numerical discretization*. John Wiley and Sons, Inc. New York, NY, USA.
- [8] Liu GR, Liu MB (2003) *Smoothed particle hydrodynamics: a meshfree particle method*. World Scientific, Singapore.
- [9] Liu GR, Gu YT (2005) An Introduction to meshfree methods and their programming. Springer, Dordrecht, p 479
- [10] Li S, Liu WK (2002) Meshfree and particle methods and their applications. *Appl Mech Rev* 55(1):1C34
- [11] Belytschko T, Krongauz Y, Organ D, Fleming M, Krysl P (1996) Meshless methods: an overview and recent developments. *Comput Methods Appl Mech Eng* 139(1C4):3C47
- [12] Idelsohn SR, Onate E (2006) To mesh or not to mesh? That is the question. *Comput Methods Appl Mech Eng* 195(37C40):4681C4696
- [13] Nguyen VP, Rabczuk T, Bordas S, Duflot M (2008) Meshless methods: a review and computer implementation aspects. *Math Comput Simul* 79(3):763C813
- [14] Liu GR, Nguyen-Thoi T, H. N-X, Lam KY (2008) A node-based smoothed finite element method (NS-FEM) for upper bound solutions to solid mechanics problems. *Comput Struct* 87:14C26
- [15] Liu GR, Zhang GY (2008) Upper bound solution to elasticity problems: a unique property of the linearly conforming point interpolation method (LC-PIM). *Int J Numer Methods Eng* 74:1128C1161

- [16] Liu GR, Nguyen-Thoi T, Lam KY (2009) An edge-based smoothed finite element method (ES-FEM) for static, free and forced vibration analyses in solids. *J Sound Vib* 320:1100C1130
- [17] Zhang GY, Liu GR, Nguyen TT, Song CX, Han X, Zhong ZH, Li GY (2007) The upper bound property for solid mechanics of the linearly conforming radial point interpolation method (LCRPIM). *Int J Comput Methods* 4(3):521C541
- [18] G. R. Liu, George X. Xu. A gradient smoothing method (GSM) for fluid dynamics problems. *International Journal for Numerical Methods in Fluids*, 58: 1101C1133, 2008.
- [19] J. Zhang, G. R. Liu, K.Y. Lam, H. Li, G. Xu. A gradient smoothing method (GSM) based on strong form governing equation for adaptive analysis of solid mechanics problems. *Finite Elements in Analysis and Design*, 44: 889C909, 2008.
- [20] Lucy LB. 1977, *Astron. J.* 82:1013-24.
- [21] Gingold RA, Monaghan JJ. 1977, *MNRAS* 181:375-389.
- [22] Benz W (1988) Applications of smooth particle hydrodynamics (SPH) to astrophysical problems. *Comput Phys Commun* 48(1):97C105
- [23] Frederic AR, James CL (1999) Smoothed particle hydrodynamics calculations of stellar interactions. *J Comput App Math* 109:213C230
- [24] Hultman J, Pharayn A (1999) Hierarchical, dissipative formation of elliptical galaxies: is thermal instability the key mechanism? Hydrodynamic simulations including supernova feedback multiphase gas and metal enrichment in cdn: structure and dynamics of elliptical galaxies. *Astron Astrophys* 347:769C798
- [25] Thacker RJ, Couchman HMP (2001) Star formation, supernova feedback, and the angular momentum problem in numerical cold dark matter cosmogony: halfway there. *Astrophys J* 555(1):L17CL20
- [26] Monaghan JJ, Lattanzio JC (1991) A simulation of the collapse and fragmentation of cooling molecular clouds. *Astrophys J* 375(1):177C189
- [27] Berczik P (2000) Modeling the star formation in galaxies using the chemodynamical SPH code. *Astrophys Space Sci* 271(2):103C126
- [28] Monaghan JJ. 1994. Simulating free surface flows with SPH. *J. Comput. Phys.* 110:399-406.
- [29] Monaghan JJ, Kocharyan A (1995) SPH simulation of multiphase flow. *Comput Phys Commun* 87:225C235

- [30] Colagrossi A, Landrini M (2003) Numerical simulation of interfacial flows by smoothed particle hydrodynamics. *J Comput Phys* 191(2):448C475
- [31] Liu J, Koshizuka S, Oka Y (2005) A hybrid particle-mesh method for viscous, incompressible, multiphase flows. *J Comput Phys* 202(1):65C93
- [32] Bonet J, Kulasegaram S (2000) Correction and stabilization of smooth particle hydrodynamics methods with applications in metal forming simulations. *Int J Numer Methods Eng* 47(6):1189C1214
- [33] Benz W, Asphaug E (1995) Simulations of brittle solids using smooth particle hydrodynamics. *Comput Phys Commun* 87(1):253C265
- [34] Cleary PW, Ha J, Ahuja V (2000) High pressure die casting simulation using smoothed particle hydrodynamics. *Int J Cast Met Res* 12(6):335C355
- [35] Chen JS, Pan C, Roque C, Wang HP (1998) A Lagrangian reproducing kernel particle method for metal forming analysis. *Comput Mech* 22(3):289C307
- [36] Monaghan JJ. 1992, *Annu. Rev. Astron. Astrophys.* 1992. 30: 543-74.
- [37] Daniel J. Price, arXiv:1012.1885.
- [38] Swegle JW, Hicks DL, Attaway SW (1995) Smoothed particle hydrodynamics stability analysis. *J Comput Phys* 116(1):123-134.
- [39] Chen JK, Beraun JE, Jih CJ (1999) An improvement for tensile instability in smoothed particle hydrodynamics. *Comput Mech* 23(4):279-287.
- [40] Morris JP (1996) *Analysis of Smoothed Particle Hydrodynamics with Applications*. Monash University.
- [41] Monaghan JJ (2000) SPH without a tensile instability. *J Comput Phys* 159(2):290-311.
- [42] Gray JP, Monaghan JJ, Swift RP (2001) SPH elastic dynamics. *Comput Method Appl M* 190(49):6641-6662.
- [43] M.B. Liu, G.R.Liu, *Arch Comput Methods Eng* (2010) 17:25-76.
- [44] Springel V. 2010. Smoothed particle hydrodynamics in astrophysics. *Annu. Rev. Astron. Astrophys.* 48:391-430.
- [45] Benz. W(1988) Applications of smooth particle hydrodynamics (SPH) to astrophysical problems. *Comput Phys Commun* 48(1):97-105.
- [46] Monaghan JJ. 1994. Simulating free surface flows with SPH. *J. Comput. Phys.* 110:399-406.
- [47] Monaghan, J.J., Gingold, R. A. 1983. *J. Comput. Phys.* 52: 374.

- [48] Crespo AJC, Gomez-Gesteira M, Dalrymple RA (2007) 3D SPH simulation of large waves mitigation with a dike. *J Hydraul Res* 45(5):631C642
- [49] Libersky, L.D. and Petschek, A.G., 1990, Smooth particle hydrodynamics with strength of materials, in: *Advances in the Free-Lagrange Method*, Trease and Crowley, eds., (Springer, Berlin) p. 248.
- [50] Wingate, C.A., and Fisher, H.N., 1993, Strength Modeling in SPHC, Los Alamos National Laboratory report, LA-UR-93-3942.
- [51] Benz, W., and Asphaug, E., 1994, *Icaros*, 107, 98-116.
- [52] Benz W, Asphaug E (1995) Simulations of brittle solids using smooth particle hydrodynamics. *Comput Phys Commun* 87(1):253-265.
- [53] LiuMB, Liu GR, Lam KY, Zong Z (2003) Smoothed particle hydrodynamics for numerical simulation of underwater explosion. *Comput Mech* 30(2):106C118
- [54] Chen JK, Beraun JE (2000) A generalized smoothed particle hydrodynamics method for nonlinear dynamic problems. *Comput Method Appl M* 190:225-239.
- [55] Liu MB, Liu GR, Lam KY (2003) A one-dimensional meshfree particle formulation for simulating shock waves. *Shock Waves* 13(3):201-211.
- [56] Sibilla, S. An Algorithm to Improve Consistency in Smoothed Particl Hydrodynamics. *Computers and Fluids*,118, 148-158.
- [57] G.R. Liu, M.B. Liu, *Smoothed particle hydrodynamics, A Meshfree Particle Method*, World Scientific Publishing, 2003.
- [58] L.D. Landau, *Izv. Akad. Nauk SSSR* 17 (1953) 51.
- [59] I.M. Khalatnikov, *Zh. Eksp. Teor. Fiz.*27 (1954) 529.
- [60] Cheuk-Yin Wong, Abhisek Sen, Jochen Gerhard, Giorgio Torrieri, Kenneth Read, *Analytical Solutions of Landau (1+1)-Dimensional Hydrodynamics*, arXiv: 1408.3343v2.
- [61] Y. Hama, T. Kodama, O. Socolowski Jr. *Braz.J.Phys.*35:24-51,2005.
- [62] Y. Hama and F.W. Pottag, *Resolution of Hydrodynamical Equations for Transverse Expansions - II*, Aug 1984. 28 pp.